Università di Napoli Federico II

Faculty of Agriculture

Doctoral School in
Valorization and Management of Agricultural and Forestal Resources

Immobilization of a biomimetic catalyst on clay minerals. Study of the activity of the supported catalysts on the oxidative coupling of humic molecules and precursors.

Tutor
Prof. Alessandro Piccolo

Candidate
Dr. Assunta Nuzzo

Coordinator
Prof. Guido D'Urso

2008-2011

INDEX

SUMMARY

Two novel heterogeneous biomimetic catalysts were synthesized by immobilizing a meso-tetra(2,6-dichloro-3-sulfonatophenyl)porphyrinate of manganese (III) chloride [Mn(TDCPPS)Cl] on both kaolinite (K) and montmorillonite (M) clay minerals, previously functionalized with a molecular spacer ending with an imidazole group, whose nitrogen atom firmly coordinates the metal in the porphyrin ring. The clay functionalization by a 3-(1-imidazolyl)propylcarbamoyl-3′-aminopropyl-triethoxysilane spacer was proved by DRIFT-IR, ^{13}C- and ^{29}Si-CPMAS-NMR spectroscopies, and the percent of Mn(TDCPPS)Cl immobilized by the spacer coordination was calculated. The efficiency of the catalysis induced by the novel heterogeneous catalysts was evaluated in the oxidative coupling reaction of catechol, a humic phenolic precursor, in the presence of H_2O_2 as oxygen donor, following the disappearance of the substrate by HPLC. The catalytic activity of the catalyst immobilized on spacer-functionalized K was, then, verified in the oxidative coupling reaction of a dissolved humic acid under either chemical (H_2O_2) or UV-light oxidation. The change in molecular size of the polymerized humic acid was followed by high-performance size exclusion chromatography (HPSEC) with both UV-Vis and refractive index (RI) detectors. The rate of catechol oxidation catalyzed by both K and M heterogeneous catalysts was about four times as rapid as that catalyzed by the free manganese-porphyrin in a homogeneous catalysis, and the activity of the heterogeneous catalysts remained effective for at least two sequential reaction cycles, although a rate decrease in catechol transformation was observed. Furthermore, the kaolinite-supported heterogeneous catalyst increased the apparent weight-average molecular weight (*Mw*) of polymerized humic acid, without significant difference between chemical and light-induced oxidation. The enhancement

in the apparent molecular mass of humic matter subjected to catalyzed oxidative polymerization was also confirmed by HPSEC chromatograms recorded after acetic acid addition, thereby suggesting that the heterogeneous biomimetic catalysis promoted the stabilization of loosely bound humic conformations by the formation of intermolecular covalent bonds during the oxidative coupling reaction. These findings suggest that metal-porphyrins immobilized on clay minerals through a flexible spacer may represent a valid tool to implement the heterogeneous biomimetic catalysis in the remediation of contaminated soils and waters and in the control of natural organic matter transformation.

CHAPTER 1 -

INTRODUCTION

1.1 Sequestration of organic carbon in soil

Agricultural activity contributes considerably to green-house gas emissions in the earth's atmosphere (Paustian et al., 1997). Extensive deforestation and intensive agricultural management have led to an increasing transfer of carbon from soil organic matter to atmospheric CO_2 (Schlesinger, 1997). It is generally accepted that reforestation of previously cleared areas may reverse the trend by increasing carbon storage in woody tissues (Idso & Kimball, 1993). Nevertheless, it is still debated if carbon storage in agricultural crops or even fast growing forest would ever equal the carbon contained in the original forest (Smith & Shugart, 1993).

As a result of Kyoto protocol established at the United Nations Framework Convention on Climate change, an effort has been made to look towards soils and living biomass for carbon sequestration, defined as the long term storage of C in soils (Wang & Hsieh, 2002). Soils are good candidates for carbon sequestration since they represent the largest carbon reservoir in terrestrial ecosystems (Schlesinger, 1997).

Soil carbon storage is primarily controlled by two fundamental processes: (i) primary production input and (ii) decomposition. Sources of C input include the amount of aboveground and belowground biomass returned to soil. The output or losses of C out of the soil system are mainly influenced by topography, composition of the mineral soil component, crop and vegetation cover, soil temperature and moisture (Nieder et al., 2003). Increased primary production would result in an increased carbon storage, whereas increased decomposition would have an opposite effect. Other factors, such as erosion, leaching, and fire also affect soil C dynamics, though in lesser and variable degrees.

The key element in soil C dynamics is the ability of soil to stabilize soil organic matter (SOM). Three main stabilizing mechanisms have been proposed (Stevenson, 1994; Six et al., 2002; Jastrow & Miller, 1998): (1) biochemical recalcitrance, (2) chemical stabilization, and (3) physical protection.

Biochemical stabilization is understood as the stabilization of SOM due to its complex chemical composition (e.g. recalcitrant compounds such as lignin and polyphenols). This C pool is sometimes referred to the passive SOM pool and its size has been assimilated to the non-hydrolyzable fraction. Chemical stabilization results from the chemical or physicochemical binding between SOM and soil minerals. The amount of C protection increases with increased silt and clay proportion of the soil. Physical protection occurs when organic matter is situated in soils in such a way that it is physically inaccessible for the microorganisms and their enzymes, thus becoming protected against decomposition. One of such arrangement involves the incorporation of SOM into soil aggregates. According to some of the studies, macroaggregate structure (> 250 μm) exerts a minimal amount of physical protection and the majority of SOM is physically protected from the decomposition predominantly at the microaggregate (< 250 μm) level.

1.2 Remediation of contamined soils and waters

Environmental pollution is one of the most problematic topics of our time. Halogenated phenols constitute a major group of pollutants having been extensively used as wood preservatives, pesticides and herbicides. They are also formed as by-products of many industrial activities and they are widely found in all the ecological sectors. Some of these organic halogenated compounds are resistant to degradation and

may persist and accumulate in aquatic ecosystems modifying their equilibrium by eliminating or reducing populations of organisms.

To overcome the problem of environmental pollution by halogenated phenols, a number of methods with different approach are available. However, an interesting method is the oxidative coupling reaction mediated by peroxidases enzymes because of their low environmental impact. In soil the oxidative coupling reactions are the main degradative reactions of contaminants which occur with the formation of covalent bonds between phenolic components of humic matter and phenolic pollutants (Bollag, 1992) via a radical mechanism. The reaction products are oligomerized and polymerized phenols and they result to be less bioavailable, less mobile and less toxic. Because of this, oxidative coupling reactions are largely used for soil and water remediation.

1.3 Humic Substances

Humic substances (HS), otherwise referred to as natural organic matter (NOM), are ubiquitous natural compounds, arising from the chemical and biological degradation of plant and animal residues and occurring in soils, sediments, coals, waters, and other natural materials (Stevenson, 1994). HS are of paramount importance in controlling both the biogeochemistry of organic carbon in the global ecosystem and the fate of environmental pollutants (Piccolo et al., 2003).

Despite their significant role in environmental processes, their basic chemical knowledge is still a matter of research. The great diversity of views regarding sizes, shapes, formation and reactivity of HS are hindered in particular due to their high complexity and heterogeneous nature. The large chemical complexity originates from the contribution of random decay of plant tissues, microbial metabolites, and of

different properties of each ecosystem, like climate and vegetation, in which HS are formed (Piccolo et al., 2003). Moreover the chemical composition of humic fraction is governed by extraction, fractionation and purification procedures (Saiz-Jimenez, 1996).

Unlike most naturally occurring compounds, HS are not defined in terms of their chemical composition or functional group content (Swift, 1999). Instead, they are traditionally classified into three major operational groups according to their solubility at different pH. This fractionation identifies 1) fulvic acids soluble in all pH conditions, 2) humic acids soluble only under alkaline conditions, and 3) humin insoluble at any pH.

Up to about 15 years ago, it has been believed that HS were macromolecular polymers, coiled-down in globular conformations at high concentrations, low pH and high ionic strength, and flexible linear colloids at neutral pH, low ionic strength and low concentration (Cozzolino et al., 2001). However, this macromolecular theory has never been unequivocally demonstrated (Piccolo, 2001). In fact, the macromolecular understanding has begun to be gradually abandoned and, instead, a supramolecular view of the HS conformation is now gaining consensus (Piccolo et al., 1996; Piccolo, 2002; Simpson, 2002).

According to this new view (Piccolo et al., 1996; Piccolo, 2001, 2002; Cozzolino et al., 2001; Piccolo et al., 2003), rather than being constituted by macromolecular polymers, as traditionally believed, HS may be better described as supramolecular associations of heterogeneous molecules that have average mass lower than 1000-2000 Da (Piccolo, 2001; Wershaw, 2004) and are held together by relatively weak forces (π-π, CH-π, and van der Waals interactions) in contiguous hydrophilic and hydrophobic domains of apparently high molecular sizes (Piccolo, 2002; Peuravuori, 2005).

Such humic associations show only apparent high molecular dimensions which can be reversibly disrupted by either treating humic solutions with low concentrations of mineral and monocarboxylic acids (Piccolo et al., 1999) or slightly varying the mobile phases composition but keeping ionic strength constant (Conte & Piccolo, 1999) into fractions of lower molecular size. New formation of intermolecular hydrogen bonding and alteration of pre-existing hydrophobic interactions accounted for the disruption of original supramolecular associations of humic matter.

The supramolecular theory was primarily formulated to give an adequate explanation for the results obtained by low and high performance size exclusion chromatography (HPSEC) of HSs (Piccolo et al., 1996; Piccolo, 2001, 2002). The HPSEC chromatograms, achieved by measuring the absorbance with UV and refractive index detectors, indicated a decrease in the molecular size of humic solutions, demonstrated by the shift toward larger elution volume for both detectors, and a concomitant reduction of absorbance at UV detector when treated with HCl or acetic acid. Such finding was attributed to a hypochromic effect, by which an increasing distance among chromophores leads to decreased intensity of absorbance (Cantor & Schimmel, 1980). The increased distance among chromophores was attributed to the disaggregation of humic clusters.

Further HPSEC experiments, involving direct modification of the mobile phase with methanol, hydrochloric acid and acetic acid, showed a progressive alteration of the chromatographic behaviour of humic materials, but did not modify that of polystyrensulphonates and polysaccharides (Piccolo et al., 2001), clearing definitively the different nature of HS and polymers. Similar comparison of original and acid-treated humic solution was followed by DOSY-NMR (diffusion ordered) spectroscopy

(Simpson, 2002; Smejkalova & Piccolo, 2008) demonstrating once more that HS have only apparent large molecular weight. Further evidence in support of the supramolecular association of HS was given by low and high resolution electrospray mass spectrometry (ESI-MS). The average molecular mass of humic material observed with this method was found to be ranging from 700 to 1200 Da (Stenson et al., 2002, 2003; Piccolo & Spiteller, 2003; Piccolo et al., 2010).

1.4 Biomimetic catalysis

If humic substances are weakly bound supramolecular associations, the unstable conformation of humic superstructures could be stabilized by increasing the number of intermolecular covalent bonds and thus enhance their resistance to further biotic or abiotic degradation (Piccolo et al., 2000). Previous works have shown that the humic superstructure can be stabilized by oxidation in the presence of oxi-reductive enzymes (containing natural metalporphyrins), such as horseradish peroxidase (Piccolo et al., 2000; Cozzolino & Piccolo, 2002). Naturally occurring oxidoreductases, namely peroxidases, are well known to catalyze the oxidative polymerization of phenols (Kobayashi et al., 2001) and are suggested to be involved in the formation of HS (Martin & Haider, 1971; Dec & Bollag, 2000; Park et al., 1999), as by the previous and erroneous understanding of humic substances as macropolymers.

Since the isolation and purification of any enzyme to be practically employed in real systems is rather problematic, synthetic biomimetic catalysts are a favorable alternative to be applied to mimic the activity of natural oxidative enzymes in an efficient and economic way (Gonsalves & Pereira, 1996). Biomimetic synthetic catalysts are artificial compounds formed by the same active prosthetic group present in

that natural enzymes, functionalized to be more soluble in water and more stable under oxidative conditions (Crestini et al., 1999; Milos, 2001), overcoming the disadvantages of natural enzymes (Gianfreda & Bollag, 1994, 1996) and mimicking their catalytic activity.

Research concerning synthetic alternatives to peroxidases was mainly focused on the development of their active sites, formed by metal-porphyrins (Sheldon, 1994; Nam et al., 2000). Synthetic metal-porphyrins (examples of iron- and manganese-porphyrin are shown in Figure 1), have been successfully applied to catalyze oxidation reaction of various hydrocarbons, such as polychlorinated aromatics and other pollutants (Meunier & Sorokin, 1997; Fukushima et al., 2003), drugs (Hendrickson et al., 1987), various lignin models (Artaud et al., 1993), and humic substances (Piccolo et al., 2005).

In all cases, singlet oxygen donors, such as hydrogen peroxide, were required to produce high-valent metal-oxo species. These oxo species, for the first time characterized as the key intermediates in the catalytic cycle of natural oxygenases by Groves and coworkers (Groves et al., 1981), show strong oxidizing ability (Moro-oka, 1998). Therefore, once they are formed, the organic substrate can undergo an oxidation giving unstable free radicals that are stabilized by spontaneous mutual coupling without additional involvement of a catalyst (Dec et al., 2001).

The formation of high-valent metal-oxo species is also observed when the system is exposed to light. The photocatalytic effect of synthetic metal-porphyrins have been demonstrated using hydrocarbons, such as alkanes and alkenes in the presence of dioxygen (Weber et al., 1994; Maldotti et al., 2002). However, this time molecular dioxygen $^3O_2$ is involved as an oxygen donor. According to this mechanism, light

causes an intramolecular transfer which leads to the formation of M(II)porphyrin (where M = Fe or Mn) (eq. 1) that can coordinate O_2 and form highly reactive metal-oxo species (Hendrickson et al., 1987; Maldotti et al., 2002).

$$M^{III}(TDCPPS)Cl \xrightarrow{h\nu} M^{II}(TDCPPS) + Cl^{\bullet} \quad (1)$$

Even though hydrogen peroxide is considered to be an environmentally clean oxidant, and hence a suitable singlet oxygen donor, synthetic metal-porphyrins in the presence of excess H_2O_2 may form unreactive oxometal(IV)-porphyrin complexes because of their instability under oxidizing conditions.

One approach to minimize oxidative degradation of metal-porphrins, is their immobilization on adequate supports (Que & Tolman, 2008; Mansuy, 2008), which provide site isolation of the metal center, thus limiting considerably catalyst self-destruction and dimerization (Mansuy, 1993).

Moreover, the use of immobilized catalysts is both operationally and economically advantageous since it allows an easy separation and recycling of the catalyst for further reactions.

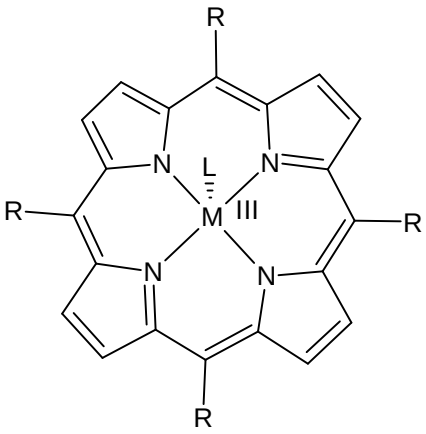

M = Fe, Mn

L = Cl

R =

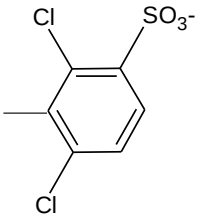

TDCPPS

Figure 1. Chemical structure of Fe- and Mn- (TDCPPS)Cl.

CHAPTER 2 – WORK OBJECTIVES

2.1 Work objectives

Extensive deforestation and intense agricultural management have led to land degradation, mineralization of soil organic carbon (SOC) and the subsequent loss of SOC as CO_2 emitted to the atmosphere. Since SOC is related to chemical, physical, and biochemical soil properties, the decrease of SOC has also led to the loss of soil quality, as well as sustainability of soil fertility and its productivity. The humic matter is considered essential in the stabilization, accumulation and dynamics of soil organic carbon. Therefore, an increased stability of humic substances against biotic and abiotic degradation can lead to an increased carbon sequestration.

Within the supramolecular understanding of HS structure, it could be reasoned to enhance the stability of humic conformations by increasing the number of non hydrolysable intermolecular covalent bonds among small humic molecules through catalyzed oxidative reactions and thus increase the molecular size of HS. This result implies, also, that it could be possible to reduce the toxicity and the bioavailability of halogenated phenols in the environment by forming covalent bonds between these contaminants and the phenolic constituents of the humic matter (Hahn et al., 2007). Both natural peroxidases containing metal-porphyrin as prosthetic group (Cozzolino & Piccolo, 2002), and synthetically prepared metal-porphyrin catalysts (Piccolo et al., 2005), have already been successfully applied to increase the conformational rigidity of humic substances. The oxidative coupling of humic superstructures was induced by either the addition of hydrogen peroxide as an oxidizing agent or photochemically. The biomimetic catalysis operated directly in soils was shown to also induce a significant reduction of soil respiration and, thus, of CO2 emissions to the atmosphere (Piccolo et al., 2011).

The aim of this work was: (a) to synthesize two heterogeneous biomimetic catalysts, by immobilizing a meso-tetra(2,6-dichloro-3-sulfonatophenyl)porphyrinate of manganese(III) chloride [Mn(TDCPPS)Cl] on both kaolinite and montmorillonite clay minerals previously functionalized with a molecular spacer to allow a coordinative interaction with the metal center of the porphyrin ring; (b) to evaluate the efficiency of the catalysis induced by two immobilized biomimetic catalysts in the oxidative coupling reaction of the catechol, a humic phenolic precursor, using H_2O_2 as oxygen donor; (c) to verify the catalytic activity of the Mn(TDCPPS)Cl immobilized on spacer-functionalized kaolinite in the oxidative coupling of a dissolved lignite humic acid under either H_2O_2 oxidant or photo-oxidation.

Finally, Chapter 7 deals with cucurbiturils, which are interesting macrocyclic molecules representing a developing area of Host-Guest Supramolecular Chemistry. This preliminary study aimed to investigate the pH-controlled release of indole-3-acetic acid from macrocyclic cucurbit[7]uril, as potential carrier of this phytohormone to cell membranes of plant roots and leaves. The work was conducted under the supervision of Dr. Oren A. Scherman, in the Chemistry Department of University of Cambridge (Cambridge, UK).

CHAPTER 3 –

MATERIALS AND

METHODS

3.1 Materials

All solvents and reagents used were of Reagent Grade (Sigma-Aldrich), and used without further purification.

Catechol

Catechol or 1,2-dihydroxybenzene was purchased from Sigma-Aldrich (Germany), with purity ranging between 97 and 99%, and used without further purification.

Humic acid

The humic acid (HA) used in this study was extracted from a North Dakota leonardite provided by Mammoth, Int. Chem. Co. (USA). The original material was shaken overnight in a 0.5 M NaOH and 0.1 M $Na_4P_2O_7$ solution under N_2 atmosphere. The HA was precipitated from alkaline extract by adding 6 M HCl until pH 1 and further purified by three cycles of dissolution in 0.1 M NaOH and subsequent precipitation in 6 M HCl. Then the HA was treated with a 0.5% (v/v) HCl-HF solution for 48 h, dialyzed (Spectrapore, 3500 Mw cut-off) against deionised water until was chloride-free and freeze-dried. An aliquot of HA was then suspended in 100 ml of deionised water and titrated (VIT 90 Videotitrator, Radiometer, Copenhagen, Denmark) with a CO_2-free solution of 0.1 M KOH to pH 7. The resulting potassium humate was filtered through a Millipore 0.45 μ, freeze-dried and homogenized in agate mortar.

Water-Soluble Manganese(III)-Porphyrin (Mn(TDCPPS)Cl)

The procedure for the synthesis of water-soluble meso-tetra(2,6-dichloro-3-sulfonatophenyl)porphyrinate of manganese(III) chloride [Mn(TDCPPS)Cl], has been described elsewhere (Piccolo et al., 2005).

Clay minerals

The clay minerals used in this work were a kaolinite (K) from Washington County, Georgia, USA, and a Na-montmorillonite (M) from Crook County, Wyoming, USA. Both have been supplied by the Source Clay Minerals Repository (University of Missouri, USA).

3.2 Procedures for the synthesis of heterogeneous biomimetic catalysts

Functionalization of clay minerals

Kaolinite and montmorillonite clay minerals were first protonated by suspending 30 g of either K or M in 1 L of a 2 M HCl solution and stirred for 48 hours to remove inorganic cations in here. This procedure was repeated 3 times. After proton saturation, clay minerals were first dialyzed (3500 Da dialysis tubes) against water until pH 5-6, and then freeze-dried and pulverized. The molecular spacer, 3-(1-imidazolyl)propylcarbamoyl-3′-aminopropyl-triethoxysilane (Imi-APTS), was synthesized as described elsewhere (Zucca et al., 2007). Briefly, 260 µL (10 mmol) of (3-isocyanatopropyl)triethoxysilane and 140 µL (11 mmol) of N-(3-aminopropyl)imidazole were mixed in 2 mL of dioxane, and allowed to react overnight at room temperature under magnetic stirring. 1 g of protonated clay mineral was then

added to this reaction mixture, and the resulting slurry refluxed at 80°C overnight. The slurry was centrifuged and the residue washed sequentially with dioxane, deionized water and then freeze-dried.

The synthesized Imi-APTS spacer (0.70 mL) was dissolved in 0.30 mL of deuterated chloroform ($CDCl_3$) for the ^{1}H and ^{13}C NMR spectra acquisition. Kaolinite and montmorillonite functionalized with Imi-APTS spacer were characterized by: DRIFT-IR, ^{13}C- and ^{29}Si- CPMAS-NMR spectroscopies.

Immobilization of Mn(TDCPPS)Cl on spacer-functionalized clay minerals

Both K and M clay minerals (100 mg) functionalized with Imi-APTS were added with 5 mL of deionized water containing different amounts of Mn(TDCPPS)Cl (0.30, 0.40, and 10.00 mg) and the suspensions stirred overnight at room temperature. The solid residue was separated by centrifugation and exhaustively washed with a 1 M NaCl solution and deionized water for removing un-bonded Mn(TDCPPS)Cl. The amount of Mn(TDCPPS)Cl leached from the support was quantified by measuring the amount of Mn-porphyrin removed in the successive washings by UV-Vis spectroscopy. The adducts between Imi-APTS-functionalized clay minerals and Mn-porphyrin were, finally, freeze-dried.

In order to investigate the nature of the interaction between the metal-porphyrin and spacer-functionalized clay minerals (i.e. covalent or electrostatic bonds), a control represented by unfunctionalized K and M clay minerals was similarly prepared by employing 5 mL of a aqueous solution containing 0.30 mg of Mn(TDCPPS)Cl.

Liquid-state NMR spectroscopy

Liquid-state NMR measurements were conducted on a 400 MHz Bruker Avance spectrometer, equipped with a 5 mm Bruker BBI (Broad Band Inverse) probe, working at ^{13}C and ^{1}H frequencies of 100.6 and 400.13 MHz, respectively, at a temperature of 298 +/- 1 K.

^{13}C-NMR spectrum was acquired with 10 s of thermal equilibrium delay and a 90° pulse length of 12.64 us. An 80 ms length Waltz16 decoupling scheme, with around 15.6 dB as power level, was employed to decouple carbon from proton nuclei. The spectrum was acquired with 400 transients and 32768 time domain points.

The spectral width of ^{13}C NMR spectrum was 200 ppm (20124.6 Hz). The free induction decay (FID) was multiplied by 1.5 Hz exponential factor, without zero filling. The spectrum was baseline corrected and processed by Bruker Topspin Software (v.1.3).

Solid-state NMR spectroscopy

Carbon-13 cross-polarization magic angle spinning nuclear magnetic resonance (^{13}C-CPMAS-NMR) spectra were obtained with a 300 MHz Bruker Avance spectrometer equipped with a 4mm wide-bore MAS probe, operating at 75.47 MHz on the carbon and with a rotor spin rate of 13000±1 Hz. A recycle time of 1 s and an acquisition time of 33 ms were used. The ^{29}Si-CPMAS-NMR spectra were obtained similarly to those of carbon but operating at 59.63 MHz on the silicon with a rotor spin rate of 5000±1 Hz, and a recycle time of 5 s.

DRIFT spectroscopy

Diffuse reflectance infrared (DRIFT) spectra were measured on a Perkin-Elmer Spectrum-One FT-IR spectrometer in the 4000-600 cm^{-1} range. Both un- and functionalized clay minerals samples were prepared by mixing 10 mg of sample with 90 mg of KBr in an agate mortar. Spectra were acquired with 8 scans. Automatic subtraction of water, smoothing, and base line correction was achieved by the Perkin-Elmer Spectrum 5.0 FTIR software.

UV-Vis spectroscopy

UV-Vis spectra of Mn(TDCPPS)Cl and of the washings of adducts between Imi-APTS-functionalized clay minerals and Mn(TDCPPS)Cl, were recorded using an Perkin Elmer Lambda 25 UV/Vis Spectrometer at λ_{max} = 467.4 nm.

3.3 Catechol coupling under biomimetic catalysis

Cathecol oxidation under heterogeneous catalysis

The oxidation reaction of catechol was conducted under stirring and at room temperature. The reaction mixture consisted in a final volume of 3 mL of 0.25 M potassium phosphate buffered at pH=6 and containing 50 ppm of catechol, Mn(TDCPPS)Cl immobilized on spacer-functionalized solid K or M in the μmoles amount described hereafter, and 5 mM of H_2O_2. The following reaction and control mixtures were prepared in triplicate: (a) 12 μmol of Mn(TDCPPS)Cl immobilized on Imi-APTS-functionalized K; (b) 12 μmol of Mn(TDCPPS)Cl immobilized on Imi-APTS-functionalized M; (c) 240 μmol of Mn(TDCPPS)Cl immobilized on Imi-APTS-functionalized K; (d) 240 μmol of Mn(TDCPPS)Cl immobilized on Imi-APTS-

functionalized M; (e) without the immobilized catalyst; (f) without the immobilized catalyst and with 12 μmol of free water-soluble Mn(TDCPPS)Cl; (g) without the immobilized catalyst and with 240 μmol of free water-soluble Mn(TDCPPS)Cl. The progress of the oxidative coupling of catechol was followed by reverse-phase HPLC analysis.

The multicyclic use of immobilized catalysts was verified by employing them in sequential reaction cycles: 2 cycles for the 12 μmol immobilized catalysts, and 3 cycles for the 240 μmol immobilized catalysts. At the end of each cycle, the solid heterogeneous catalyst was separated by centrifugation from the supernatant, washed extensively with deionized water, and freeze-dried before being used in the subsequent reaction cycle.

HPLC analysis

A Perkin-Elmer LC 200 pump, equipped with a 10 μL sample loop on a 7125 Rheodyne Rotary Injector, a Sphereclone 5 ODS column (250 mm_4.6 mm, 5 μm, Phenomenex), and two detectors in series (a Perkin-Elmer LS-3B fluorescence spectrometer and a Gilson 118 UV/Vis detector) was used to follow the disappearance of catechol in oxidation reaction. The UV detector was set at 280 nm, whereas the excitation/emission wavelengths set in the fluorescence detector were 278/360 nm. The eluent solution was a binary phase of methanol (A) and 0.75% trifluoroacetic acid solution in MilliQ grade water (Millipore) (v/v) (B), that was pumped at 1.2 mL min^{-1} with the following gradient mode: eluent A was held for 1 min at 2%, increased to 100% in 10 min, decreased to 2% in 3 min, and finally held at 2% for 3 min. A Perkin-Elmer TotalChrom 6.2.0 software was employed to acquire and elaborate

chromatograms. Quantitative analysis was based on a calibration curve built with known concentrations of catechol in the 10-50 ppm interval.

3.4 Oxidative polymerization of HA and determination of humic molecular size by HPSEC analysis

Oxidative polymerization of HA by heterogeneous biomimetic catalysis

Control and reaction mixtures of HA were prepared by re-dissolving 0.95 mg of potassium humate in 1.9 mL of a 0.25 M potassium phosphate buffer at pH=6. These mixtures were modified as follows: (a) addition of 0.01 mmol of H_2O_2 (100 μL of a 0.1 M freshly prepared solution) and then incubation in darkness to prevent photo-oxidation and to obtain a second control; (b) irradiation with UV light to obtain a third control; (c) as in (a) and with 12 μmol of Mn(TDCPPS)Cl immobilized on Imi-APTS-functionalized kaolinite, otherwise referred to as K-Imi-APTS-MnP, as heterogeneous catalyst (9.06 mg of a 3.44×10^{-3} $mg^{MnP}/mg^{K\text{-}Imi\text{-}APTS\text{-}MnP}$) to induce the oxidative polymerization reaction; (d) as in (b) and with the same amount of heterogeneous catalyst as above. For all mixtures, the final volume was 2 mL.

The mixtures were stirred at room temperature and analyzed at different reaction times: 2, 24 and 72 h by HPSEC. Therefore, at each reaction time, the supernatant was passed through a 0.45-μm filter and injected in the HPSEC system. Both control and reaction mixtures were then added with glacial acetic acid until pH 3.5 and re-analyzed by HPSEC.

HPSEC analysis

The HPSEC system consisted of a Shimadzu LC-10-ADVP pump and two detectors in series: a UV-Vis variable wavelength detector (Perkin-Elmer LC-295) operating at 280 nm and a refractive index detector (Fisons Instruments, Refractomonitor IV). A rheodyne rotary injector, equipped with a 100-μL sample loop, was used to load the calibration standard and humic solutions. A Polysep-GFC-P-3000 600×7.5 mm i.d. column and a Polysep-GFC-P-3000 75×7.5 mm i.d. pre-column (Phenomenex, Inc., CA, USA) were used. The elution flow rate was set to 0.6 mL min^{-1} for an eluting solution made of 0.1 M NaH_2PO_4, buffered at pH 7, filtered through Millipore 0.45 μm, and degassed with He. The column total (Vt=15.47 mL) and void volume (V0=6.29 mL) were measured with water and a Blue dextran (Mw=2.000 kDa) aqueous solution, respectively, and calibrated with polystyrene sulphonates of known molecular weights (130.000, 32.000, 16.800, 6.780, and 4.300 Da, Polymer Standard Service, Germany). Size-exclusion chromatograms for both the UV and RI detectors were evaluated by using a Unipoint Gilson Software to record automatically each run.

Statistical analysis

ANOVA and the Tukey's test were used to compare apparent weight-averaged molecular weight (Mw) values obtained for control and reaction mixtures, and difference was considered to be significant at the level of $P \leq 0.05$. Mw values were calculated from triplicate HPSEC chromatograms, as previously reported (Piccolo et al., 2005).

3.5 Synthesis and isolation of cucurbit[n]urils (Chapter 7)

Synthesis of glycolurils

A modification of the literature procedure was used here (Buschmann et al., 1997). To a solution of urea (600 g, 10 mol) in water (1 L) was added a 40% aqueous solution of glyoxal (500 g, 3.45 mol) and HCl 35% (86 mL). The resulting solution was heated at 85-90°C until a heavy precipitate was formed. The reaction mixture was allowed to cool to room temperature and filtered. The filter cake was washed with copious amounts of water (2 L) followed by acetone to remove residual water. The resulting white solid (397.5 g) was dried under high vacuum and analyzed by ^{1}H–NMR spectroscopy in d-DMSO.

Synthesis of cucurbit[n]urils

Powdered glycoluril (795 g, 5.59 mol) and powdered paraformaldehyde (354 g, 11.20 mol) were mixed thoroughly. An ice-cold concentrated HCl solution (1130 mL) was added gradually while stirring with a large glass rod. After the addition of about 100 mL, stirring was no longer possible as the reactants were transformed into a brick-like material. At this point the reaction becomes highly exothermic. The heterogeneous mixture was gradually heated to 80°C over 2.5 hours and maintained at that temperature for an additional 2.5 hours at which point all of the solid had dissolved. The homogeneous red solution was heated to 100°C for 14 hours. After cooling to room temperature, the purification process was begun.

Purification of CB[5], CB[6], CB[7], CB[8]

The reaction mixture was evaporated to a minimum volume (~ 600 mL). This slurry was poured into water (2.5 L). The solid, containing CB[6], CB[7] and CB[8], was collected by filtration. The filtrate was evaporated to about 600 mL and then slowly poured into a mixture of MeOH (3 L) and water (200 mL) with vigorous stirring. After stirring overnight, the precipitate, containing mainly CB[7] and CB[5], was isolated by filtration.

Separation procedure to isolate CB[7] from CB[5]/CB[7] mixture

CB[5]/CB[7] mixture (less than 4 mmol CB[7]), containing a small amount of CB[6], was dissolved in 250 mL of water and centrifuged to remove CB[6]. The 1-alkyl-3-methylimidazolium [C_4mim]Br ionic liquid guest (4.5 mmol) was added to CB[5]/CB[7] aqueous solution to obtain CB[7]-[C_4mim]Br complex in solution. NH_4PF_6 salt (4.5 mmol) was added to CB[7]-[C_4mim]Br complex and, centrifuging the system, a CB[7]-[C_4mim]PF_6 complex was formed, which had poor solubility and precipitated from water. The CB[7]-[C_4mim]PF_6 complex was isolated, leaving an aqueous solution of CB[5], whose cavity was too small to bind the [C_4mim] guest, and it was readily recrystalized to give pure CB[5]. CB[7]-[C_4mim]PF_6 complex was washed with methanol. The final key step in this purification method for CB[7] was the dissociation of the CB[7]-[C_4mim]PF_6 complex based on a solid state ion exchange. [C_4mim]Br (5 mmol) was added to CB[7]-[C_4mim]PF_6 complex in 200 mL of water and it was heated up at 80°C until most solid dissolved for converting back CB[7]-[C_4mim]PF_6 to the bromide counter ion. CB[7]-[C_4mim]Br aqueous solution was concentrated, mixed with 150 mL of methanol at 80°C for 20 minutes, cooled down at

room temperature and centrifuged to obtain CB[7]-[C_4mim]Br solid. Then, CB[7]-[C_4mim]Br complex was dissociated through a solid state metathesis reaction with NH_4PF_6 (6 mmol) upon refluxing in 70 mL of DCM for 5-6 days. As the reaction proceeded, [$C_n$mim]PF_6 was formed and immediately partitioned into DCM leaving NH_4Br and CB[7] in the solid state since they were insoluble in DCM. The selective removal of [$C_n$mim]PF_6 from the reaction state provided the required driving force for a quantitative decomplexation. The resulting CB[7] solid was filtered and washed with methanol, dried and analyzed by ^{1}H NMR in D_2O. CB[7]'s purity was then checked by elemental analysis.

Synthesis of 2[Npmim]Br

1-Methylimidazole (10 mmol) and 2-(bromomethyl)naphthalene (10 mmol) were mixed in 70 mL of toluene. The reaction mixture was allowed to react refluxing at 135°C under magnetic stirring overnight. Then the reaction mixture was cooled to room temperature; the top layer of the mixture was removed and the flask which contained reaction was refilled with fresh toluene and heated to 135°C for 1 hour. When the system was cooled down the bottom layer was washed with ether several times. Finally the gel-like product was dryed in the oven at 45°C and characterized by ^{1}H NMR in d-DMSO.

Separation procedure to isolate CB[8] from CB[6]/CB[8] mixture

CB[6]/CB[8] mixture (18% CB[8] ~ 0.25 mM) was dissolved in 200 mL of water with 2[Npmim]Br (0.46 mM) and centrifuged to obtain CB[8]-2[Npmim]Br complex in aqueous solution. NH_4PF_6 salt (0.5 mM) was added to CB[8]-2[Npmim]Br

and the system was centrifuged to isolate CB[8]-2[Npmim]PF_6 solid. In order to convert back CB[8]-2[Npmim]PF_6 to the bromide counter ion, 2[Npmim]Br (0.2 g) was added to CB[8]-2[Npmim]PF_6 complex in 200 mL of water and it was heated up at 80°C for 1-2 hours. The obtained not clear solution was cooled down and then extracted with DCM. CB[8]-2[Npmim]Br white milky solution was concentrated to 30-40 mL heating up at 80°C, then, 150 mL of methanol was added and the reaction mixture was cooled down at room temperature under stirring to obtain CB[8]-2[Npmim]Br solid. The solid was isolated by centrifuge washing with methanol. Then, CB[8]-2[Npmim]Br complex was dissociated through a solid state metathesis reaction with NH_4PF_6 (0.1 g) upon refluxing in 50 mL of DCM for 5-6 days. Finally, the reaction mixture was centrifuged and washed with DCM. The resulting CB[8] solid was washed with methanol and water by centrifuge, dryed and analyzed by ^{1}H NMR in 20% DCl. CB[8]'s purity was checked by elemental analysis.

^{1}H-NMR spectroscopy

Liquid-state ^{1}H-NMR measurements were conducted on a 400 MHz Bruker Avance spectrometer, equipped with a 5 mm QNP probe, working at ^{1}H frequency of 400.13 MHz at a temperature of 300.2 +/- 1 K. ^{1}H-NMR spectra were acquired with 1 s of thermal equilibrium delay and a 90° pulse length of 9.4 μs. The spectrum was acquired with 16 transients, 2 dummy scans and 32768 time domain points. The free induction decay (FID) was multiplied by 0.3 Hz exponential factor, without zero filling. The spectrum was baseline corrected and processed by Bruker Topspin Software (v.1.3).

CHAPTER 4 - ENHANCED CATECHOL OXIDATION BY HETEROGENEOUS BIOMIMETIC CATALYSTS IMMOBILIZED ON CLAY MINERALS

ENHANCED CATECHOL OXIDATION BY HETEROGENEOUS BIOMIMETIC CATALYSTS IMMOBILIZED ON CLAY MINERALS

Assunta Nuzzo[1] and Alessandro Piccolo[1,2*]

Dipartimento di Scienze del Suolo, della Pianta, dell'Ambiente e delle Produzioni Animali, Università di Napoli Federico II, Via Università, 100, 80055 Portici, Italy

Centro Interdipartimentale di Ricerca sulla Risonanza Magnetica Nucleare per l'Ambiente, l'Agroalimentare ed i Nuovi Materiali (CERMANU), Via Università, 100, 80055 Portici, Italy

*Corresponding author. E-mail: Alessandro.piccolo@unina.it

Manuscript to be submitted to *J. Mol. Catal. A – Chem.*

Abstract

Two novel heterogeneous biomimetic catalysts were synthesized by immobilizing a meso-tetra(2,6-dichloro-3-sulfonatophenyl)porphyrinate of manganese (III) chloride [Mn(TDCPPS)Cl] on both kaolinite (K) and montmorillonite (M) clay minerals, previously functionalized with a molecular spacer ending with an imidazole group, whose nitrogen atom firmly coordinated the metal in the porphyrin ring. The clay functionalization by a 3-(1-imidazolyl)propylcarbamoyl-3′-aminopropyl-triethoxysilane spacer was proved by DRIFT-IR, ^{13}C- and ^{29}Si-CPMAS-NMR spectroscopies, and the percent of Mn(TDCPPS)Cl immobilized by the spacer coordination was calculated. The activity of the novel catalysts was evaluated in the oxidative coupling reaction of catechol in the presence of H_2O_2 as oxygen donor. The rate of catechol oxidation

catalyzed by both K and M heterogeneous catalysts was about four times as rapid as that catalyzed by the free manganese-porphyrin in a homogeneous catalysis, and depended on the percent of catalyst immobilized on the clay minerals. Moreover, the activity of the heterogeneous catalysis remained effective for at least two sequential reaction cycles, although a rate decrease in catechol transformation was observed. These results showed that the immobilization of a biomimetic catalyst on clay minerals increased the catalytic efficiency and allowed the catalyst recycling and reuse for additional reactions. Metal-porphyrins immobilized on clay minerals through flexible spacers may represent an environment-friendly tool to implement heterogeneous catalysis in the remediation of contaminated soils and waters.

Key-words: clay minerals, biomimetic catalysis, manganese-porphyrin, immobilization, catechol, oxidative coupling, hydrogen peroxide, heterogeneous

INTRODUCTION

In recent years, the interest in using of metal-porphyrins as biomimetic catalysts has been progressively growing (Que & Tolman, 2008). Special attention has been focused on the ability of metal-porphyrins to act as models of cytochrome P450 monooxygenases by catalyzing several oxidation reactions of organic and inorganic compounds, under mild conditions (Que & Tolman, 2008; Mansuy, 2008) including the hydroxylation of alkanes (Traylor et al., 1992; Nam et al., 2003) and epoxidation of alkenes (Traylor et al., 1993; Rebelo et al., 2006).

Due to instability of natural metal-porphyrins under oxidizing conditions and poor water solubility (Crestini et al., 1999), attention has been devoted in developing

synthetic metal-porphyrins that are more resistant to degradative oxidation and active in aqueous media. These properties have been usually achieved by adding electron-withdrawing groups (such as sulphonatophenyl groups) in the meso positions of metal-porphyrins (Rocha-Gonsalves & Pereira, 1996). Furthermore, sterically and/or electronically protected polychlorinated or polyfluorinated porphyrins were synthesized to increase their stability (Cui et al., 1993; Crestini et al., 1999; Crestini et al., 2004). Although efficient homogeneous catalytic systems based on metal-porphyrins have been developed, (Mohajer & Solati, 2006; Stephenson. & Bell, 2006; Crestini. et al., 1999), it has been found that, when metal-porphyrins are free in solution, side reactions, such as their self-destruction or formation of μ–oxo porphyrin dimers, limit considerably their catalytic activity (Meunier, 1994). Moreover, their use in solution cannot be economically affordable on large scale due to difficul catalyst separation, recovery and recycling.

To overcome the described limitations of homogeneous catalysis, immobilization of metal-porphyrins on adequate supports has been attempted by different mechanisms: adsorption (Meunier, 1994; Bedioui, 1995; Nakagaki et al., 2002; Crestini et al., 2004), ion exchange (Mifune et al., 2005), or covalent bond formation (Martinez-Lorente et al., 1996; Kitamura et al., 2006). The supported catalysts are environmentally friendly systems, since allow easy separation of catalytic products and catalyst reuse for further reactions, with both operational and economic advantages. Several materials have been used to support metal-porphyrins and, thus, to make heterogeneous catalysts: organic synthetic polymers such as polystyrene (Barbaro & Liguori, 2009), biopolymers or inorganic matrices such as silica (Zucca et al., 2007; Martinez-Lorente et al., 1996), porous vycor glass (Nakagaki et al., 2002), zeolites

(Bedioui et al., 1995). Metal-porphyrins are reported to be immobilized on montmorillonites by adsorption (Machado et al., 2002; Crestini et al., 2004) or in the interlayer surfaces of kaolinites through their grafting by ethanolamine (Bizaia et al., 2009). However, to our knowledge, there are no earlier attempts to immobilize a metal-porphyrin on a clay mineral support functionalized with a molecular spacer, whose terminal coordinates the metal center of the catalyst, and long enough to minimize unspecific support/porphyrin interactions.

Heterogeneous catalysis through a metal-porphyrin immobilized on a spacer-functionalized clay mineral may efficiently enhance the oxidative coupling of phenols and phenol-containing humic molecules in aqueous media. The free-radical mechanism of action of metal-porphyrins is induced by an oxygen donor that produces high-valent metal-oxo species which, in turn, oxidize phenolic moieties (Sheldon, 1994). Unstable free radicals are formed and then stabilized by mutual couplings, thus resulting into polyphenols consisting of covalently linked phenylene and oxyphenylene units (Oguchi et al., 1999; Kurioka et al., 1994). Oxidative coupling reactions of reactive phenols under biomimetic catalysis have been applied to study the transformation of natural molecules in the environment (Sánchez-Cortés et al., 2001; Dec et al., 2001) and remove toxic phenolic compounds from soils and wastewaters (Aktaş & Tanyolaç, 2003). Biomimetic catalyst such as iron- and manganese-porphyrins were shown to successfully catalyze oxidative coupling reactions of humic monomeric precursors such as catechol, caffeic and *p*-coumaric acid (Šmejkalová & Piccolo, 2006; Šmejkalová et al., 2006; Šmejkalová et al., 2007), as well as dissolved humic substances under a chemical oxidant (Piccolo et al., 2005) or under photooxidation (Šmejkalová & Piccolo, 2005). However, no investigation has been reported up to date on oxidative coupling

reactions of humic phenols and humic matter catalyzed by immobilized biomimetic catalysts.

The aim of this work was, therefore, to immobilize a meso-tetra(2,6-dichloro-3-sulfonatophenyl)porphyrinate of manganese(III) chloride [Mn(TDCPPS)Cl] on both kaolinite and montmorillonite clay minerals, following their functionalization with a molecular spacer to allow a coordinative interaction with Mn. The efficiency of the catalysis induced by the immobilized Mn-porphyrin and the H_2O_2 oxidant, was studied by following the disappearance of catechol, an aromatic constituent of humic substances, and comparing the catalytic rate with that obtained by homogeneous catalysis.

EXPERIMENTAL SECTION

Materials. All solvents and reagents used were of Reagent Grade (Sigma-Aldrich), and used without further purification. The procedure for the synthesis of water-soluble meso-tetra(2,6-dichloro-3-sulfonatophenyl)porphyrinate of manganese(III) chloride [Mn(TDCPPS)Cl], has been described elsewhere (Piccolo et al., 2005). The clay minerals used in this work were a kaolinite (K) from Washington County, Georgia, USA, and a Na-montmorillonite (M) from Crook County, Wyoming, USA. Both have been supplied by the Source Clay Minerals Repository (University of Missouri, USA).

Functionalization of clay minerals. Clay minerals were first protonated by suspending 30 g of either K or M in 1 L of a 2 M HCl solution and stirred for 48 hours. This procedure was repeated 3 times. After proton saturation, clay minerals were first

dialyzed (3500 Da dialysis tubes) against water until pH 5-6, and then freeze-dried and pulverized. The molecular spacer, 3-(1-imidazolyl)propylcarbamoyl-3′-aminopropyl-triethoxysilane (Imi-APTS), was synthesized as described elsewhere (Zucca et al., 2007). Briefly, 260 µL (10 mmol) of (3-isocyanatopropyl)triethoxysilane and 140 µL (11 mmol) of N-(3-aminopropyl)imidazole were mixed in 2 mL of dioxane, and allowed to react overnight at room temperature under magnetic stirring. 1 g of protonated clay mineral was then added to this reaction mixture, and the resulting slurry refluxed at 80°C overnight. The slurry was centrifuged and the residue washed sequentially with dioxane, deionized water and then freeze-dried.

Immobilization of Mn(TDCPPS)Cl on spacer-functionalized clay minerals. Both K and M clay minerals (100 mg) functionalized with Imi-APTS were added with 5 mL of deionized water containing different amounts of Mn(TDCPPS)Cl (0.30, 0.40, and 10.00 mg) and the suspensions stirred overnight at room temperature. The solid residue was separated by centrifugation and exhaustively washed with a 1 M NaCl solution and deionized water for removing un-bonded Mn(TDCPPS)Cl. The amount of Mn(TDCPPS)Cl leached from the support was quantified by measuring the amount of Mn-porphyrin removed in the successive washings through spectrophotometric measurements with a UV-Vis spectrophotometer (Perkin Elmer Lambda 25) at λ_{max} = 467.4 nm.

The adducts between Imi-APTS-functionalized clay minerals and Mn-porphyrin were, finally, freeze-dried. A control represented by unfunctionalized K and M clay minerals was similarly prepared by employing 5 mL of a aqueous solution containing 0.30 mg of Mn(TDCPPS)Cl.

Cathecol oxidation under heterogeneous catalysis. The oxidation reaction of catechol was conducted under stirring at room temperature. The reaction mixture consisted in a final volume of 3 mL of 0.25 M potassium phosphate buffered at pH=6 and containing 50 ppm of catechol, Mn(TDCPPS)Cl immobilized on spacer-functionalized solid K or M in the μmoles amount described hereafter, and 5 mM of H_2O_2. The following reaction and control mixtures were prepared: (a) 12 μmol of Mn(TDCPPS)Cl immobilized on Imi-APTS-functionalized K; (b) 12 μmol of Mn(TDCPPS)Cl immobilized on Imi-APTS-functionalized M; (c) 240 μmol of Mn(TDCPPS)Cl immobilized on Imi-APTS-functionalized K; (d) 240 μmol of Mn(TDCPPS)Cl immobilized on Imi-APTS-functionalized M; (e) without the immobilized catalyst; (f) without the immobilized catalyst and with 12 μmol of free water-soluble Mn(TDCPPS)Cl; (g) without the immobilized catalyst and with 240 μmol of free water-soluble Mn(TDCPPS)Cl. The multicycle use of immobilized catalysts was verified by employing them in sequential reaction cycles: 2 cycles for the 12 μmol immobilized catalysts, and 3 cycles for the 240 μmol immobilized catalysts. At the end of each cycle, the solid heterogeneous catalyst was separated from the supernatant, washed extensively with deionized water, and freeze-dried before being used in the subsequent reaction cycle.

During each reaction cycle, the progress of the oxidative coupling of catechol was followed by reverse-phase HPLC analysis. HPLC system consisted of a Perkin-Elmer LC 200 pump, equipped with a 10 μL sample loop on a 7125 Rheodyne Rotary Injector, a Sphereclone 5 ODS column (250 mm_4.6 mm, 5 μm, Phenomenex), and two detectors in series (a Perkin-Elmer LS-3B fluorescence spectrometer and a Gilson 118 UV/Vis detector). The UV detector was set at 280 nm, whereas the excitation/emission

wavelengths set in the fluorescence detector were 278/360 nm. The eluent solution was a binary phase of methanol (A) and 0.75% trifluoroacetic acid solution in MilliQ grade water (Millipore) (v/v) (B), that was pumped at 1.2 mL min^{-1} with the following gradient mode: eluent A was held for 1 min at 2%, increased to 100% in 10 min, decreased to 2% in 3 min, and finally held at 2% for 3 min. A Perkin-Elmer TotalChrom 6.2.0 software was employed to acquire and elaborate chromatograms. Quantitative analysis was based on a calibration curve built with known concentrations of catechol in the 10-50 ppm interval.

NMR spectra. Liquid-state ^{13}C-NMR spectrum of Imi-APTS spacer was obtained on a 400 MHz Bruker Avance spectrometer, equipped with a 5 mm Bruker BBI (Broad Band Inverse) probe, working at a ^{13}C frequency of 100.6 MHz at 298±1 °K, and acquired with 10 s thermal equilibrium delay, 12.64 μs of 90° pulse length, and a 80 ms long proton decoupling Waltz16 sequence, with around 15.6 dB power level. The spectrum was acquired with 400 transients and 32k time domain. For a ^{13}C NMR spectral width of 200 ppm (20124.6 Hz), the spectra free induction decay (FID) was multiplied by 1.5 Hz exponential factor, without zero filling, baseline corrected and processed by Bruker Topspin Software (v.1.3). The Imi-APTS spacer (0.70 mL) was dissolved in 5 mm NMR quartz tube using 0.30 mL of deuterated chloroform ($CDCl_3$).

Carbon-13 cross-polarization magic angle spinning nuclear magnetic resonance (^{13}C-CPMAS-NMR) spectra were obtained with a 300 MHz Bruker Avance spectrometer equipped with a 4mm wide-bore MAS probe, operating at 75.47 MHz on the carbon and with a rotor spin rate of 13000±1 Hz. A recycle time of 1 s and an acquisition time of 33 ms were used. The ^{29}Si-CPMAS-NMR spectra were obtained similarly to those of

carbon but operating at 59.63 MHz on the silicon with a rotor spin rate of 5000±1 Hz, and a recycle time of 5 s.

Infrared spectra. Diffuse reflectance infrared (DRIFT) spectra were measured on a Perkin-Elmer Spectrum-One FT-IR spectrometer in the 4000-600 cm^{-1} range. Both un- and functionalized clay minerals samples were prepared by mixing 10 mg of sample with 90 mg of KBr in an agate mortar. Spectra were acquired with 8 scans, automatic subtraction of water, smoothing, and base line correction.

RESULTS AND DISCUSSION

Heterogeneous biomimetic catalysts. A structural representation of the adduct between a clay mineral surface and Mn(TDCPPS)Cl via the Imi-APTS spacer is shown in Figure 1. The evidence that K and M was actually functionalized with the Imi-APTS spacer was reached by DRIFT-IR and ^{13}C- and ^{29}Si-CPMAS-NMR spectroscopies.

The infrared spectrum of the spacer alone (Figure 2B) shows the characteristic absorptions of the spacer molecule (Bellamy, 1975): the stretching (3500-3000 cm^{-1}) and bending (1562 cm^{-1}) vibrations of the N-H amide groups, the weak CH stretching band at 3112 cm^{-1} due to the aromatic imidazole ring, the stretchings of CH_3 (2971 cm^{-1}) and CH_2 (2925 cm^{-1}) groups in the spacer chain with the corresponding skeletal bendings at around 1450 cm^{-1}, and, finally, the 1391 cm^{-1} absorption for the symmetric deformation of CH_3 groups. Moreover, the stretching vibrations for the Si-O-C bonds are visible in the 1100-1000 cm^{-1} range. When the spacer was covalently linked to a clay mineral surface (only the K DRIFT-IR spectrum is shown in Figure 2A), the

corresponding infrared spectrum (Figure 2C) became deprived of the 2971 and 1391 cm^{-1} bands, thereby proving that the ethoxyl groups in the spacer had reacted with the surface silanols and aluminols of clay minerals.

Figure 3B shows the ^{13}C-CPMAS-NMR spectrum of montmorillonite functionalized with Imi-APTS, whose signals may be compared with those in the liquid-state ^{13}C-NMR spectrum for the spacer alone (Figure 3A) and identified as carbon nuclei in the spacer molecule. Upon clay mineral functionalization, the ^{13}C-CPMAS-NMR spectrum of M reveals the disappearance of signals at 17.9 and 57.97 ppm for the CH_3 and CH_2 nuclei, respectively, in the ethoxyl groups of the spacer (Figure 3A). The lack of these signals indicates that the reaction between the triethoxysilane group in Imi-APTS and the hydroxyl groups on the clay mineral surface had occurred.

The ^{29}Si-CPMAS-NMR spectra of M and K minerals before and after their functionalization with the spacer are reported in Figure 4. The spectra of unfunctionalized clay minerals show Si signals for the minerals crystalline structure, which are positioned at -90.99, -99.20, -107.50 ppm for montmorillonite (Figure 4A) and at -91.09 ppm for kaolinite (Figure 4C). After the reaction of minerals with Imi-APTS, the ^{29}Si-CPMAS-NMR spectra of both functionalized M (Figure B) and K (Figure D) reveal three additional signals due to the progressive formation of surface Si-O-Si siloxane bonds with the three ethoxyl groups of the spacer (Lee et al., 2005; Kahraman et al., 2006). In particular, the formation of single T^1 [R-$Si{\equiv}(OSi)(OCH_2CH_3)_2$], double T^2 [R-$Si{\equiv}(OSi)_2(OCH_2CH_3)$], and triple T^3 [R-$Si{\equiv}(OSi)_3$] siloxane bonds produced signals at around -50, -59, -67 ppm, respectively. These Si resonances confirm the occurred covalent linkages between the surface

mineral silanols/aluminols and the spacer ethoxyls, thereby proving the mineral functionalization.

The percent of Mn(TDCPPS)Cl catalyst immobilized on K and M clay minerals, before and after their functionalization with the imidazole-containing spacer, and as a function of the amount of added catalyst, is reported in Table 1. The manganese-porphyrin retained on the functionalized minerals, due to axial coordination between the spacer imidazole nitrogen and the Mn(III) within the porphyrin ring, was nearly quantitative at low amounts (0.3-0.4 mg) of catalyst in solution. This is because the occurred specific coordination between Mn(TDCPPS)Cl and the functionalized clay minerals was strong enough to prevent the bound catalyst to be removed away by simple washings. The role of the imidazole-containing spacer in strongly retaining the catalyst, appeared evident when the same low amount of dissolved Mn(TDCPPS)Cl was put in contact with the unfunctionalized clay minerals (Table 1). In that case, the catalyst, being only physically and unspecifically adsorbed on mineral surfaces, was washed away completely from M and, substantially, from K, by the washing operations following the adsorption reaction.

Catalyzed oxidative coupling of catechol. Metal-porphyrins, such as manganese-porphyrins, were shown to couple phenolic compounds by way of a radical mechanism. These catalysts are thought to undergo oxidation by producing high-valent metal-oxo species, which can catalyze the oxidation of phenols and produce free radicals (Groves et al., 1981; Sheldon, 1994). The generated radicals may then be quenched by spontaneous and multiple mutual couplings (Dec et al., 2001), thus resulting into oligo- or poly-mers of large molecular weights, low solubility, and increased stability against further biological degradation.

The catalytic activity of two heterogeneous catalysts, synthesized here as Mn(TDCPPS)Cl immobilized on spacer-functionalized K and M, was verified by following the coupling of catechol under H_2O_2 oxidation, through its disappearance from solution. No substrate oxidation was observed in absence of catalysts, while the catechol absorption by the clay minerals alone was negligible (not shown).

The UV-detected chromatograms of catechol subjected to the oxidation reaction catalyzed by two synthesized heterogeneous catalysts, revealed a significant decrease of the original substrate in a time-course of about 5 h (not shown). The concomitant fluorescence-detected chromatograms showed peaks of reaction products, which eluted at larger elution volumes than catechol, thereby implying a less polar structure than the original substrate (not shown). These additional peaks detected by fluorescence may well be catechol oligomers formed during the oxidative coupling catalyzed by the heterogeneous biomimetic catalysts. This agrees with previous findings indicating that phenolic monomers are coupled into oligomers under oxidative catalysis (Šmejkalová & Piccolo, 2006; Šmejkalová et al., 2006). Moreover, some of these fluorescent peaks observed here, first increased and then declined during the time course of the catalyzed catechol oxidation, thus suggesting that they represent intermediate and unstable reaction products, which become susceptible of further oxidation, as previously observed (Šmejkalová & Piccolo, 2006).

The values for the first-order rate constants calculated for the catechol oxidation catalyzed by either 12 or 240 μmol for both the free Mn(TDCPPS)Cl catalyst and that immobilized on the spacer-functionalized K and M clay minerals are reported in Table 2. The initial 5 hours reaction time was selected to avoid interferences which may decrease reaction rates, such as oxidant decomposition or catalyst inactivation. The

initial reaction period was fitted according to the first-order rate equation, $\ln c_t/c_0 = -kt$, where c_0 and c_t (mol dm^{-3}) represent the substrate concentration in solution at the reaction time 0 and t (sec), respectively, and k (sec^{-1}) represents the first-order rate constant. First-order rate reactions were implied by the straight lines ($R^2 \geq 0.9$) obtained by plotting $\ln (c_t)$ as a function of reaction time.

The catalyst immobilized on both K and M accelerated the reaction rate of the catechol oxidation about four times in respect to the rate found for the free catalyst. Moreover, the oxidative coupling reaction was affected by the amount of metal-porphyrin immobilized on the clay minerals. In fact, the rate of catechol oxidation catalyzed by 240 μmol of Mn(TDCPPS)Cl immobilized on spacer-functionalized K and M (Table 2) was about six times larger than for the reaction catalyzed by 12 μmol of immobilized catalysts. This indicates that the more concentrated the catalyst, the larger was the number of active sites participating to the reaction and the amount of substrate that underwent oxidative couplings (Šmejkalová & Piccolo, 2006).

Moreover, the clay minerals containing the immobilized catalyst were used sequentially in a second and a third oxidation reaction. The first-order rate constants measured for such progressive reaction cycles (Table 2) showed that 12 μmol of catalyst immobilized on either K or M were still active in the second cycle, though its activity was reduced to that of the free catalyst. Similarly, 240 μmol of catalyst immobilized on K provided the same rate constant as for the free catalyst in the second cycle, but the rate substantially decreased in the third cycle. Conversely, 240 μmol of Mn(TDCPPS)Cl immobilized on M catalyzed the catechol oxidation reaction in the second cycle to a rate that was twice as fast as the free catalyst, loosing much of its activity only in the third cycle. These results thus indicate that heterogeneous adducts formed between Imi-

APTS-functionalized K and M clay minerals and Mn(TDCPPS)Cl were more efficient catalysts than the homogeneous Mn(TDCPPS)Cl catalyst. The catalytic activity of heterogeneous biomimetic catalysts significantly increased by 4-5 times in comparison to the free homogeneous catalyst and remained effective for at least two sequential reaction cycles, though with a decrease in reaction rate.

CONCLUSIONS

This work has shown that an active biomimetic catalyst such as manganese-porphyrin can be immobilized on clay minerals such as kaolinte and motmorillonite, wich are common soil constituents. The activity of the immobilized catalyst was several times larger than that observed by the free catalyst in solution towards the oxidative coupling reaction of a humic phenolic monomer, such as catechol. Such increased activity must be attributed to the method of immobilization of the catalyst on the clay minerals, which was through a spacer linked to the mineral surface by covalent bonds. The flexible spacer chain coordinated the manganese in the catalyst porphyrin ring by a imidazole dative nitrogen atom present at the spacer free end. Our results suggest that heterogeneous catalysts formed by immobilizing oxidative metal-porphyrins on the surface of spacer-functionalized soil minerals may be usefully employed as tools to reduce the toxicity of polluting phenols in contaminated soils and wastewaters.

Acknowledgments

A.N. conducted this work in partial PhD fulfillment of the Doctorate School "Valorizzazione e Gestione delle Risorse Agroforestali" of the Università di Napoli Federico II.

References

Aktaş, N.; Tanyolaç, A. Reaction conditions for laccase catalyzed polymerization of catechol. *Bioresour. Technol.* 2003, *87*, 209-214.

Barbaro, P.; Liguori, F. Ion exchange Resins: Catalyst Recovery and Recycle. *Chem. Rev.* 2009, *109*, 515-529.

Bedioui, F. Zeolite-encapsulated and clay-intercalated metal porphyrin, phthalocyanine and Schiff-base complexes as models for biomimetic oxidation catalysts: an overview. *Coord. Chem. Rev.* 1995, *144*, 39-68.

Bellamy, L. J. *The infra-red Spectra of Complex Molecules*; Third edition; Chapman and Hall, London, 1975.

Bizaia, N.; de Faria, E. H.; Ricci, G. P.; Calefi, P. S.; Nassar, E. J.; Castro, K. A. D. F.; Nakagaki, S.; Ciuffi, K. J.; Trujillano, R.; Vicente, M. A.; Gil, A.; Korili, S. A. Porphyrin-kaolinite as Efficient Catalyst for Oxidation Reactions. *ACS Appl. Mater. Interfaces* 2009, *1*, 2667-2678.

Crestini, C.; Saladino, R.; Tagliatesta, P.; Boschi, T. Biomimetic degradation of lignin and lignin model compounds by synthetic anionic and cationic water soluble manganese and iron porphyrins. *Bioorgan. Med. Chem.* 1999, *7*, 1897-1905.

Crestini, C.; Pastorini, A.; Tagliatesta, P. Metalloporphyrins immobilized on montmorillonite as biomimetic catalysts in the oxidation of lignin model compounds. *J. Mol. Catal. A - Chem.* 2004, *208*, 195-202.

Cui, F.; Wijesekera, T.; Dolphin, D.; Farrel, R.; Skerker, P. Biomimetic degradation of lignin. *J. Biotechnol.* 1993, *30*, 15-26.

Dec, J.; Haider, K.; Bollag, J.-M. Decarboxylation and demethoxylation of naturally occurring phenols during coupling reactions and polymerization. *Soil Sci.* 2001, *166*, 660-671.

Dec, J.; Haider, K.; Bollag, J.-M. Release of substituents from phenolic compounds during oxidative coupling reactions. *Chemosphere* 2003, *52*, 549-556.

Groves, J. T.; Haushalter, R. C.; Nakamura, M.; Nemo, T. E.; Evans, B. J. High-valent iron-porphyrin complexes related to peroxidase and cytochrome P-450. *J. Am. Chem. Soc.* 1981, *103*, 2884-2886.

Kahraman, M. V.; Kuğu, M.; Menceloğlu, Y.; Kayaman-Apohan, N.; Güngör, A. The novel use of organo alkoxy silane for the synthesis of organic-inorganic hybrid coatings. *J. Non-Crist. Solids* 2006, *352*, 2143-2151.

Kitamura, Y.; Mifune, M.; Hino, D.; Yokotani, S.; Saito, M.; Tsukamoto, I.; Iwado, A.; Saito, Y. Peroxidase-like catalytic activity of Mn- and Fe-tetrakis(4-carboxyphenyl)porphines bound to aminopropyl-glass bead in oxidative reaction of heterocyclic amines. *Talanta* 2006, *69*, 43-47.

Kurioka, H.; Komatsu, I.; Uyama, H.; Kobayashi, S. Enzymatic oxidative polymerization of alkylphenols. *Macromol. Rapid Commun.* 1994, *15*, 507-510.

Lee, T.-M.; Ma, C-C M.; Hsu, C.-W.; Wu, H.-L. Effect of molecular structures and mobility on the thermal and dynamical mechanical properties of thermally cured epoxy-bridged polyorganosiloxanes. *Polymer* 2005, *46*, 8286-8296.

Machado, A. M.; Wypych, F.; Drechsel, S. M.; Nakagaki, S. Study of the Catalytic Behavior of Montmorillonite/Iron(III) and Mn(III) Cationic Porphyrins *J. Colloid Interface Sci.* 2002, *254*, 158-164.

Mansuy, D. Biocatalysis and substrate chemodiversity: Adaptation of aerobic living organisms to their chemical environment. *Catal. Today* 2008, *138*, 2-8.

Martinez-Lorente, M.A.; Battioni, P.; Kleemiss, W.; Batoli, J.F.; Mansuy, D. Manganese porphyrins covalently bound to silica and montmorillonite K10 as efficient catalysts for alkene and alkane oxidation by hydrogen peroxide. *J. Mol. Catal. A - Chem.* 1996, *113*, 343-353.

Meunier, B. In: *Metalloporphyrins Catalyzed Oxidations;* Montanari, F.; Casella L.; Eds.; Kluwer Academics Publishers: Dordrecth, 1994; pp. 11-19.

Mifune, M.; Hino, D.; Sugita, H.; Iwado, A.; Kitamura, Y.; Motohashi, N.; Tsukamoto, I.; Saito, Y. Peroxidase-Like Catalytic Activity of Anion-Exchange Resins Modified with Metal-Porphyrins in Oxidative Reaction of Hetrocyclic Amines with Hydrogen Peroxide. *Chem. Pharm. Bull.* 2005, *53*, 1006-1010.

Mohajer, D.; Solati, Z. Rapid and highly selective epoxidation of alkenes by tetrabutylammonium monopersulfate in the presence of manganese meso-tetrakis(pentafluorophenyl)porphyrin and tetrabutylammonium salts or imidazole co-catalysts. *Tetrahedron Lett.* 2006, *47*, 7007-7010.

Nakagaki, S.; Ramos, A.R.; Benedito, F.L.; Peralta-Zamore, P.G.; Zarbin, A.J.G. Immobilization of iron porphyrins into porous vycor glass: characterization and study of catalytic activity. *J. Mol. Catal. A - Chem.* 2002, *185*, 203-210.

Nam, W.; Park, S.E.; Lim, I.K.; Lim, M.H.; Hong, J.; Kim, J. First Direct Evidence for Stereospecific Olefin Epoxidation and Alkane Hydroxylation by an Oxoiron(IV) Porphyrin Complex. *J. Am. Chem. Soc.* 2003, *125*, 14674-14675.

Oguchi, T.; Tawaki, H.; Uyama, S.-i.; Kobayashi, S. Soluble polyphenol. *Macromol. Rapid Commun.* 1999, *20*, 401-403.

Piccolo, A.; Conte, P.; Tagliatesta, P. Increased conformational rigidity of humic substances by oxidative biomimetic catalysis. *Biomacromolecules* 2005, *6*, 351-358.

Powell, M.F.; Pai, E.F.; Bruice, T.C. Study of (Tetraphenylporphinato)manganese(111)-Catalyzed Epoxidation and Demethylation Using p-Cyano-N,N-dimethylanilinNe -Oxide as Oxygen Donor in a Homogeneous System. Kinetics, Radiochemical Ligation Studies, and Reaction Mechanism for a Model of Cytochrome P-450. *J. Am. Chem. Soc.* 1984, *106*, 3277-3285.

Que, L., Jr.; Tolman, W. B. Biologically inspired oxidation catalysis. *Nature* 2008, *455*, 333-340.

Rocha-Gonsalves, A.M.A.; Pereira, M.M. State of the art in the development of biomimetic oxidation catalysts. *J. Mol. Catal. A - Chem.* 1996, *113*, 209-221.

Rebelo, S.L.H.; Gonçalves, A.R.; Pereira, M.M.; Simoes, M.M.Q.; Neves, M.G.P.M.S.; Cavaleiro, J.A.S. Epoxidation reactions with hydrogen peroxide activated by a novel heterogeneous metalloporphyrin catalyst. *J. Mol. Catal. A - Chem.* 2006, *256*, 321-323.

Sánchez-Cortés, S.; Francioso, O.; García-Ramos, J.V.; Ciavatta, C.; Gessa, C. Catechol polymerization in the presence of silver surface. *Colloids Surf., A* 2001, *176*, 177-184.

Sheldon, R. A. Oxidations catalysis by metalloporphyrins. In *Metalloporphyrins in Catalytic Oxidations*; Sheldon, R. A.; Ed.; Marcel Dekker Inc.: New York, 1994.

Šmejkalová, D.; Piccolo, A. Enhanced Molecular Dimension of a Humic Acid Induced by Photooxidation Catalyzed by Biomimetic Metalporphyrins. *Biomacromolecules* 2005, *6*, 2120-2125.

Šmejkalová, D.; Piccolo, A. Rates of Oxidative Coupling of Humic Phenolic Monomers Catalyzed by a Biomimetic Iron-Porphyrin. *Environ. Sci. Technol*. 2006, *40*, 1644-1649.

Šmejkalová, D.; Piccolo, A.; Spiteller, M. Oligomerization of Humic Phenolic Monomers by Oxidative Coupling under Biomimetic Catalysis *Environ. Sci. Technol*. 2006, *40*, 6955-6962.

Šmejkalová, D.; Conte, P.; Piccolo, A. Structural Characterization of Isomeric Dimers from the Oxidative Oligomerization of Catechol with a Biomimetic Catalyst. *Biomacromolecules* 2007, *8*, 737-743.

Stephenson., N.A.; Bell, A.T. The influence of substrate composition on the kinetics of olefin epoxidation by hydrogen peroxide catalyzed by iron(III) [tetrakis(pentafluorophenyl)] porphyrin. *J. Mol. Catal. A - Chem.* 2006, *258*, 231-235.

Traylor, T.G.; Hill, K.W.; Fann, W.P.; Tsuchiya, S.; Dunlap, B.E. Aliphatic Hydroxylation Catalyzed by Iron(111) Porphyrins. *J. Am. Chem. Soc.* 1992, *114*, 1308-1312.

Traylor, T.G.; Tsuchiya, S.; Byun, Y.S.; Kim, C. High-Yield Epoxidations with Hydrogen Peroxide and tert-Butyl Hydroperoxide Catalyzed by Iron(111) Porphyrins: Heterolytic Cleavage of Hydroperoxides. *J. Am. Chem. Soc.* 1993, *115*, 2775-2781.

Zucca, P.; Mocci, G.; Rescigno, A.; Sanjust, E. 5,10,15,20-Tetrakis(4-sulfonato-phenyl)porphine-Mn(III) immobilized on imidazole-activated silica as a novel lignin-peroxidase-like biomimetic catalyst. *J. Mol. Catal. A - Chem.* 2007, *278*, 220-227.

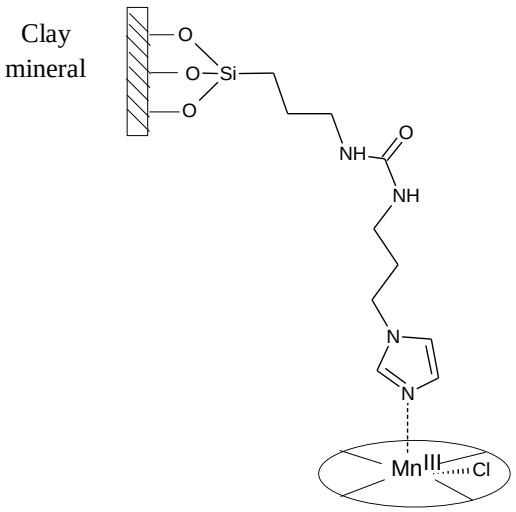

Figure 1. Schematic representation of the coordinative interaction between the imidazole terminal of the spacer covalently linked to clay mineral surfaces and [Mn(TDCPPS)Cl].

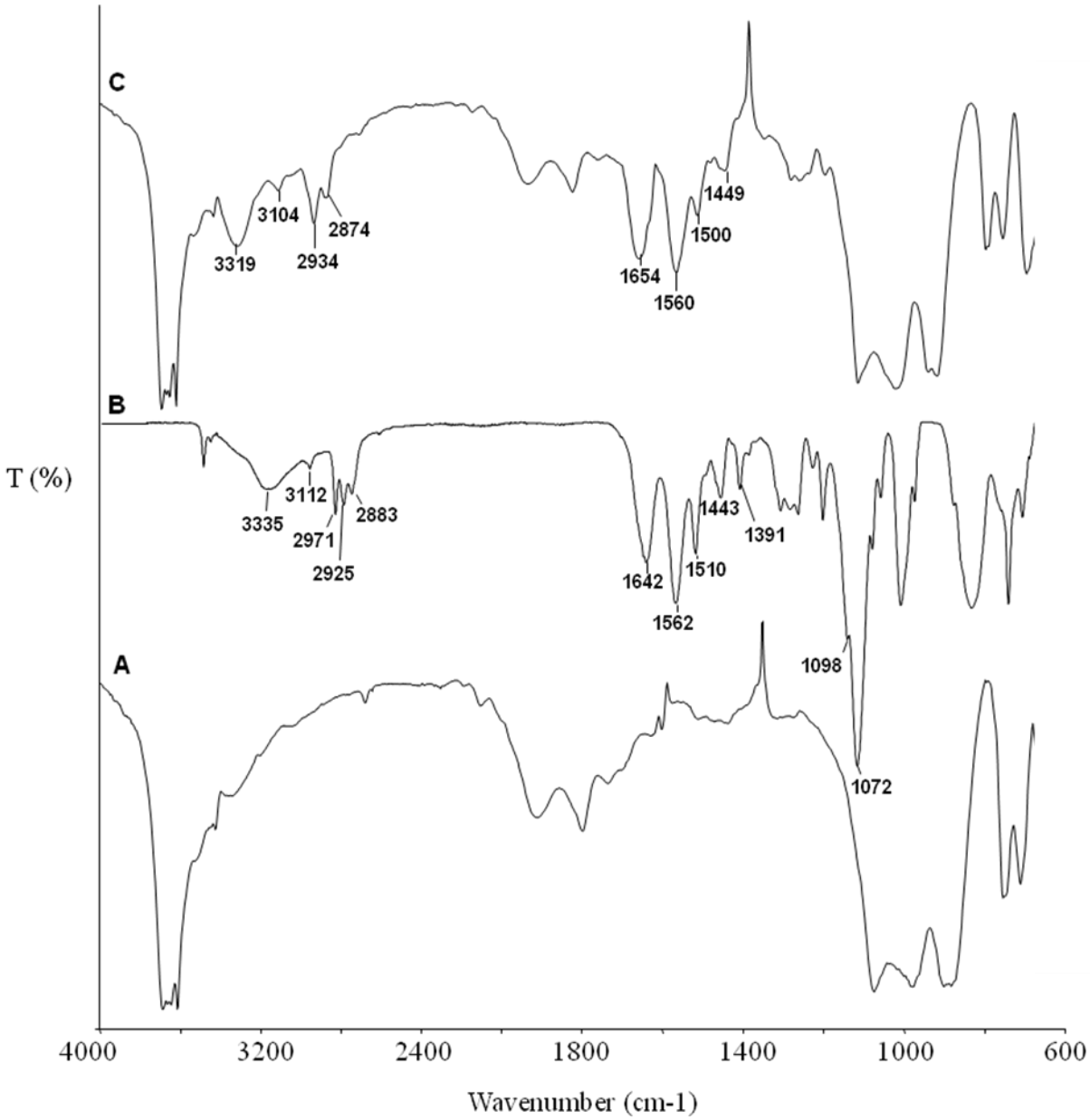

Figure 2. Infrared absorption spectra of: K clay mineral (A); Imi-APTS (B); K functionalized with Imi-APTS (C).

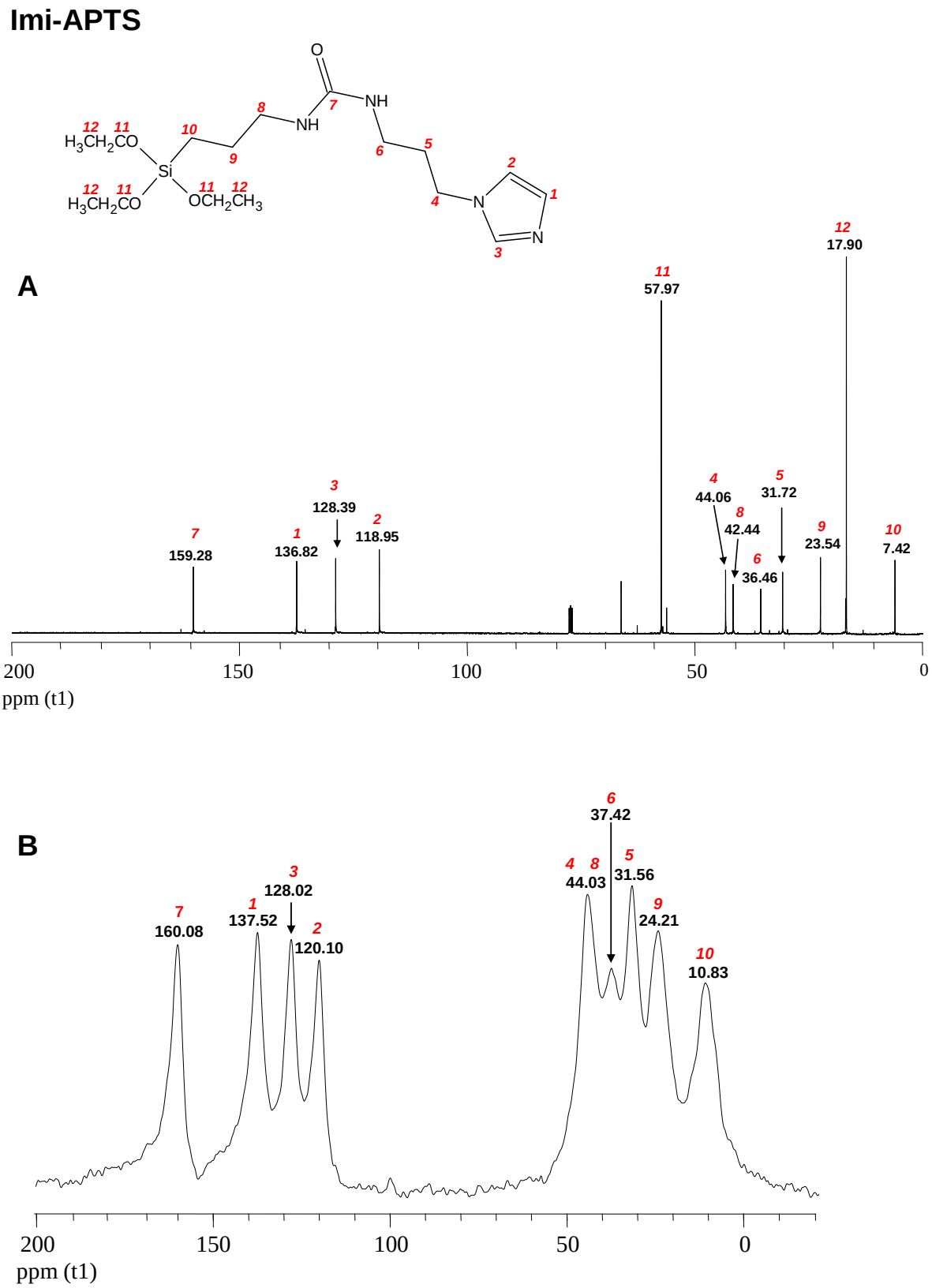

Figure 3. Liquid-state ^{13}C NMR spectrum of Imi-APTS spacer (A); solid-state ^{13}C-CPMAS-NMR spectrum of M clay mineral functionalized with Imi-APTS spacer (B). Numbers on spectral signals correspond to different carbons in the Imi-APTS structure.

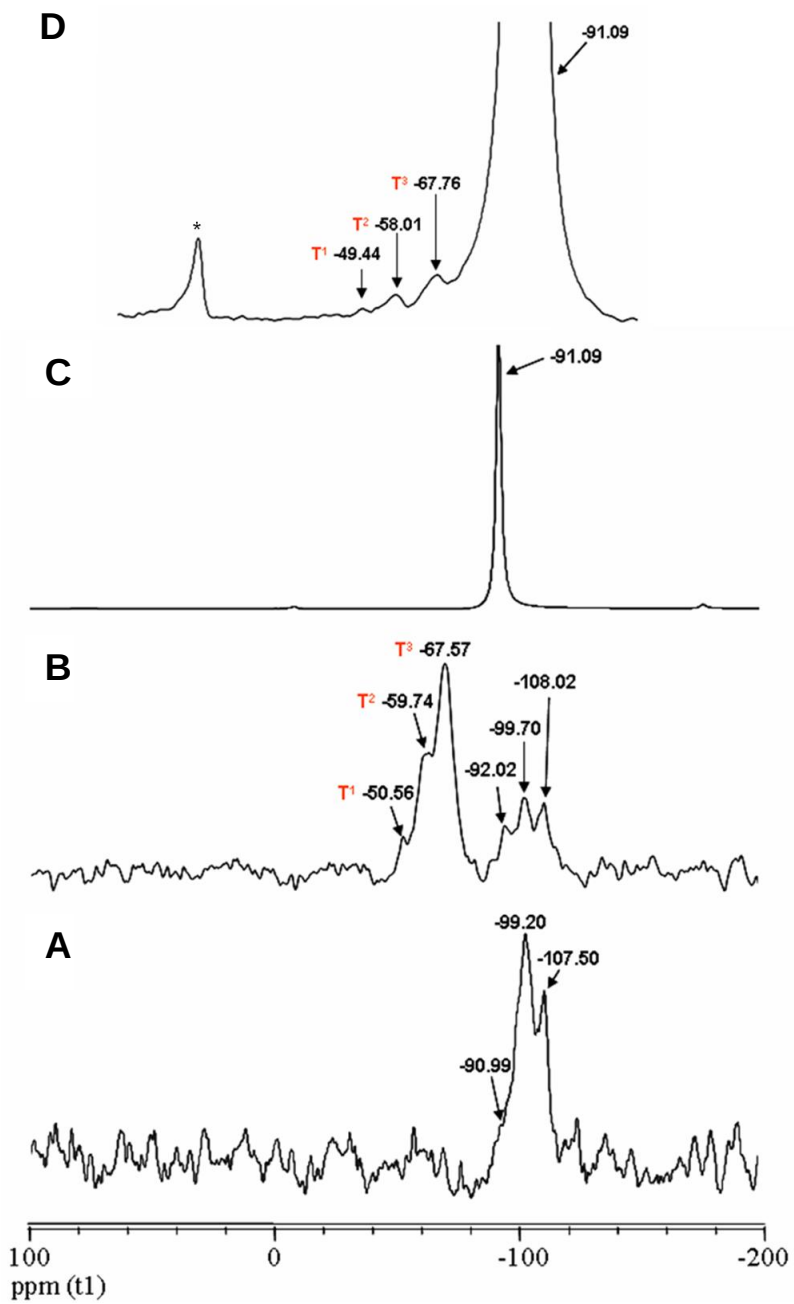

Figure 4. ^{29}Si-CPMAS-NMR spectra of: unfunctionalized M (A); M functionalized with Imi-APTS (B); unfunctionalized K (C); expanded spectrum of K functionalized with Imi-APTS (D); (* = side band).

Table 1. Percentage (%) of catalyst immobilized on kaolinite (K) and montomorillonite (M) clay minerals before and after functionalization with Imi-APTS spacer, as a function of increasing addition (mg) of Mn(TDCPPS)Cl.

Clay Minerals	Added Mn(TDCPPS)Cl (mg)		
	0.3	0.4	10.0
	Immobilized Mn(TDCPPS)Cl (%)		
K	33.3	ND	ND
K-Imi-APTS	96.7	85.0	84.1
M	0.00	ND	ND
M-Imi-APTS	90.0	97.5	85.5

ND. Not Determined

Table 2. First-Order Rate Constants[a] ($k \times 10^{-5}$ sec^{-1} ± SD) for catechol oxidation catalyzed by different amounts (μmol) of free or immobilized Mn(TDCPPS)Cl catalyst, for subsequent reaction cycles.

Catalyst Amount (μmol)	12		240		
Cycle number	1	2	1	2	3
Mn(TDCPPS)Cl	0.84± 0.12		5.06± 1.98		
K-Imi-APTS/Mn(TDCPPS)Cl	3.12± 0.65	1.03± 0.74	20.41±3.65	4.82± 0.85	1.27± 0.55
M-Imi-APTS/Mn(TDCPPS)Cl	3.30± 0.26	0.96± 0.05	21.69± 2.51	10.41± 2.40	1.73± 0.30

SD = Standard deviation.

a. 5 h reaction course.

CHAPTER 5 - OXIDATIVE POLYMERIZATION OF A HUMIC ACID BY HETEROGENEOUS BIOMIMETIC CATALYSIS

OXIDATIVE POLYMERIZATION OF A HUMIC ACID BY HETEROGENEOUS BIOMIMETIC CATALYSIS

Assunta Nuzzo[1] and Alessandro Piccolo[1,2*]

Dipartimento di Scienze del Suolo, della Pianta, dell'Ambiente e delle Produzioni Animali, Università di Napoli Federico II, Via Università, 100, 80055 Portici, Italy

Centro Interdipartimentale di Ricerca sulla Risonanza Magnetica Nucleare per l'Ambiente, l'Agroalimentare ed i Nuovi Materiali (CERMANU), Via Università, 100, 80055 Portici, Italy

*Corresponding author. E-mail: alessandro.piccolo@unina.it

Manuscript in preparation for *Environ. Sci. Technol.*

Abstract

The oxidative coupling reaction of humic molecules was conducted with either chemical (H_2O_2) or UV-light oxidation under heterogeneous biomimetic catalysis. The meso-tetra(2,6-dichloro-3-sulfonatophenyl)porphyrinate of manganese(III) chloride [Mn-(TDCPPS)Cl] biomimetic catalyst was immobilized on kaolinite clay mineral through a molecular spacer with a terminal imidazole to hold a coordination bond with the metal in the porphyrin ring. The change in molecular size of a dissolved humic acid subjected to oxidative coupling by the catalyst supported on spacer-functionalized kaolinite was followed by high-performance size exclusion chromatography (HPSEC) with UV-Vis and refractive index (RI) detectors in series. Both detectors indicated that

the heterogeneous biomimetic catalysis favoured the polymerization by significantly increasing the apparent weight-average molecular weight (*Mw*) of the humic acid. However, the RI detector showed that the humic mass increased within 72 h of reaction time, whereas absorbance variations due to altered mutual arrangements among humic chromophores made results by UV detector less consistent with increasing reaction time. HPSEC chromatograms recorded again after lowering the pH of polymerized humic samples from 6 to 3.5 by acetic acid addition, showed that their molecular size was significantly modified as compared to control. Both UV and RI detectors indicated an increased size distribution for the polymerized humic matter undergone heterogeneous catalysis under either chemical or UV-light oxidation. These findings suggest that the heterogeneous biomimetic catalysis promoted the stabilization of loosely bound humic conformations by forming new intermolecular covalent bonds during oxidative coupling. The fact that no significant differences were found between chemical and light-induced oxidation indicates a multiple potential application of the kaolinite-supported heterogeneous catalysis in either the remediation of contaminated soils and waters or the control of natural organic matter transformation.

Keywords: oxidative polymerization, heterogeneous catalysis, biomimetic catalyst, humic matter

INTRODUCTION

Humic substances (HS) are ubiquitous natural compounds arising from the chemical and biological degradation of plant and animal residues (Piccolo, 1996). HS are crucial in ecosystems because they regulate the global carbon and nitrogen cycles,

the growth of plants and microorganisms, the fate and transport of anthropogenic compounds and heavy metals, and the stabilization of soil structure (Piccolo, 1996; Nardi et al., 2002). A general consensus regards HS as supramolecular associations of heterogeneous and relatively small (<1000 Da) molecules, which are held together in only apparently large molecular sizes by weak forces, such as hydrogen and hydrophobic bonds (Piccolo, 2002), and whose conformations can be disrupted by the action of weak organic acids (Piccolo et al., 1999).

The supramolecular understanding of HS suggests the possibility of increasing the molecular size and complexity by polymerizing aromatic humic molecules with the formation of new intermolecular covalent bonds. Such polymerization would chemically stabilize humic matter and enhance its resistance to biotic and abiotic degradation (Piccolo et al., 2000; Cozzolino & Piccolo, 2002). Previous works have shown that humic superstructures were oxidatively polymerized in the presence of biomimetic catalysts, such as water-soluble iron- and manganese-porphyrins, by using chemical oxidation (Piccolo et al., 2005) or photo-oxidation (Šmejkalová & Piccolo, 2005). Biomimetic catalysts promote oxidative coupling reactions between humic phenols via a free radical mechanism (Shaik et al., 2007), induced by oxygen activation. Singlet oxygen donors, such as hydrogen peroxide, are required to produce highly reactive oxoiron(IV)-porphyrin radical cations which show strong oxidizing ability. These radical species in turn oxidize phenolic substrate giving unstable free radicals which spontaneously couple into molecules of larger mass. In the case of photo-oxidation, light leads instead to the formation of metal(II)-porphyrin. The reduced metal may then coordinate a dissolved dioxygen molecule, generating metal(III)-peroxyalkyl complex, which can undergo subsequent reactions resulting in a formation of reactive

oxoferryl porphyrinate π cation radicals, as in the case of chemical oxidation (Šmejkalová & Piccolo, 2005).

Metal-porphyrins successfully catalyzed the oxidative polymerization of phenols and phenol-containing humic matter in aqueous solution by either chemical or photo-oxidation (Šmejkalová & Piccolo, 2006; Šmejkalová et al., 2006). Oxidation of humic phenolic precursors, such as catechol and coumaric and caffeic acids, catalyzed by biomimetic metal-porphyrins, produced up to tetramer olygomers (Šmejkalová et al., 2006). The occurrence of the photo-polymerization of humic molecules catalyzed by a water-soluble iron-porphyrin *in situ* in soil was also proved on three different soils. The catalyzed photo-polymerization induced not only an increased soil structural stability but also a reduction of soil respiration, due to the larger microbial recalcitrance of polymerized soil organic matter (Piccolo et al., 2011). Thus, an *in situ* photo-catalyzed polymerization of soil humus may have important ecological and environmental consequences, such as promoting carbon sequestration in soil and reducing CO_2 emission from soil. Furthermore, an enhanced molecular mass of humic matter would facilitate soil particles association into larger soil aggregates, thus improving soil physical quality and resistance to soil erosion (Tisdall & Oades, 1982; Baldock & Skjemstad, 2000).

Nevertheless, a limitation of the use of water-soluble metal-porphyrins in soil systems may be accounted to their high solubility in water that may reduce reactivity on soil surface due to excessive down-leaching, especially in loosely textured soils. Moreover, the instability of free water-soluble metal-porphyrins under oxidizing conditions may be an additional limitation of homogeneous catalysis. Conversely, the immobilization of these biomimetic catalysts on adequate supports may be a winning

strategy to reduce both their oxidative degradation (Nuzzo & Piccolo, 2011) and their loss by leaching. Moreover, supported heterogeneous catalysts seem advantageous in comparison with their homogeneous counterparts, since they allow an easier catalyst recovery and recycling, thereby enhancing overall cost-efficiency. We showed that the use of two heterogeneous biomimetic catalysts, synthesized by immobilizing Mn-porphyrin on both spacer-functionalized kaolinite and montmorillonite, successfully enhanced the rate of oxidative coupling of catechol in respect to corresponding homogeneous catalyst (Nuzzo & Piccolo, 2011).

The aim of this work was hence to verify whether the heterogeneous catalysis was capable to oxidatively polymerize a humic acid isolated from lignin. The catalytic activity was exerted by a Mn-porphyrin immobilized on a kaolinite support previously functionalized with a molecular spacer. The humic polymerization was induced by either H_2O_2 or photo-oxidation, and the changes in molecular size followed by size-exclusion chromatography.

EXPERIMENTAL SECTION

Materials. All solvents and reagents used were of Reagent Grade (Sigma-Aldrich), and used without further purification. The synthesis of the meso-tetra(2,6-dichloro-3-sulfonatophenyl)porphyrinate of Mn(III) chloride [Mn(TDCPPS)Cl] has been previously described (Piccolo et al., 2005). The humic acid (HA) was extracted from North Dakota leonardite (Mammoth, Int. Chem. Co., USA), purified, and turned into potassium humate, as described elsewhere (Fontaine & Piccolo, 2011). The kaolinite

(K) clay mineral originated from Washington County, Georgia (USA), and was supplied by the Source Clay Minerals Repository (University of Missouri, USA).

Functionalization of kaolinite. Kaolinite (30 g) was first protonated by suspending in 1 L of a 2 M HCl solution and stirred for 48 hours. After proton saturation, K was first dialyzed (3500 Da dialysis tubes) against water until pH 5-6, and, then, freeze-dried and pulverized. The molecular spacer, 3-(1-imidazolyl)propylcarbamoyl-3′-aminopropyl-triethoxysilane (Imi-APTS), was synthesized as described elsewhere (Zucca et al., 2007). Briefly, 260 µL (10 mmol) of (3-isocyanatopropyl)triethoxysilane and 140 µL (11 mmol) of N-(3-aminopropyl)imidazole were mixed in 2 mL of dioxane, and allowed to react overnight at room temperature under magnetic stirring. Protonated K (1 g) was then added to this reaction mixture, and the resulting slurry refluxed at 80°C overnight. The slurry was centrifuged and the residue washed sequentially with dioxane, deionized water and then freeze-dried.

Immobilization of Mn(TDCPPS)Cl on spacer-functionalized kaolinite. Imi-APTS-functionalized K (100 mg) was added with 5 mL of deionized water containing 0.40 mg of Mn(TDCPPS)Cl and the suspensions stirred overnight at room temperature. The solid residue was separated by centrifugation and exhaustively washed with a 1 M NaCl solution and deionized water for removing un-bonded Mn(TDCPPS)Cl. The amount of Mn(TDCPPS)Cl leached from the support was quantified by measuring the amount of Mn-porphyrin removed in the successive washings through spectrophotometric measurements with a UV-Vis spectrophotometer (Perkin Elmer Lambda 25) at λ_{max} = 467.4 nm. The adduct between Imi-APTS-functionalized K and Mn-porphyrin was, finally, freeze-dried.

Oxidative polymerization of HA by heterogeneous biomimetic catalysis. A control solution contained 0.95 mg of potassium humate dissolved in 1.9 mL of a 0.25 M potassium phosphate buffer at pH=6, while other control and reaction mixtures were obtained by modifying this humic solution as it follows: (a) a second control made by adding 0.01 mmol of H_2O_2 (100 μL of a 0.1 M freshly prepared solution) and then incubated in darkness to prevent photo-oxidation; (b) a third control made by subjecting the humic solution to a UV light irradiation at 254 nm in a UV-Vis spectrophotometer (Perkin Elmer Lambda 25); (c) the same solution as in (a) but added with a Imi-APTS-functionalized kaolinite on which 12 μmol of Mn-porphyrin was immobilized (K-Imi-APTS-MnP), as heterogeneous catalyst (9.06 mg of a 3.44×10^{-3} $mg^{MnP}/mg^{K\text{-}Imi\text{-}APTS\text{-}MnP}$); (d) the same solution as in (b) and with the same amount of heterogeneous catalyst as that added in (c). For all mixtures, the final volume was 2 mL. The mixtures were stirred at room temperature, and after 2, 24 and 72 h of reaction times, were centrifuged at 10,000 rpm and the supernatant injected in the HPSEC system after filtering through a 0.45-μm filter. Then, the same supernatants were added with glacial acetic acid until a pH 3.5 was reached and analyzed again by HPSEC.

HPSEC. The HPSEC system consisted of a Shimadzu LC-10-ADVP pump and two detectors in series: a UV-Vis variable wavelength detector (Perkin-Elmer LC-295) operating at 280 nm and a refractive index detector (Fisons Instruments, Refractomonitor IV). A rheodyne rotary injector, equipped with a 100-μL sample loop, was used to load the calibration standard and humic solutions. A Polysep-GFC-P-3000 600×7.5 mm i.d. column and a Polysep-GFC-P-3000 75×7.5 mm i.d. pre-column (Phenomenex, Inc., CA, USA) were used. The elution flow rate was set to 0.6 mL min^{-1} for an eluting solution made of 0.1 M NaH_2PO_4, buffered at pH 7, filtered through

Millipore 0.45 μm, and degassed with He. The column total (Vt=15.47 mL) and void volume (V0=6.29 mL) were measured with water and a Blue dextran (Mw=2.000 kDa) aqueous solution, respectively, and calibrated with polystyrene sulphonates of known molecular weights (130.000, 32.000, 16.800, 6.780, and 4.300 Da, Polymer Standard Service, Germany). Size-exclusion chromatograms for both the UV and RI detectors were automatically recorded and evaluated by using a Unipoint Gilson Software for each run. Calculation of the apparent weight-average molecular weight values (*Mw*) was done by the method of Yau et al. (1979) using the following equation:

$$Mw = \sum_{i=1}^{N} hi(Mi) \Big/ \sum_{i=1}^{N} hi$$

where *hi* is the height of the size exclusion chromatogram of each sample eluted at volume *i*. The relative standard deviation of calculated values among triplicates of each chromatogram varied to a maximum of 7%.

Liquid- and solid-state ^{13}C-NMR NMR spectroscopy. Liquid-state ^{13}C-NMR spectrum of Imi-APTS spacer was obtained on a 400 MHz Bruker Avance spectrometer, equipped with a 5 mm Bruker BBI (Broad Band Inverse) probe, working at a ^{13}C frequency of 100.6 MHz at 298±1 °K, and acquired with 10 s thermal equilibrium delay, 12.64 □s of 90° pulse length, and a 80 ms long proton decoupling Waltz16 sequence, with around 15.6 dB power level. The spectrum was acquired with 400 transients and 32k time domain. For a ^{13}C NMR spectral width of 200 ppm (20124.6 Hz), the spectra free induction decay (FID) was multiplied by 1.5 Hz exponential factor, without zero filling, baseline corrected and processed by Bruker

Topspin Software (v.1.3). The Imi-APTS spacer (0.70 mL) was dissolved in 5 mm NMR quartz tube using 0.30 mL of deuterated chloroform ($CDCl_3$).

Carbon-13 cross-polarization magic angle spinning nuclear magnetic resonance (^{13}C-CPMAS-NMR) spectra were obtained with a 300 MHz Bruker Avance spectrometer equipped with a 4mm wide-bore MAS probe, operating at 75.47 MHz on the carbon and with a rotor spin rate of 13000±1 Hz. A recycle time of 1 s and an acquisition time of 33 ms were used.

Statistical analysis. ANOVA and the Tukey's test were used to compare apparent weight-averaged molecular weight (Mw) values obtained for control and reaction mixtures, and difference was considered to be significant at the level of $P \leq 0.05$. Mw values were calculated from triplicate HPSEC chromatograms, as previously reported (Piccolo et al., 2005).

RESULTS AND DISCUSSION

The structural characterization of the Imi-APTS-functionalized kaolinite was conducted earlier by both infrared and solid-state ^{29}Si-CPMAS-NMR spectroscopy (Nuzzo & Piccolo, 2011). It was found that the reaction between the spacer ethoxyl groups and silanol and aluminol groups on the clay mineral surface had occurred, and the Imi-APTS spacer resulted covalently bound to kaolinite.

Here, we employed ^{13}C-NMR spectroscopy to further prove the kaolinite functionalization with the Imi-APTS molecular spacer. The liquid-state ^{13}C-NMR spectrum of Imi-APTS spacer alone (Figure 1A) was compared with the solid-state ^{13}C-

CPMAS-NMR spectrum of kaolinite after functionalization with the Imi-APTS spacer (Figure 1B). The functionalization reaction determined the disappearance of signals at 17.9 and 57.97 ppm due to CH_3 and CH_2 nuclei , respectively, in the spacer triethoxysilane group, thereby proving that the silicon atom in Imi-APTS had reacted with the silanols and aluminols of the kaolinite surface. As shown earlier (Nuzzo & Piccolo, 2011), the Imi-APTS spacer-functionalized kaolinite was used as support for the stable immobilization of the Mn(TDCPPS)Cl catalyst. This was reached through formation of an axial coordination between the imidazole nitrogen contained in the spacer and the metal center of Mn-porphyrin.

The oxidative polymerization of HA, catalyzed by the K-Imi-APTS-MnP adduct, was evaluated by measuring the apparent weight-average molecular weights (*Mw*) of the reaction solutions subjected to either H_2O_2 or UV-light oxidation. The *Mw* values obtained from the corresponding UV-detected size-exclusion chromatograms are shown in Figure 2. These values for control HA and control HA exposed to UV light did not vary significantly within the 72 h of reaction time (not shown) . Conversely, the humic solutions subjected for 2 h to the polymerization reaction under heterogeneous catalysis revealed significantly larger *Mw* values than control HA for both H_2O_2 and light-induced oxidation.

This significant enhancement was maintained after 24 h of reaction time, with a *Mw* value for HA subjected to the catalyzed polymerization under photo-oxidation greater than for H_2O_2 oxidation (Figure 2). However, after 72 h of reaction time, the *Mw* value for HA undergone heterogeneous catalysis with H_2O_2 oxidation became similar to that of control, whereas that for control HA treated with only H_2O_2 increased significantly. For the same reaction time, the *Mw* value of humic matter subjected to

heterogeneous catalysis under photo-oxidation was, instead, still larger than control, and did not differ significantly from control HA added with H_2O_2.

In UV-detected chromatograms the intensities of chromatographic peaks depend only on the presence of chromophores in HA, rather than on the totality of humic components. Moreover, the molecular absorptivity is due to a multitude of heterogeneous chromophores, whose cumulative absorbance may change when the mutual orientation of the transition dipole moments of neighboring chromophores is altered (Piccolo, 2002). Such hypochromic/hyperchromic effect may explain the inconsistent results observed for the catalyzed polymerization reactions at 72 h of reaction time. In fact, the re-orientation of the chromophoric dipole moments induced by the formation of new covalent bonds during the polymerization reaction, may cause unpredictable variations in the absorbance of size-exclusion chromatographic peak. To overcome this limitation, a refractive index (RI) detector has been employed to evaluate the variation of humic molecular sizes (Piccolo, 2002; Song et al., 2010). In fact, the RI detector enables to follow the overall mass distribution of humic matter, including non-cromophore-bearing components, thereby providing more reliable information on the conformational changes of the bulk humic mass induced by chemical variations (Piccolo et al., 2003).

The *Mw* values calculated from the RI-detected size exclusion chromatograms for the humic material subjected to catalyzed oxidative polymerization are shown in Figure 3. At all reaction times, the oxidative polymerization of humic matter under heterogeneous biomimetic catalysis with either H_2O_2 oxidation or UV-light irradiation, increased significantly the *Mw* values in respect to control HA. The catalyzed chemical oxidation invariably showed larger *Mw* values than control HA, while this was true for

the catalyzed photo-polymerization at only 72 h of reaction time. These results showed that the heterogeneous catalysis enhanced the HA molecular dimensions by both oxidation methods, though the H_2O_2 oxidation resulted more rapid than photo-oxidation.

The solutions of both control and polymerized HA mixtures were then brought to pH 3.5 with glacial acetic acid and injected again in the HPSEC system. The acetic acid treatment is reported to disrupt the loose humic conformations, by forming new and stronger intermolecular hydrogen bonds among complementary acidic functional groups in HA (Piccolo et al. 1999, 2002, 2003; Cozzolino et al., 2001). Conversely, when humic conformational structures are stabilized by new intermolecular covalent bonds induced by oxidative coupling catalyzed by water-soluble metal-porphyrins, the addition of acetic acid does not alter the original HPSEC profile of the solution (Piccolo et al., 2005; Šmejkalová & Piccolo, 2005).

The UV-detected size-exclusion chromatograms of humic solutions lowered to pH 3.5 by acetic acid addition before injection into the HPSEC system are shown in Figure 4. Both control and reaction solutions were analyzed after 2, 24 and 72 h of reaction time. At all reaction times, all solutions of reacted HA showed a different profile than control HA. While the latter revealed distinct chromatographic peaks at about 12.4 and 13.3 mL of elution volume (Figure 4a), these signals were modified in intensity in the HA solution added with H_2O_2 and shifted to slightly larger elution volumes (Figure 4b). For the HA solutions subjected to the catalyzed polymerization reactions, the acetic acid addition reduced the intensity of the 12.4 mL peak and somewhat shifted it at lower elution time, whereas the second peak almost disappeared at 2 and 24 h after reaction start (Figure 4c, d). However, after 72 h of reaction time,

the second peak was slightly resumed in the sample catalyzed under H_2O_2 oxidation (Figure 4c). At the same reaction time, the HA undergone the catalyzed photo-polymerization revealed a still different elution profile with the absorbance of both peaks significantly reduced and the peak around 8.8 mL become most relevant (Figure 4d).

These findings suggest that the oxidative polymerization by either chemical or photo oxidation under heterogeneous catalysis enabled a rearrangement of chromophores inside the HA superstructures. The substantial decrease of the peaks eluting at larger volumes than for control, seems to indicate that humic matter was increased in mass size by the catalyzed polymerization reaction. However, this explanation may not hold true because of the possible variation in peak absorbance discussed above and attributed to an uncontrolled hypochromic/hyperchromic effect rather than to real changes in molecular size.

To confirm the suggestion that heterogeneous catalysis enabled a real mass increase in HA, the RI-detected size-exclusion chromatograms were also evaluated for the same HA solutions brought to pH 3.5 (Figure 5). The RI detector showed that the elution profile of the HA solution treated with H_2O_2 (Figure 5b) was either very similar to control HA (Figure 5a) or was slightly less in absorbance. Conversely, the elution profiles of HA undergone polymerization by heterogeneous catalysis by both H_2O_2 (Figure 5c) or photo oxidation (Figure 5d) invariably showed a significant shift to lower elution volumes and even a more intense peak at the around the void volume (8.8 mL). Therefore, the findings by RI detector support the observations that the heterogeneous catalysis, exerted by the Mn-porphyrin immobilized on kaolinite under either H_2O_2

oxidation or UV-light irradiation, turns weakly associated humic superstructures into more stable conformations.

In conclusion, we provided evidence that humic molecules in solution undergo formation of intermolecular covalent bonds when exposed to an oxidative coupling reaction under heterogeneous catalysis. Calculations of weight-average molecular weight values from size-exclusion chromatograms of humic solutions suggest that the molecular mass of humic superstructure was enhanced by the coupling reaction catalyzed by a metal-porphyrin immobilized on kaolinite. Moreover, the *Mw* values showed that there was no significant difference whether H_2O_2 oxidation or photo-oxidation was employed to conduct the catalyzed polymerization reaction. The increase in molecular mass of the humic material subjected to the oxidative catalyzed reaction was confirmed by shift of the size-exclusion chromatography profiles to lower elution volumes after treating humic matter with acetic acid to lower the solution pH from the original 7 of control HA to 3.5. These results suggest that a biomimetic catalyst supported on a clay mineral may be usefully employed to reduce toxicity of phenols, as done in the case of homogeneous catalysis (Fontaine & Piccolo, 2011), and control the stability of humic matter in soil (Piccolo et al., 2011).

Acknowledgements

A.N. conducted this work in partial fulfillment of a PhD degree in the Doctorate School "Valorizzazione e Gestione delle Risorse Agroforestali" of the Università di Napoli Federico II.

References

Baldock, J. A.; Skjemstad, J. O. Role of the matrix and minerals in protecting natural organic materials against biological attack. *Org. Geochem.* 2000, *31*, 697–710.

Cozzolino, A.; Conte, P.; Piccolo, A. Conformational changes of soil humic substances induced by some hydroxy-, cheto-, and sulphonic acids. *Soil Biol. Biochem.* 2001, *33*, 563-571.

Cozzolino, A.; Piccolo, A. Polymerization of dissolved humic substances catalyzed by peroxidase. Effects of pH and humic composition. *Org. Geochem*. 2002, *33*: 281-294.

Fontaine, B.; Piccolo, A. Co-polymerization of penta-halogenated phenols in humic substances by catalytic oxidation using biomimetic catalysis. *Environ. Sci. Pollut. Res.* 2011, DOI 10.1007/s11356-011-0626-x.

Nardi, S.; Pizzeghello, D.; Muscolo, A.; Vianello, A. Physiological effects of humic substances on higher plants. *Soil Biol. Biochem.* 2002, *34*, 1527-1536.

Nuzzo, A.; Piccolo, A. Enhanced catechol oxidation by heterogeneous biomimetic catalysts immobilized on clay minerals. 2011. Manuscript to be submitted for *J. Mol. Catal. A – Chem., also reported in this thesis.*

Piccolo, A. Humus and Soil Conservation. In *Humic Substances in Terrestrial Ecosystems*; Piccolo, A., Ed.; Elsevier: Amsterdam, The Netherlands, 1996; pp 225-264.

Piccolo, A. The supramolecular structure of humic substances: a novel understanding of humus chemistry and implication in soil science. *Adv. Agron.* 2002, *75*, 57-134.

Piccolo, A.; Conte, P.; Cozzolino, A. Effects of mineral and monocarboxylic acids on the molecular association of dissolved humic substances. *Eur. J. Soil Sci.* 1999, *50*, 687-694.

Piccolo, A.; Cozzolino, A.; Conte, P.; Spaccini, R. Polymerization of humic substances by an enzyme-catalyzed oxidative coupling. *Naturwissenschaften* 2000, *87*, 391-394.

Piccolo, A.; Conte, P.; Trivellone, E.; Van Lagen, B.; Buurman, P. Reduced heterogeneity of a lignite humic acid by preparative HPSEC following interaction with an organic acid. Characterization of size-separates by PYR-GC-MS and ^{1}H-NMR spectroscopy. *Environ. Sci. Technol.* 2002, *36*, 76-84.

Piccolo, A.; Conte, P.; Cozzolino, A.; Spaccini, R. The conformational structure of humic substances. In: Benbi DK, Nieder R. (eds) *Handbook of processes and modeling in the soil-plant system.* The Haworth Reference Press, New York, 2003.

Piccolo, A.; Conte, P.; Tagliatesta, P. Increased conformational rigidity of humic substances by oxidative biomimetic catalysis. *Biomacromolecules* 2005, *6*, 351-358.

Piccolo, A.; Spaccini, R.; Nebbioso A.; Mazzei P**.** Carbon sequestration in soil by *in situ* catalyzed photo-oxidative polymerization of soil organic matter. *Environ. Sci. Technol.* 2011, *45*, 6697–6702.

Shaik, S.; Hirao, H.; Kumar, D. Reactivity of high-valent iron_oxo species in enzymes and synthetic reagents: a tale of many states. *Acc. Chem. Res.* 2007, *40*, 532-542.

Šmejkalová, D.; Piccolo, A. Enhanced molecular dimension of a humic acid induced by photooxidation catalyzed by biomimetic metalporphyrins. *Biomacromolecules* 2005, *6*, 2120-2125.

Šmejkalová, D.; Piccolo, A. Rates of oxidative coupling of humic phenolic monomers catalyzed by a biomimetic iron-porphyrin. *Environ. Sci. Technol.*, 2006, *40*, 1644-1649.

Šmejkalová, D.; Piccolo, A.; Spiteller, M. Oligomerization of humic phenolic monomers by oxidative coupling under biomimetic catalysis. *Environ. Sci. Technol.*, 2006, *40*, 6955-6962.

Song, J.; Huang, W.; Peng, P.; Ma, B. X. Y. Humic Acid Molecular Weight Estimation by High-Performance Size-Exclusion Chromatography with Ultraviolet Absorbance Detection and Refractive Index Detection. *Soil Sci Soc. Am. J.* 2010, *74*, 2013-3020.

Tisdall, J. M.; Oades, J. M. Organic matter and water-stable aggregates in soils. *J. Soil Sci.* 1982, *33*, 141–163.

Yau, W. W.; Kirkland, J. J.; Bly, D. D. *Modern Size Exclusion Chromatography*; Wiley Interscience: New York, 1979; p 318-326.

Zucca, P.; Mocci, G.; Rescigno, A.; Sanjust, E. 5,10,15,20-Tetrakis(4-sulfonato-phenyl)porphine-Mn(III) immobilized on imidazole-activated silica as a novel lignin-peroxidase-like biomimetic catalyst. *J. Mol. Catal. A - Chem.* 2007, *278*, 220-227.

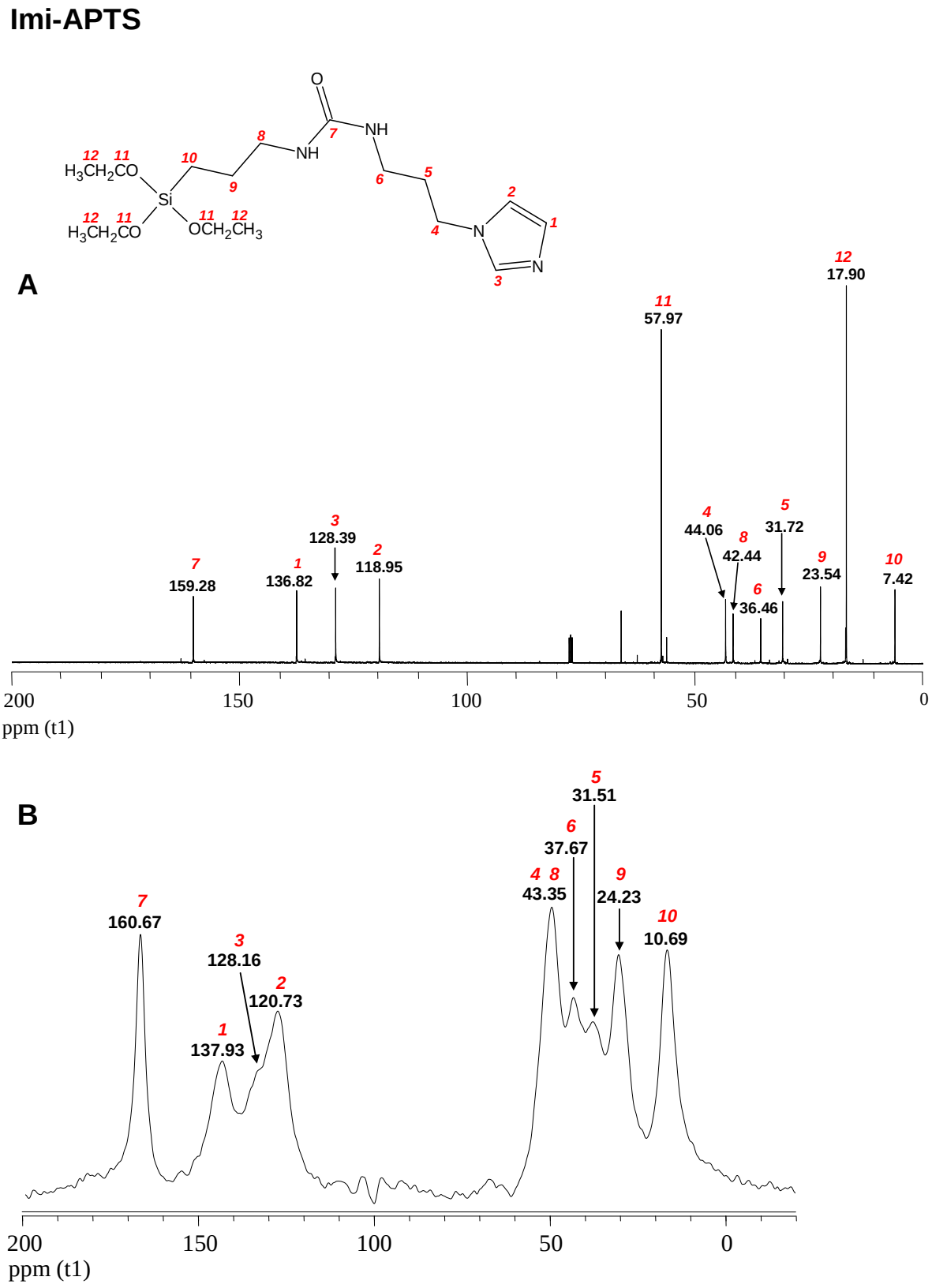

Figure 1. Liquid-state ^{13}C NMR spectrum of Imi-APTS spacer (A); solid-state ^{13}C-CPMAS-NMR spectrum of kaolinite functionalized with Imi-APTS (B). Numbers on spectral signals correspond to different carbons in the Imi-APTS structure.

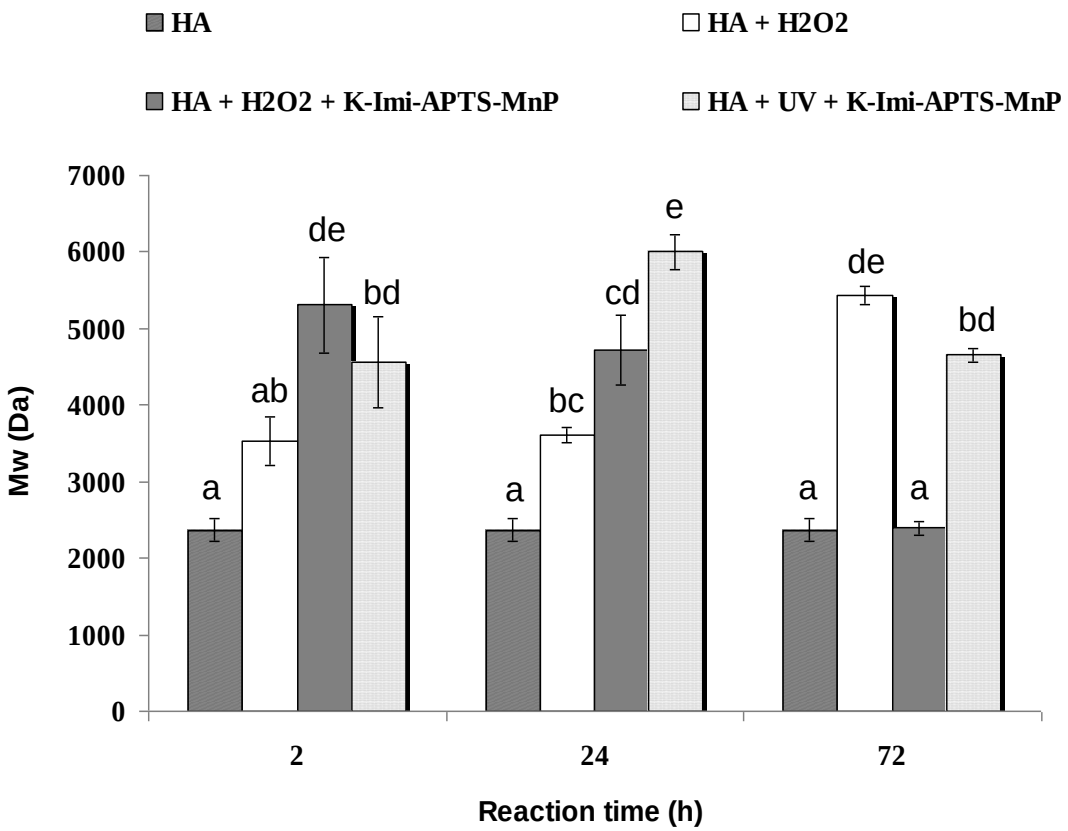

Figure 2. UV-derived apparent weight-average molecular weight (*Mw*) for the lignite humic acid (HA), before and after polymerization under heterogeneous catalysis by MnP-Imi-APTS-K and oxidation by either H_2O_2 or UV light irradiation. *Mw* values for control and reaction mixtures were for 2, 24 and 72 hours of reaction time as by UV-HPSEC chromatograms. Error bars indicate standard error (n=3) and different letters indicate significant differences by the Tukey's test at $P \leq 0.05$.

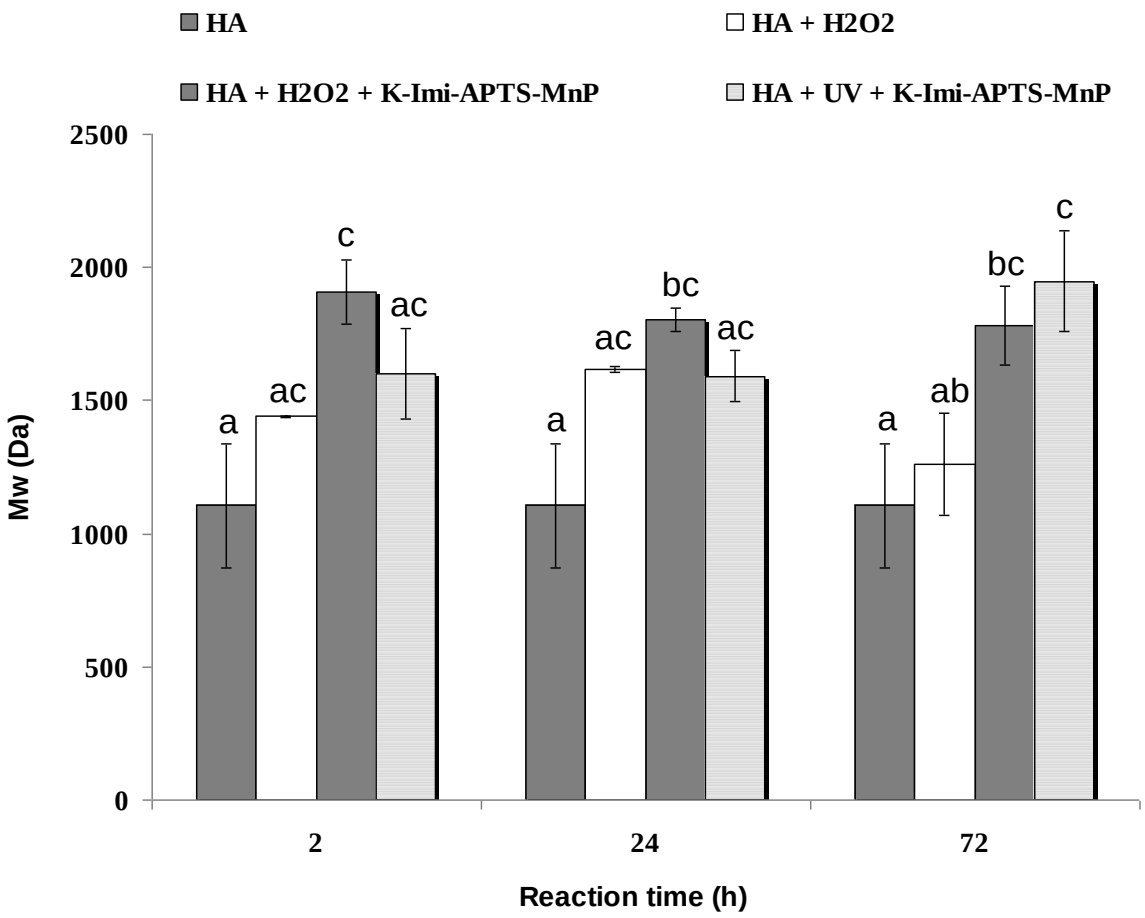

Figure 3. RI-derived apparent weight-average molecular weight (*Mw*) for the lignite humic acid (HA), before and after polymerization under heterogeneous catalysis by MnP-Imi-APTS-K and oxidation by either H_2O_2 or UV-light irradiation. *Mw* values for control and reaction mixtures were for 2, 24 and 72 hours of reaction time as by RI-HPSEC chromatograms. Error bars indicate standard error (n=3) and different letters indicate significant differences by the Tukey's test at $P \leq 0.05$.

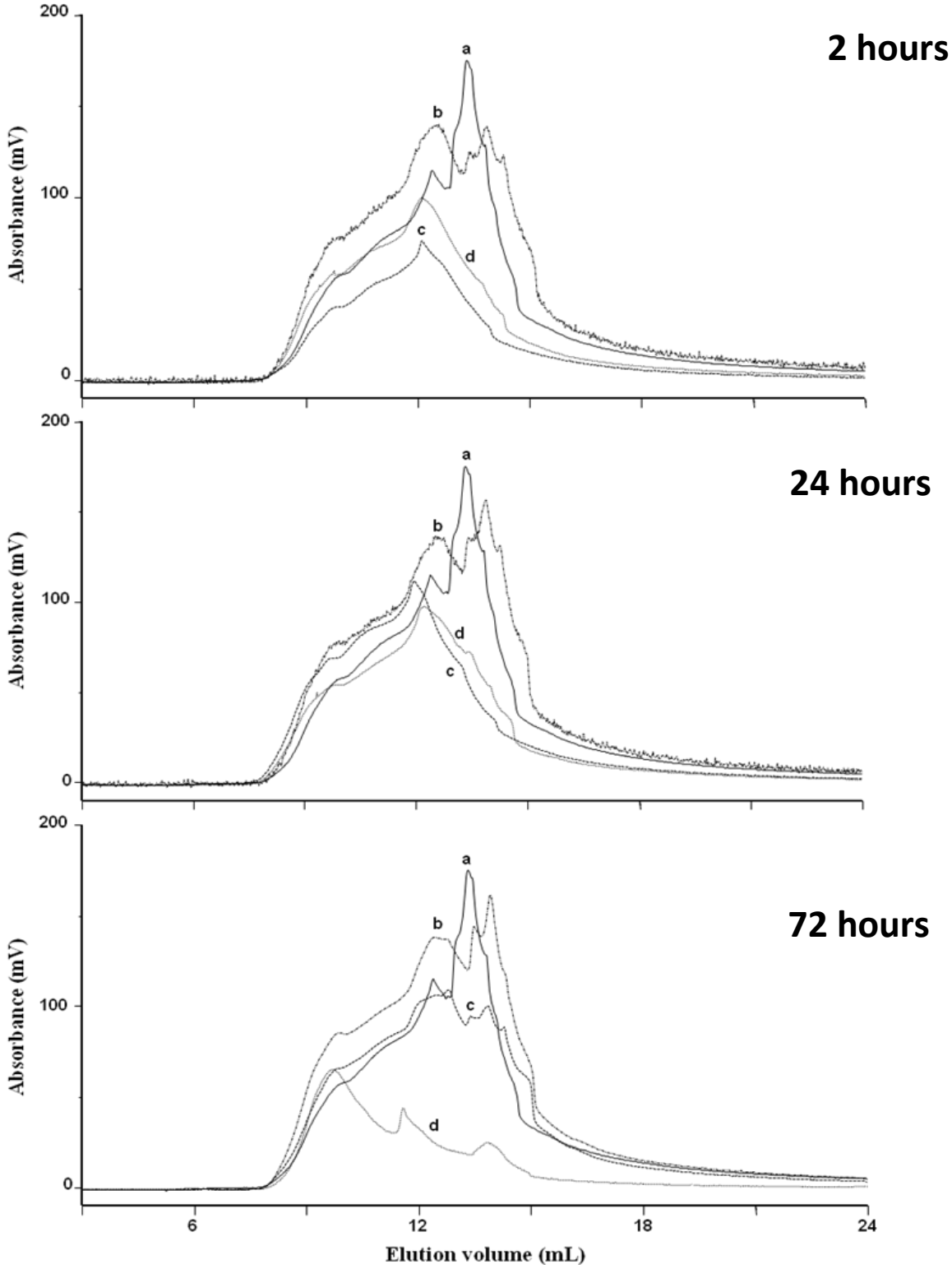

Figure 4. UV-detected HPSEC chromatograms of humic solutions treated with acetic acid to reach pH 3.5: (a) control HA; (b) control HA+H_2O_2; (c) HA+ H_2O_2+K-Imi-APTS-MnP; (d) HA+ K-Imi-APTS-MnP and exposed to UV light. Solutions were analyzed after 2, 24 and 72 h of reaction time.

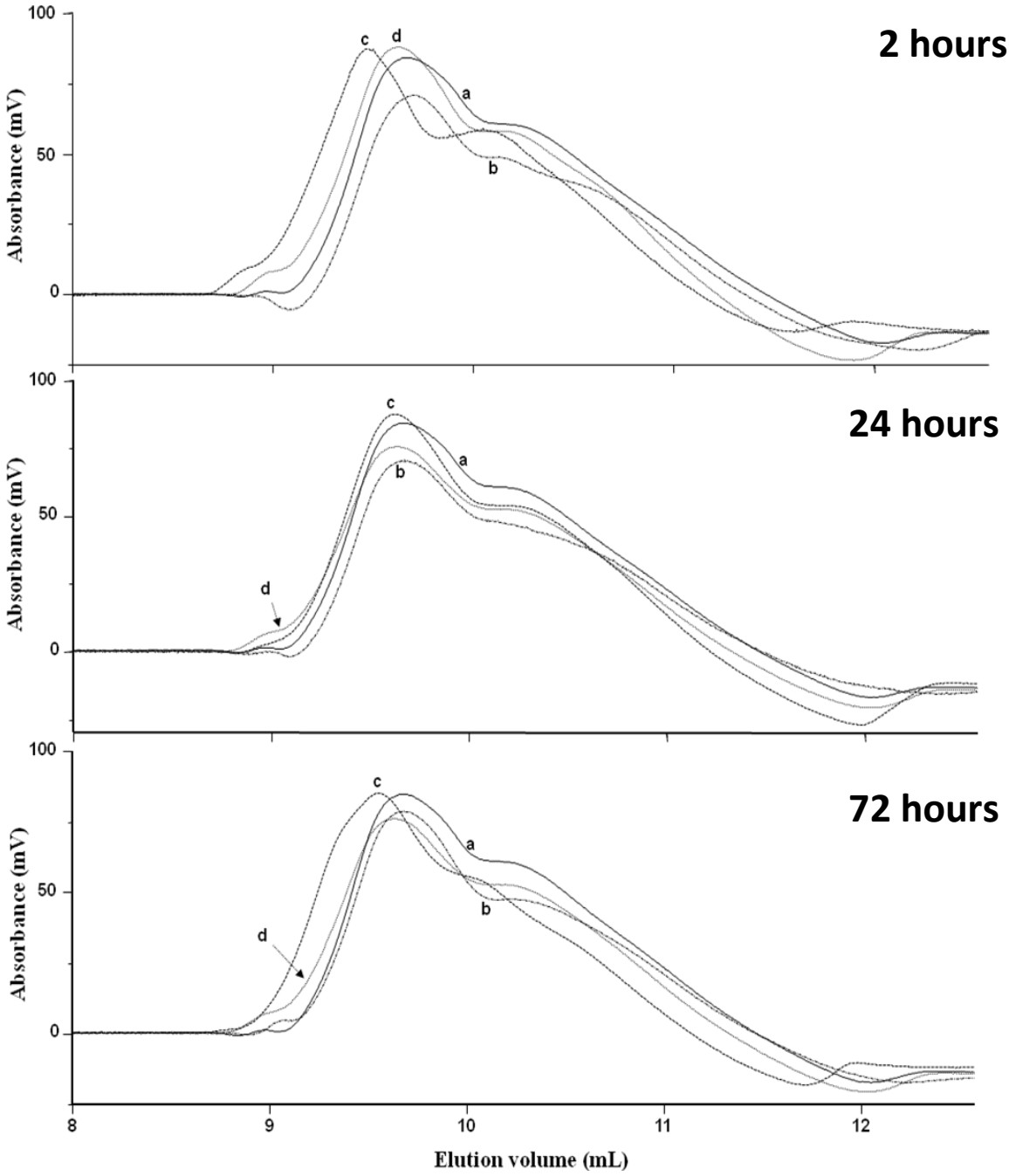

Figure 5. RI-detected HPSEC chromatograms of humic solutions treated with acetic acid to reach pH 3.5: (a) control HA; (b) control HA+H_2O_2; (c) HA+ H_2O_2+K-Imi-APTS-MnP;, (d) HA+ K-Imi-APTS-MnP and exposed to UV light. Solutions were analyzed after 2, 24 and 72 h of reaction time.

Supporting Information

Table 1. Apparent weight-average molecular weight (*Mw*) values and their standard deviation (±SD) of the lignite humic acid under different treatments, as measured from UV-detected HPSEC chromatograms after acetic acid addition. Values followed by the same letter within columns are not significantly different by Tukey's test at the level of $P \leq 0.05$.

	Mw		
Reaction time	2	24	72
HA	2367.65 ± 151.12 a	2367.65 ± 151.12 a	2367.65 ± 151.12 a
HA + H_2O_2	3528.32 ± 310.85 ab	3604.04 ± 102.55 bc	5436.51 ± 117.10 de
HA + H_2O_2 + K-Imi-APTS-MnP	5307.63 ± 628.95 de	4713.61 ± 460.01 cd	2390.46 ± 91.45 a
HA + UV + K-Imi-APTS-MnP	4560.96 ± 596.69 bd	6005.46 ± 229.46 e	4655.90 ± 86.26 bd

Table 2. Apparent weight-average molecular weight (*Mw*) values and their standard deviation (±SD) of the lignite humic acid under different treatments, as measured from RI-detected HPSEC chromatograms after acetic acid addition. Values followed by the same letter within columns are not significantly different by Tukey's test at the level of $P \leq 0.05$.

	Mw		
Reaction time	2	24	72
HA	1105.88 ± 234.37 a	1105.88 ± 234.37 a	1105.88 ± 234.37 a
HA + H_2O_2	1439.18 ± 2.53 ac	1615.83 ± 12.21 ac	1261.82 ± 190.24 ab
HA + H_2O_2 + K-Imi-APTS-MnP	1907.48 ± 121.35 c	1805.33 ± 44.16 bc	1779.89 ± 147.24 bc
HA + UV + K-Imi-APTS-MnP	1602.56 ± 169.06 ac	1591.28 ± 95.06 ac	1948.87 ± 190.62 c

CHAPTER 6 - GENERAL CONCLUSIONS

6.1 General conclusions

Results of this work indicate that metal-porphyrins immobilized on clay minerals through a molecular spacer are promising heterogeneous biomimetic catalysts, capable of turning weakly-associated humic superstructures into more stable covalently-bound oligo- or poly-mers, by means of radical oxidative transformation induced by either H_2O_2 oxidant or exposure to UV light.

By subjecting a humic phenolic precursor, such as the catechol, to oxidative coupling reaction, it was shown that the rate of the reaction catalyzed by immobilized catalysts was significantly larger than that catalyzed by the corresponding water-soluble catalyst in a homogeneous catalysis.

Afterwards, a dissolved humic acid was subjected to the oxidative coupling reaction catalyzed by the Mn-porphyrin supported on spacer-functionalized kaolinite and induced by either chemical or photo oxidation. The increase in the apparent molecular mass of the polymerized humic acid was shown both before and after acetic acid addition, thereby suggesting that the heterogeneous catalysis favoured the polymerization of the humic matter by increasing its apparent size distribution, through formation of C-O-C and C-C bonds during the oxidative coupling reaction.

These observations suggest the potential use of heterogeneous biomimetic catalysis in any environmental condition in which the coupling of phenols may be desired. In particular, it seems that a technology employing the supported catalysts described here may be more efficient than the corresponding water-soluble catalysts in the ecological and environmental control of soil organic matter processes and in the decontamination of soils and waters from organic pollution.

CHAPTER 7 -

CUCURBITURILS

7.1 Introduction

The cucurbit[n]uril (CB[n]; n= number of glycoluril units) story begins in 1905, when the scientist Robert Behrend described the acid-catalyzed condensation reaction between glycoluril and formaldehyde (Behrend et al., 1905). The substance formed during this reaction was insoluble in all common solvents but could be recrystallized from hot H_2SO_4, which yielded a well-defined substance. Although Behrend was not able to structurally characterize this substance, he did demonstrate that it forms complexes with a wide variety of species including $KMnO_4$, $AgNO_3$ and methylene blue.

It was not until 1981 that Mock and coworkers reported that the product of Behrend's reaction was the macrocyclic pumpkin-shaped cucurbit[6]uril (Figure 1) comprising six equivalents of glycoluril and twelve equivalents of formaldehyde (Freeman et al., 1981). They coined the name "cucurbituril" in reflection of the botanical name for pumpkin "cucurbitaceae".

Research on the CB[n] family received momentum only when four other homologues (CB[5], CB[7], CB[8] and mostly recently CB[10]) were isolated from the mixture by the research groups of Kim, Day and Isaac (Kim et al., 2000; Day et al., 2001; 2002; Liu et al., 2005). Since then a notable amount of work has been published in the literature on the host-guest chemistry of the CB[n] family and their utilization in chemistry, biology, materials science and nano-technology (Lagona et al., 2005; Lee et al., 2003).

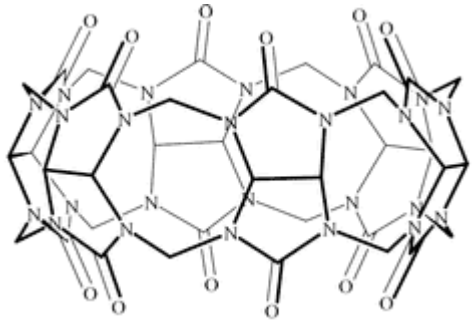

Figure 1. Chemical structure of cucurbit[6]uril.

7.2 Guests of CB[n]s

CB[n]s are a family of macrocyclic container molecules composed of glycoluril monomers joined by pairs of methylene bridges (Lagona et al., 2005; Mock, 1996; Lee et al., 2003; Marquez et al., 2004). All CB[n]s have a highly symmetrical, pumpkin-shaped structure with two identical carbonyl-fringed portals and an interior hydrophobic cavity (Lee et al., 2003, Liu et al., 2002). In recent years, CB[n]s have been established as versatile and interesting host molecules, which form stable inclusion complexes with a wide range of guest molecules. Although ionic species such as ammonium salts are the most studied guests for CB[n] hosts, neutral species could also be encapsulated in the cavity of CB[n]s. Kim and coworkers reported the encapsulation of THF and Xe by CB[6] in aqueous solution with various buffer salts (Jeon et al., 1996; Whang et al., 1998; Haouaj et al., 2001). Cations from the buffer solutions were present in the portal regions in the crystal structures of the isolated CB[6] complexes, thereby physically blocking the escape of any guest inside. In every example of complexes reported between neutral guests and CB[n] hosts, cations are likely acting as "lids" trapping the neutral molecules inside the cavity. In 2009 Scherman and coworkers reported (Liu et al., 2009) for the first time the isolation of a lid-free and charge-free inclusion complex

with CB[6]. The crystal structure analysis of diethylether encapsulated within CB[6] did not show any trace of ions at the portal region. This result indicated that the CB[6] hydrophobic cavity could act as a good "shelter" to poorly solvated molecules such as diethylether in aqueous media.

CB[n]s form host-guest complexes also with room temperature ionic liquids (RTIL). Imidazolium RTILs are promising guests for CB[n] hosts, since their physical properties can be altered in a straightforward manner by varying both counterion and the chemical nature of the alkyl substituent. Moreover, small changes in alkyl chain length of substituents can alter the binding mode and stochiometry of the inclusion complexes between RTIL guests and CB[n] hosts (Liu et al., 2008).

7.3 pH-controlled release of indole-3-acetic acid from cucurbit[7]uril

Auxin is the generic name of a small class of molecules (plant hormones) that have an important role in coordination of many growth processes in the plant's life cycle and are essential for plant body development. The most important member of the auxin family is the indole-3-acetic acid (IAA). It generates the majority of auxin effects in intact plants, and is the most potent native auxin. We report here a preliminary work aimed to study the influence of pH on the release of indole-3-acetic acid from CB[7], in order to control the transport of this phytohormone to cell membranes of plant roots and leaves, in an aqueous system. In water IAA exists in two forms in equilibrium, one being neutraI and the other one being anionic. Only the neutral form forms inclusion complex with CB[7] (Figure 2).

Controlled catch and release of auxins with CB[7] might represent a very innovative technology to induce growth responses in plants, avoiding the risk that excess ethylene is producted (high doses of auxin are responsible for it), which can inhibit elongation growth, cause leaf abscission and even kill the plant.

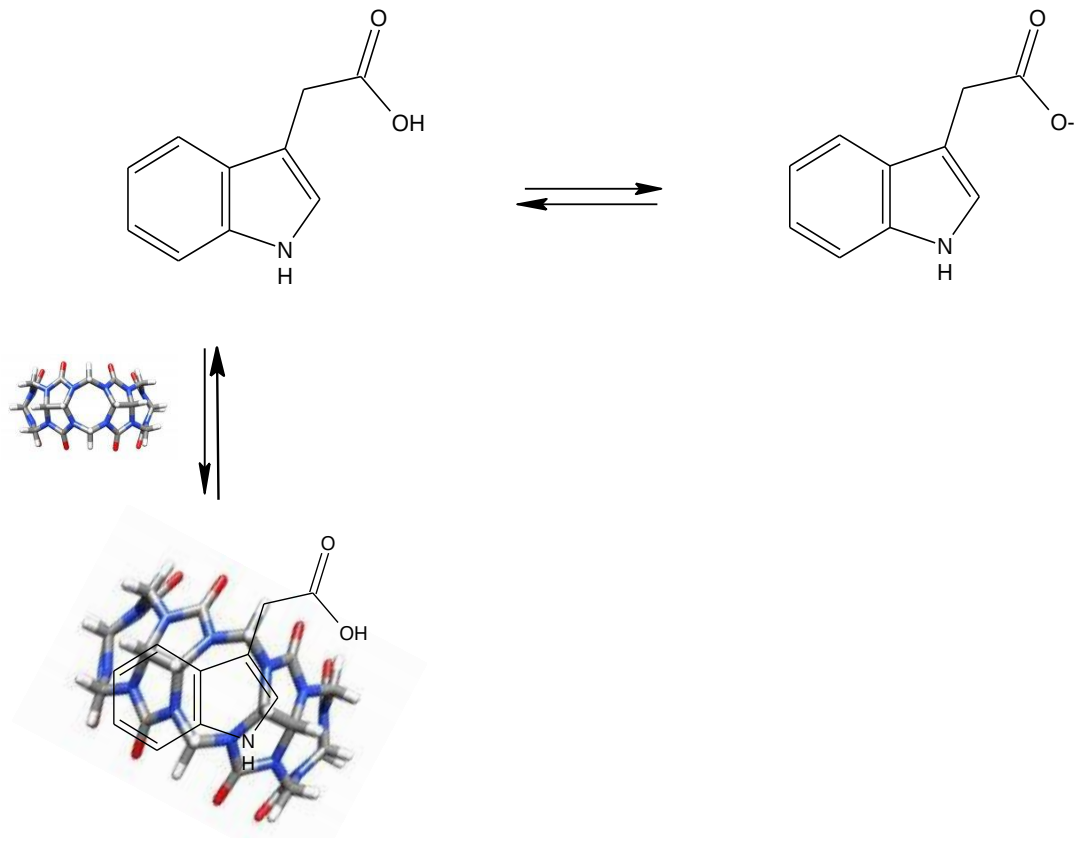

Figure 2. Equilibrium between neutral and anionic IAA species and complexation of the neutral IAA with CB[7].

7.4 Synthesis and isolation of CB[n]s

The synthesis of CB[n]s occurs by the condensation reaction of one equivalent of glycoluril and two equivalents of formaldehyde in concentrated HCl as reported first

by Behrend in 1905 (Behrend et al., 1905) and then by Mock and coworkers (Freeman et al., 1981).

The traditional methods of isolation of CB[n]s analogues primarily rely on the different solubility of CB[n]s in various solvents, such as acetone-water and methanol-water mixtures (Kim et al., 2000; Day et al., 2001). The relatively greater solubility (about 10^3) of CB[5] and CB[7] in water over other members allows for the separation of these two analogues from the complex mixture by precipitation of the even-numbered analogues. Further separation of the individual analogues is based on their solubility in different solvent mixtures (Kim et al., 2000; Day et al., 2001). For the standard separation routes, it is difficult to obtain CB[n]s in high purity as both CB[5] and CB[7] have low solubility in the mixed solvent systems requiring multiple solvent-based separation cycles. Recently, Scherman and coworkers have reported a new more environmentally friendly method to isolate CB[7] from CB[5]/CB[7] mixture based on ionic liquid binding and a solid state metathesis reaction (Jiao et al., 2010). The new technique not only provides a greener method for CB isolation (the free ionic liquid can easily be extracted from the reaction solution and re-used), and high yield (71%), but also reduces the separation time to a few days. A similar approach has also been applied to separate CB[6] and CB[8] (Jiao et al., PCT/GB2010/002330).

7.5 Elemental analysis

CB[7] and CB[8] were purified according to the method reported by Jiao et al. (2010) and Jiao et al. (PCT/GB2010/002330), respectively, and their purity was, then, checked by elemental analysis.

CB[7]'s elemental analysis. Expected values: C=43.33%; H=3.61%; N=33.70%. Experimental values: C=33.66%; H=3.78%; N=26.08%.

CB[8]'s elemental analysis. Expected values: C=43.33%; H=3.61%; N=33.70%. Experimental values: C=33.32%; H=3.15%; N=23.00%.

7.6 ^{1}H NMR spectroscopy

Mode of inclusion of IAA and methyl indole-3-acetate into the cavity of CB[7] in aqueous solution was investigated by using ^{1}H-NMR spectroscopy (Figures 3-11). In the ^{1}H-NMR spectra of CB[n] host-guest complexes, the complexation-induced shift changes (CIS) in the proton resonances of the guest molecule are informative as to the average location of the guest with respect to the CB[n] cavity. Upfield shifts are observed for guest protons located in the shielding region of the cavity, while guest protons located near the carbonyl oxygens of the portals experience deshielding and downfield CIS value.

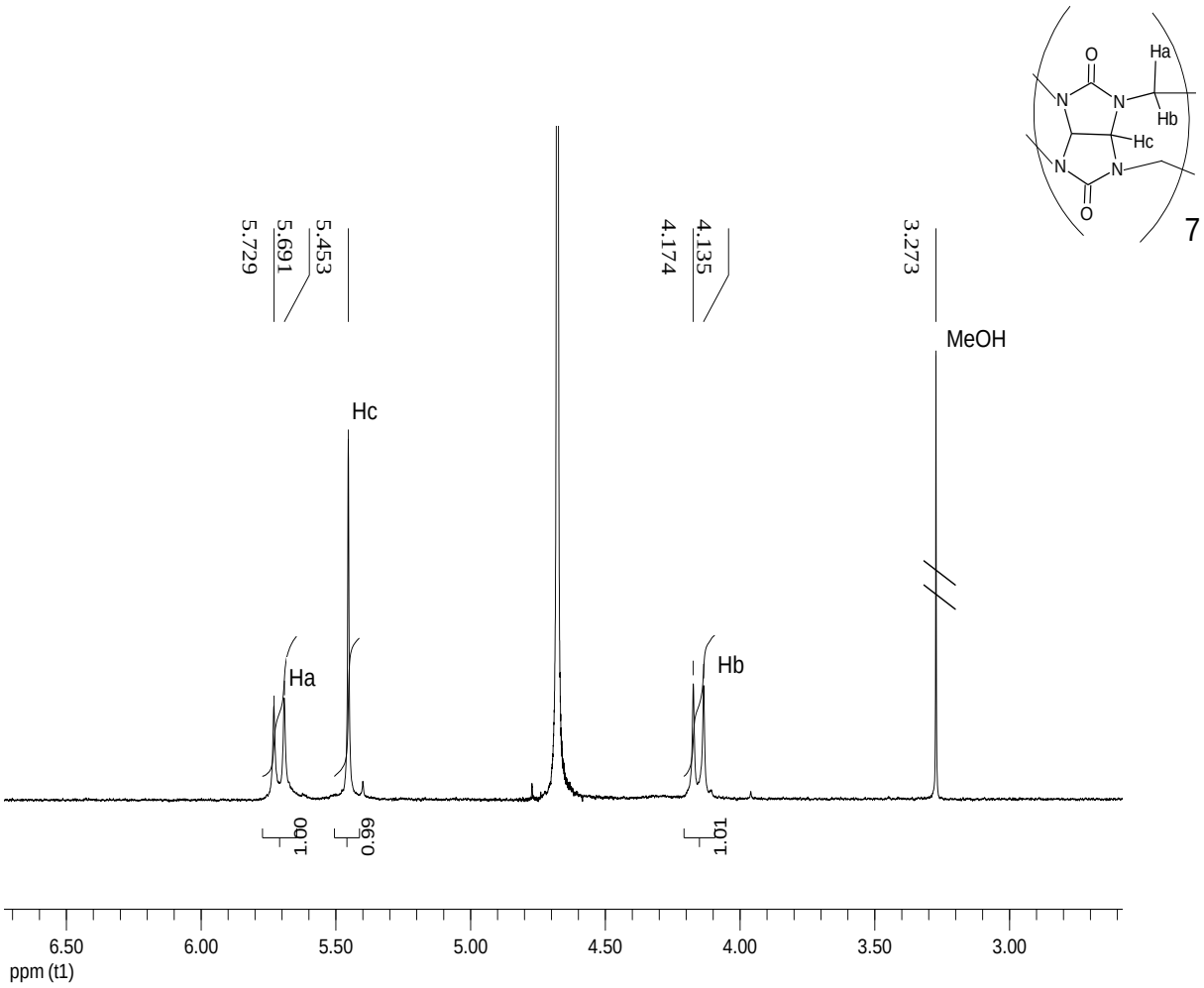

Figure 3. ^{1}H-NMR spectrum (in D_2O) of CB[7].

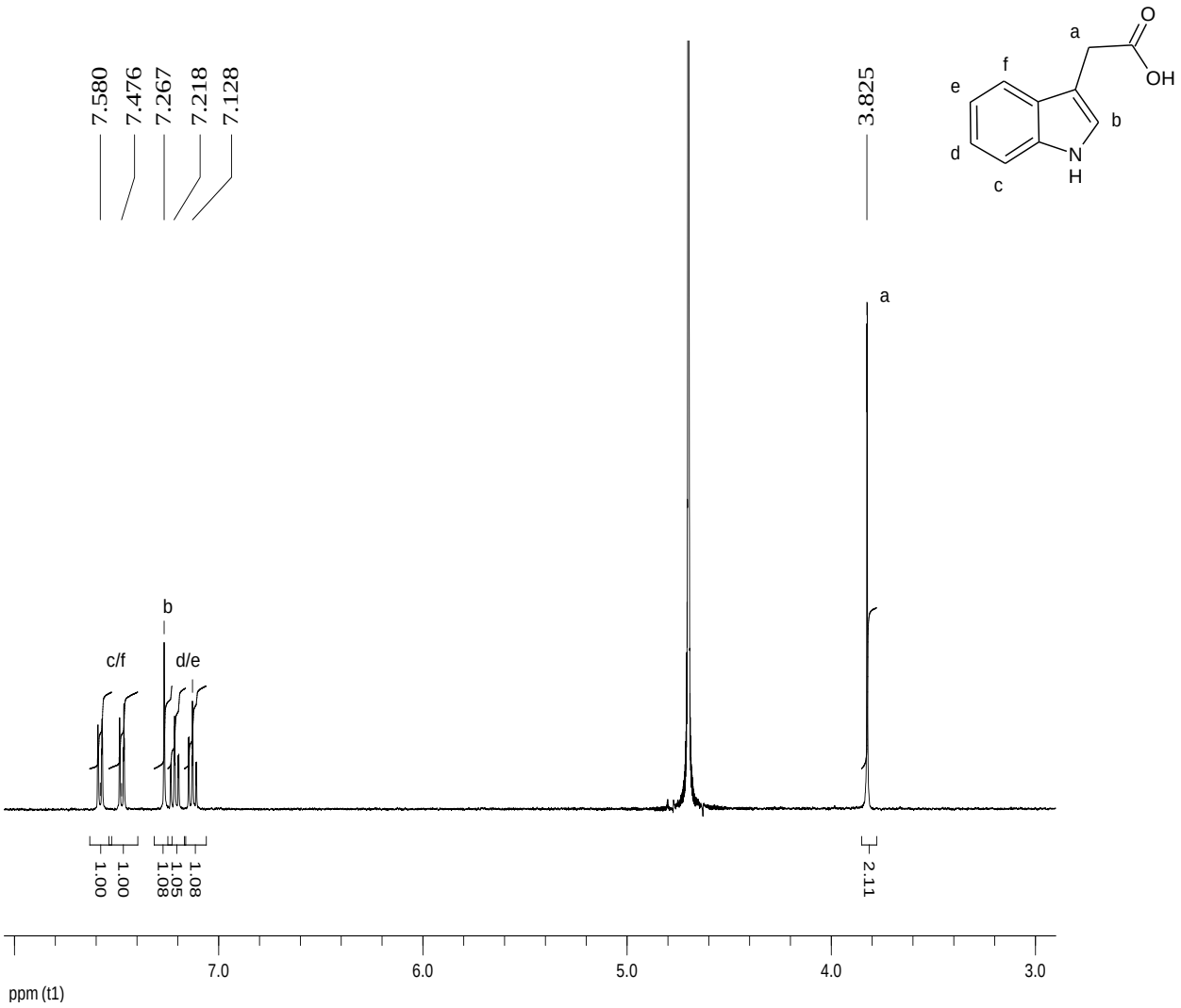

Figure 4. ^{1}H-NMR spectrum (in D_2O) of IAA.

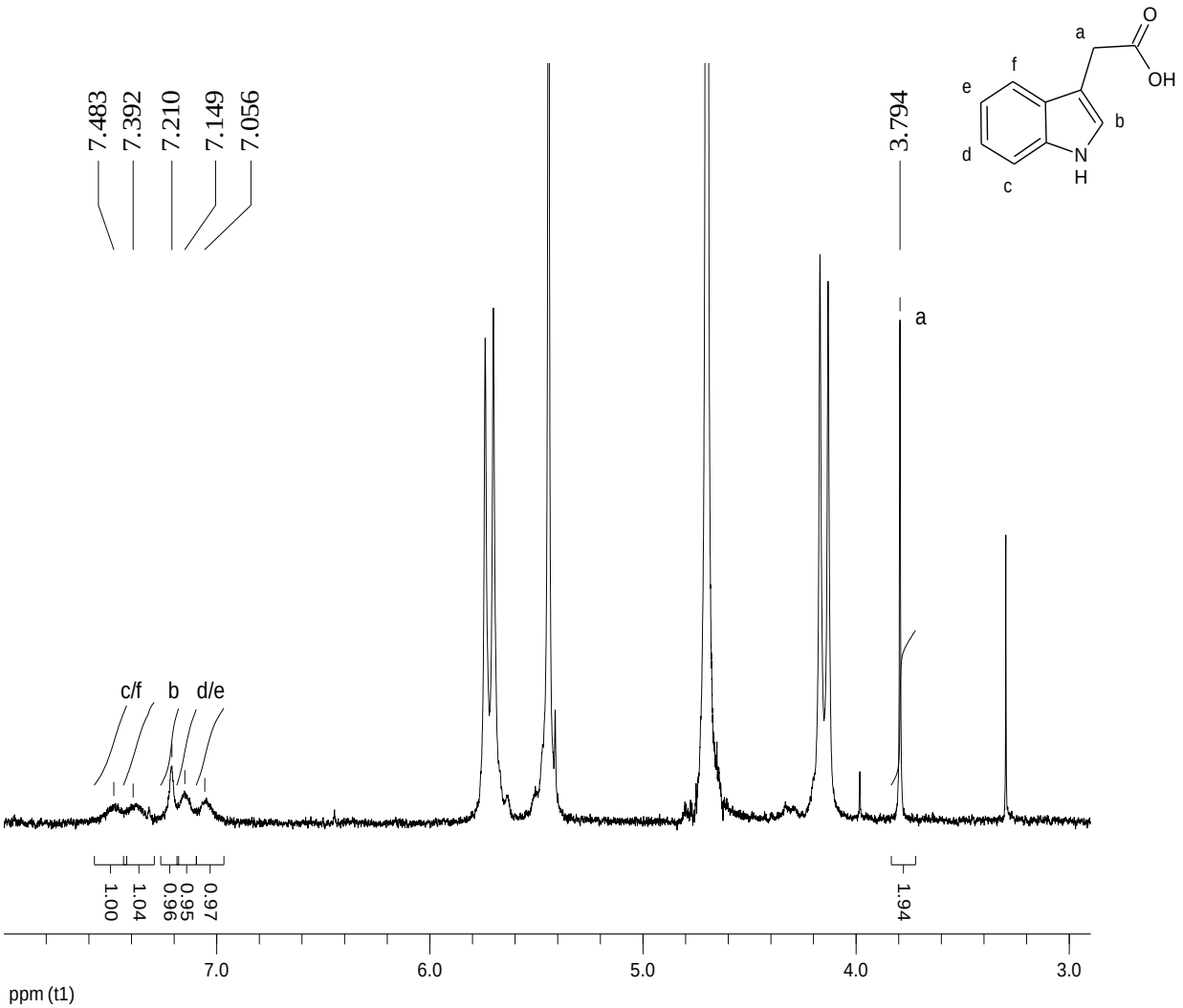

Figure 5. ^{1}H-NMR spectrum (in D_2O) of CB[7]-IAA complex. The IAA/CB[7] molar ratio is 1:1.

The ^{1}H-NMR spectrum of the IAA alone (Figure 4) showed signals in the 7.6-7.1 ppm range due to aromatic protons contained in the indole-acetic ring and a signal at 3.8 ppm corresponding to ethylene protons. When the IAA was complexed with CB[7], the corresponding ^{1}H-NMR spectrum (Figure 5) showed that indole-acetic ring protons, located in the shielding region of the CB[7] cavity, were slightly upfield shifted, while for ethylene protons, placed outside the shielding region of the CB, the shift was

negligible. The only slight upfield shift of the aromatic protons of IAA after complexation suggests that the CB[7]-IAA complex occurred.

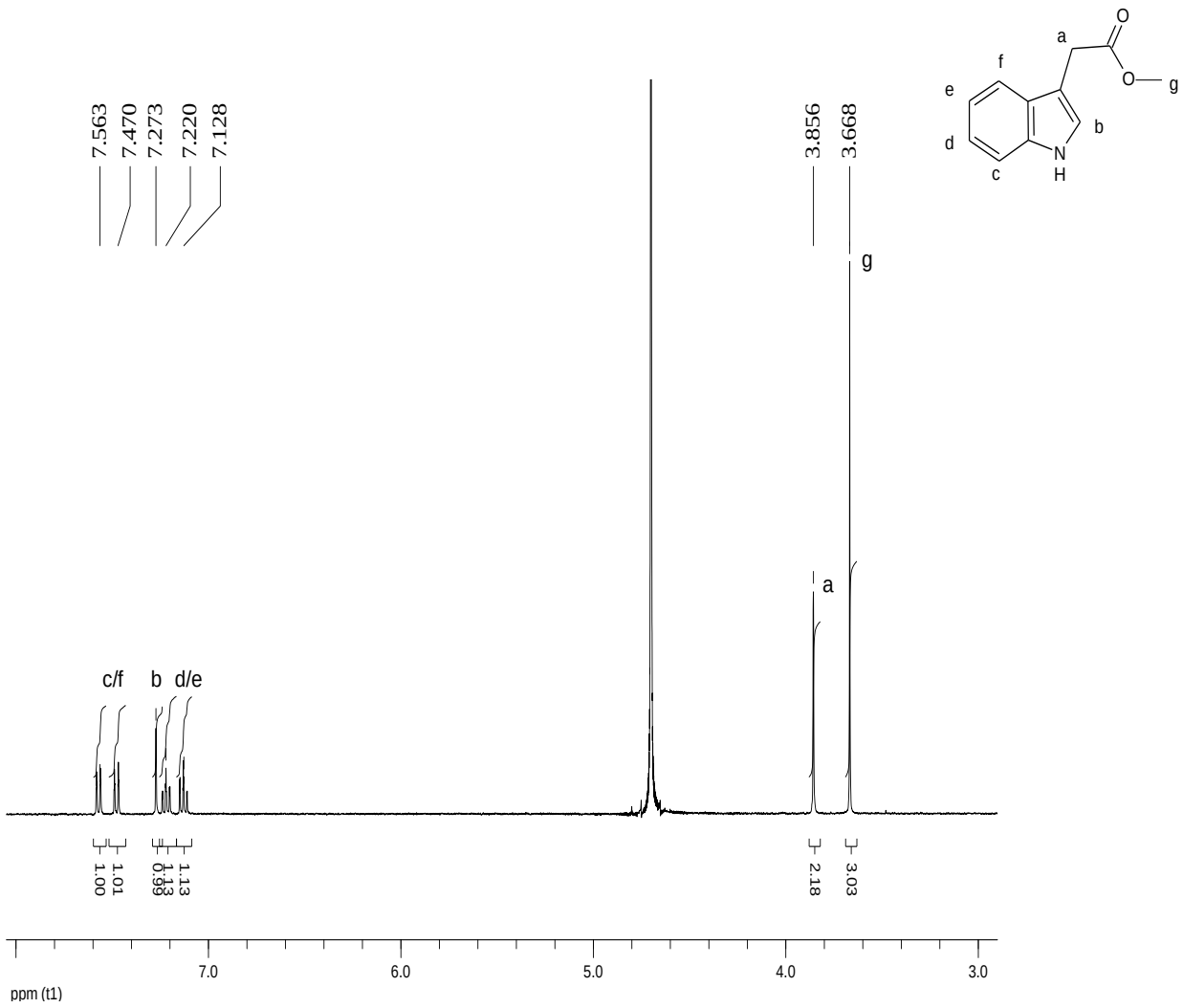

Figure 6. ^{1}H-NMR spectrum (in D_2O) of methyl indole-3-acetate.

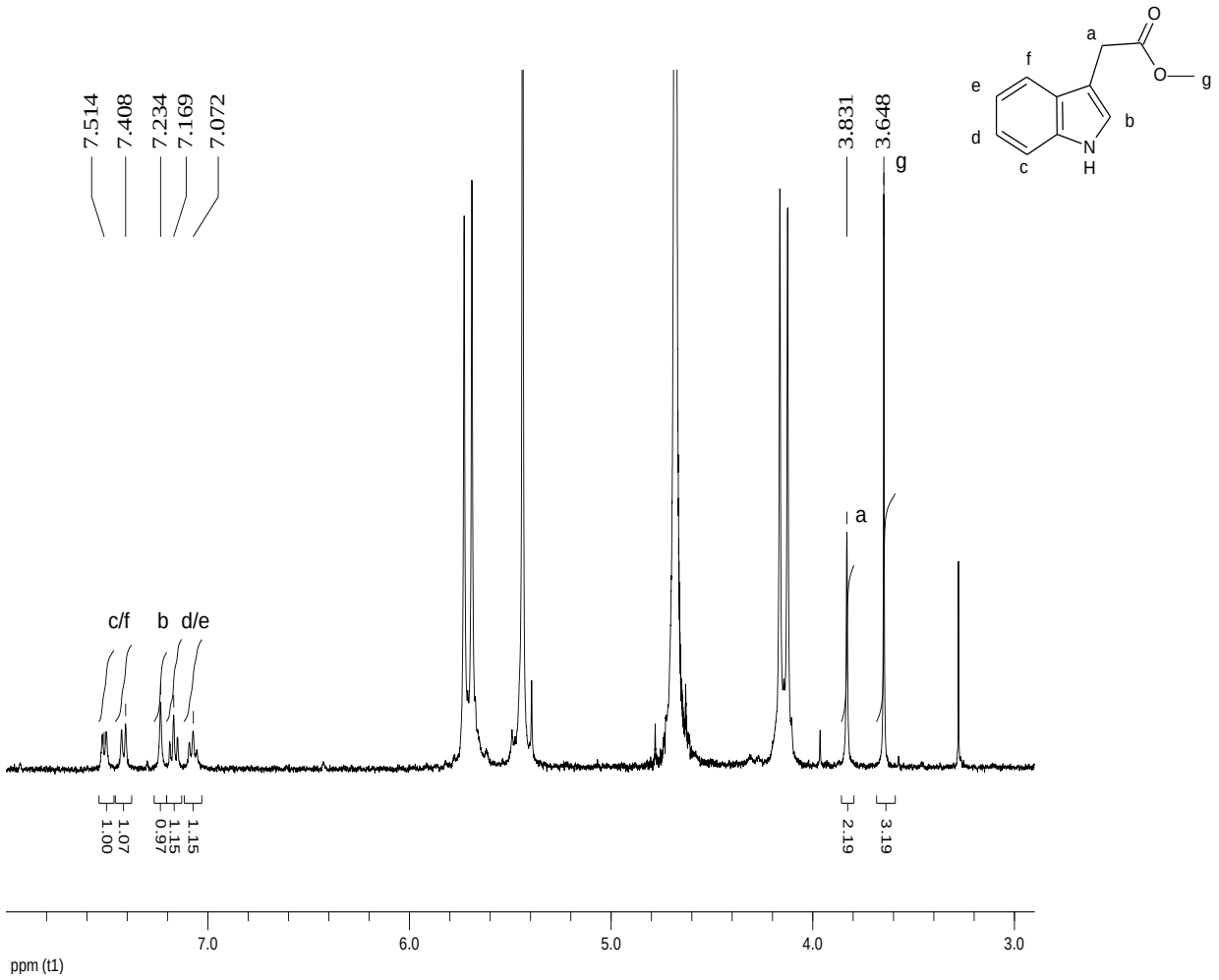

Figure 7. ^{1}H-NMR spectrum (in D_2O) of CB[7]-methyl indole-3-acetate complex. The guest/CB[7] molar ratio is 1:1.

Figure 6 shows the ^{1}H-NMR spectrum of methyl indole-3-acetate molecule, whose signals may be compared with those in the ^{1}H-NMR spectrum of the methyl indole-3-acetate complexed with CB[7] (Figure 7). Upon complexation, the ^{1}H-NMR spectrum of the guest molecule revealed a slight upfield shift of signals in the 7.6-7.1 ppm range for indole-acetic ring protons, because they became shielded in the hydrophobic cavity of the CB, while for both ethylene protons at 3.8 ppm and methylene protons at 3.6 ppm, both located in the deshielding region of the CB, the shift was negligible. These

findings suggest that the complex between the methyl indole-3-acetate and CB[7] was formed.

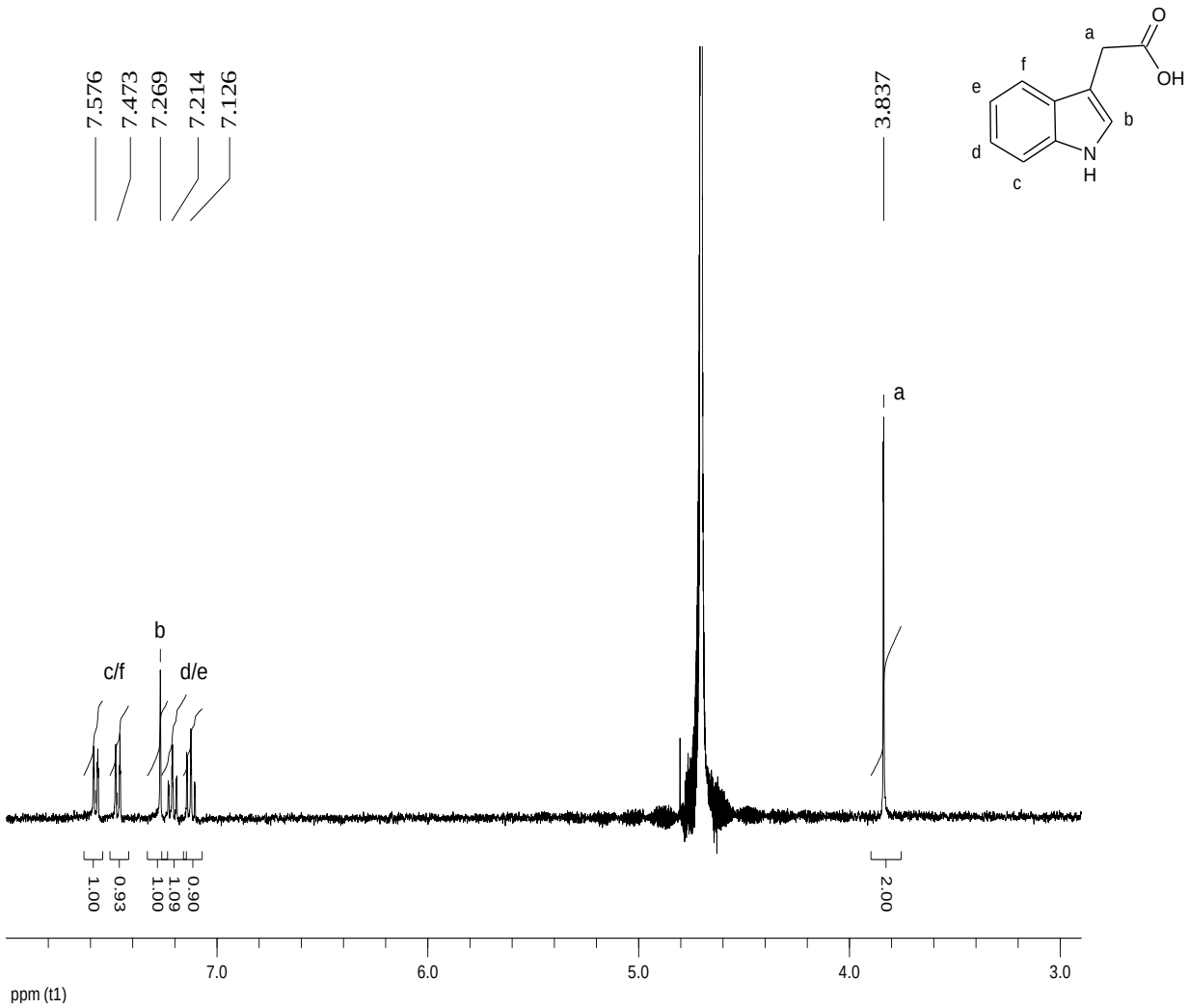

Figure 8. ^{1}H-NMR spectrum (in D_2O) of IAA at pH 1. The pH value of solution has been adjusted by adding the required amount of DCl.

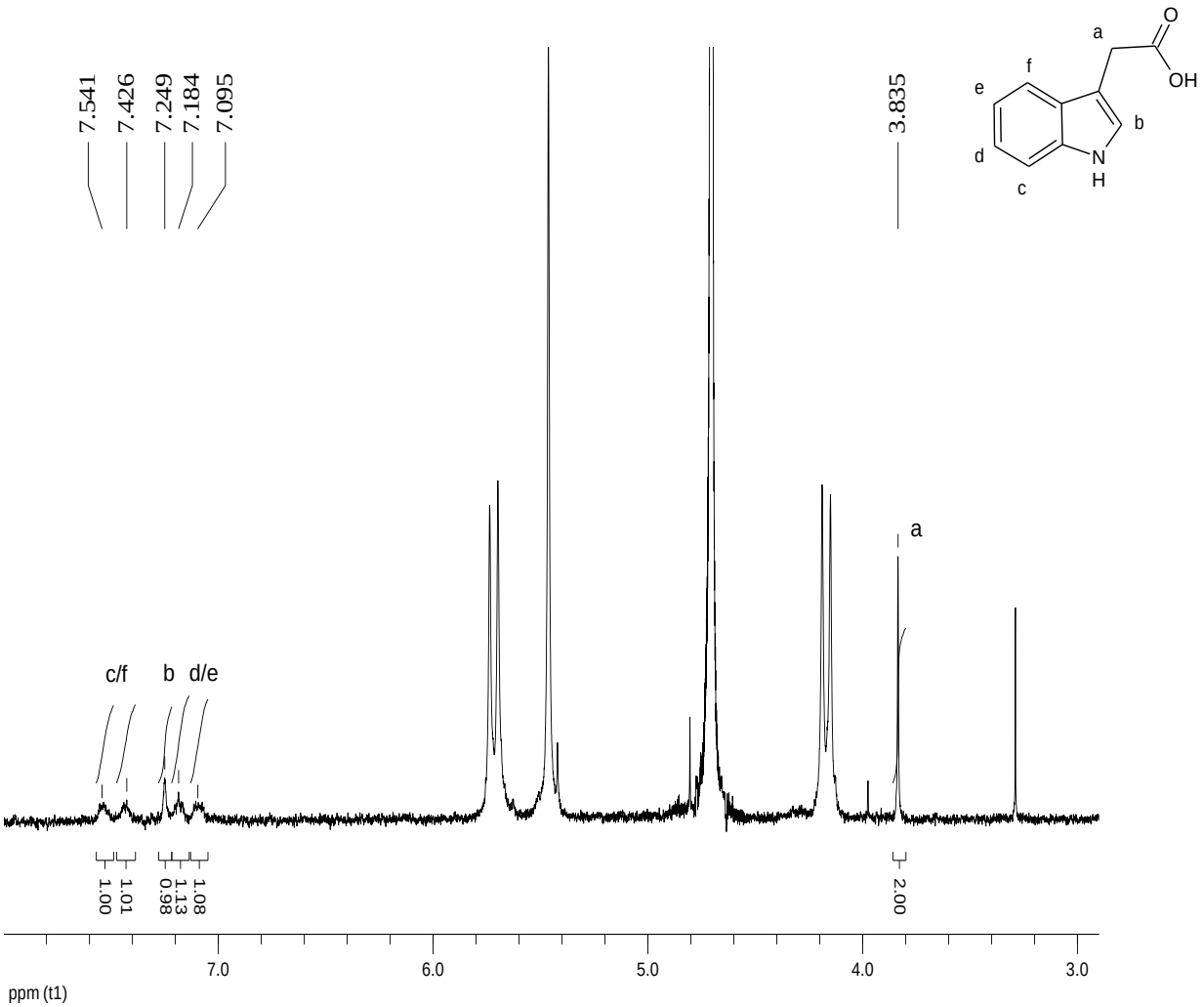

Figure 9. ^{1}H-NMR spectrum (in D_2O) of CB[7]-IAA complex at pH 1. The IAA/CB[7] molar ratio is 1:1 and the pH value of solution has been adjusted by adding the required amount of DCl. The solution is pink.

The ^{1}H-NMR spectra of IAA before and after complexation with CB[7] at pH 1 are reported in Figures 8 and 9, respectively. After complexation with the CB[7] host, the ^{1}H-NMR spectrum of IAA showed aromatic protons signals slightly upfield shifted, thus suggesting that they are located in the shielding region of the CB[7] cavity, whereas the lack of shift for the ethylene protons signal indicates that the ethylene protons were placed in line with the deshielding carbonyl groups of the portals. The

upfield shift of the IAA aromatic protons, after complexation, may be interpreted as a preferential encapsulation of the indole-acetic ring inside the CB[7] macrocycle, while the remaining part of the IAA molecule is located near the carbonyl groups of the portals or slightly outside. This behavior suggests the formation of a CB[7]-IAA complex that also gave a pink colour to the sample solution.

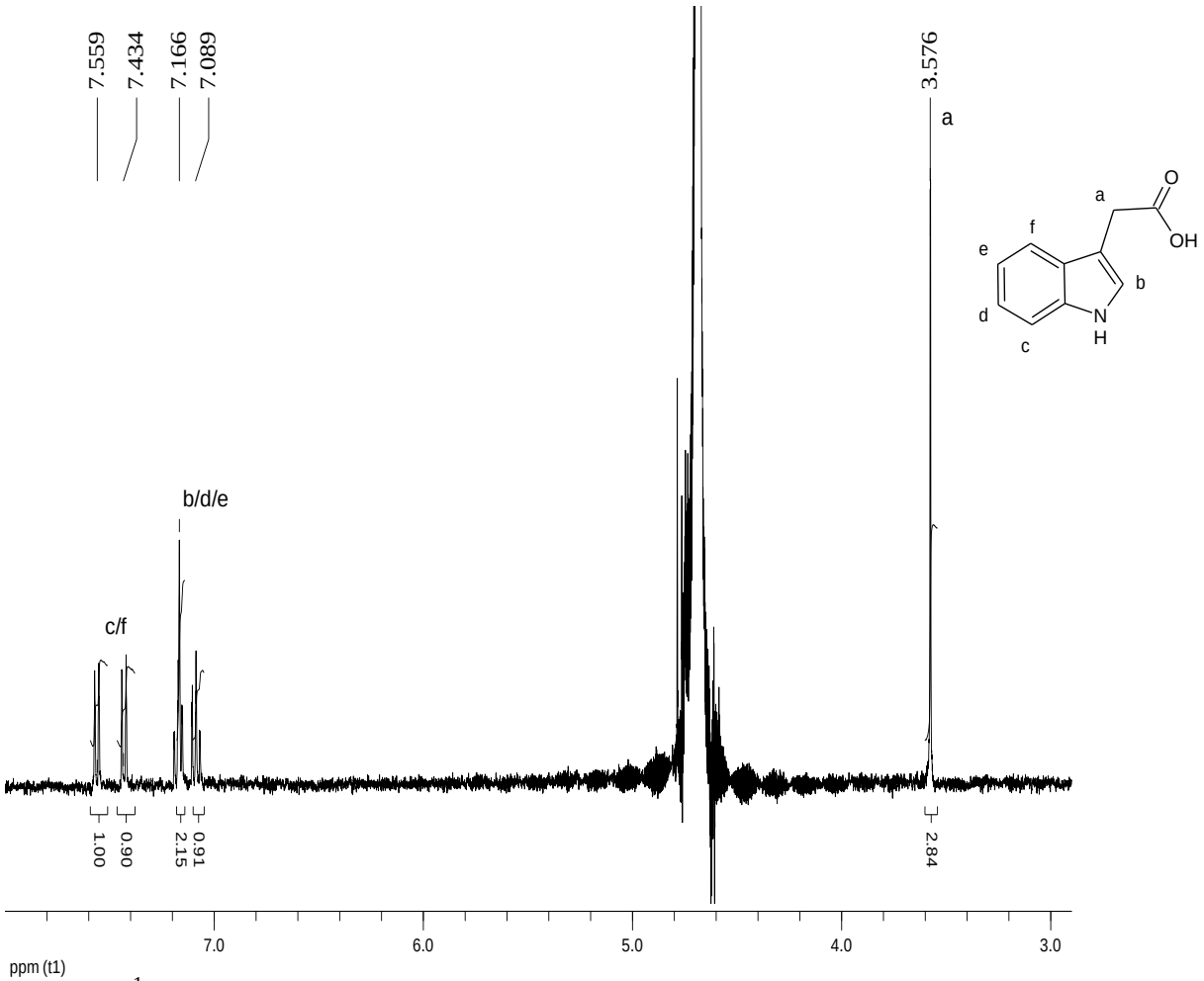

Figure 10. ^{1}H-NMR spectrum (in D_2O) of IAA at pH 12. The pH value of solution has been adjusted by adding the required amount of NaOD.

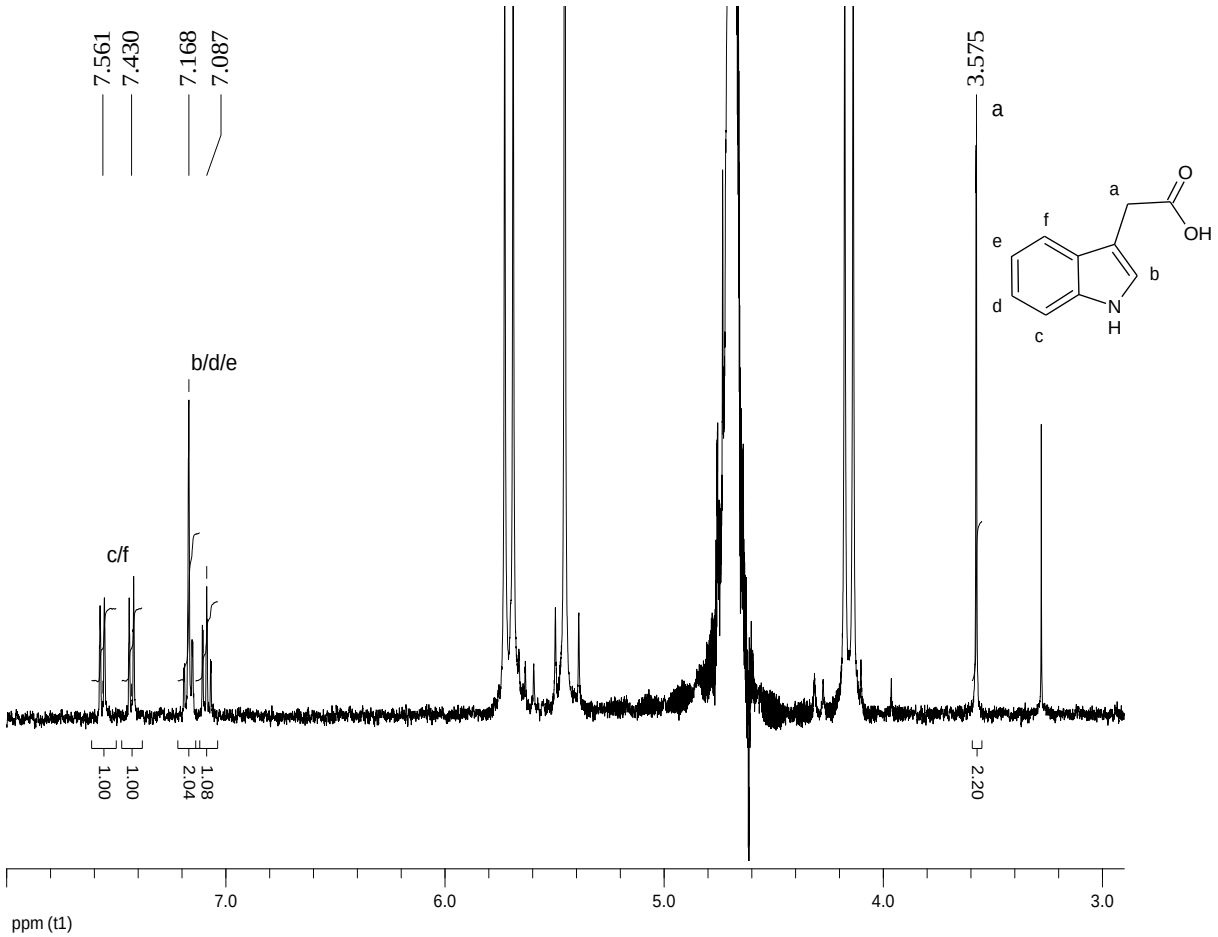

Figure 11. ^{1}H-NMR spectrum (in D_2O) of IAA with CB[7] at pH 12. The IAA/CB[7] molar ratio is 1:1 and the pH value of solution has been adjusted by adding the required amount of NaOD. The solution is uncoloured.

The ^{1}H-NMR spectra of IAA alone and IAA with CB[7] at pH 12 are reported in Figures 10 and 11, respectively. At basic pH both aromatic signals and the ethylene signal of IAA were not shifted suggesting that they were located outside the shielding region of the CB[7] cavity. It means that the CB[7]-IAA complex was not formed.

In conclusion, Figures 8 and 9 showed that at pH 1 the CB[7]-IAA complex was formed because IAA, in aqueous solution, was in the neutral form, the only one form that permits an inclusion complex with CB[7], while, as the solution became basic, the

IAA was deprotonated and it was not longer able to complex with CB[7] through the carboxylat group in the IAA molecule and the carbonyl groups of CB[7] (Figures 10 and 11). These results indicate that a pH-controlled release of indole-3-acetic acid guest from CB[7] was found to occur.

7.7 Outlook

Following the preliminary notes on the possibility to control the movement of the auxin molecules in and out the cucurbituril macrocyle, the host-guest chemistry of IAA-CB[7] complex in aqueous solution will be further investigated by determining:

• the binding constant, by ITC (Isothermal Titration Calorimetry), UV/Vis and ^{1}H NMR spectroscopy, and the stochiometry of the IAA-CB[7] complex at pH 1;

• pH values ranging from 2 to 11, at which it is possible to have either the only IAA anionic form or the only IAA-CB[7] complex (by checking the binding mode with ^{1}H-NMR spectroscopy and calculating the binding constant).

Moreover, the direct functionalization of CB[7] with an alkyl chain might be a potential strategy to favour the potential adsorption of the IAA-CB[7] complex on the hydrophobic cell membranes of plant roots and leaves, whereby the auxin might be released.

Finally, it will be interesting to also compare the ability of IAA to form CB[7] a host-guest complex with that of another auxin, for example indole-3-butyric acid (IBA), whose longer spacer between the carboxyl group and the indole-acetic ring may influence the binding mode of the complex, at varying solution pH.

In conclusion, the development of a technology based on the use of cucurbiturils for the pH-controlled release of auxins in plant systems might represent an interesting application of these macrocycle molecules.

CHAPTER 8 -

REFERENCES

8.1 References

Aktaş, N.; Tanyolaç, A. Reaction conditions for laccase catalyzed polymerization of catechol. *Bioresour. Technol.* 2003, *87*, 209-214.

Artaud, I.; Ben-Aziza, K.; Mansuy, D. Iron porphyrin-catalyzed oxidation of 1,2-dimethoxyarenes: a discussion of the different reactions involved and the competition between the formation of methoxyquinones or muconic dimethyl esters. *J. Org. Chem.* 1993, *58*, 3373-3380.

Baldock, J. A.; Skjemstad, J. O. Role of the matrix and minerals in protecting natural organic materials against biological attack. *Org. Geochem.* 2000, *31*, 697–710.

Barbaro, P.; Liguori, F. Ion exchange Resins: Catalyst Recovery and Recycle. *Chem. Rev.* 2009, *109*, 515-529.

Bedioui, F. Zeolite-encapsulated and clay-intercalated metal porphyrin, phthalocyanine and Schiff-base complexes as models for biomimetic oxidation catalysts: an overview. *Coord. Chem. Rev.* 1995, *144*, 39-68.

Behrend, R.; Meyer, E.; Rusche, F. Ueber Condensationsproducte aus Glycoluril und Formaldehyd. *Justus Liebigs Ann. Chem.* 1905, *339*, 1-37.

Bellamy, L. J. *The infra-red Spectra of Complex Molecules*; Third edition; Chapman and Hall, London, 1975.

Bizaia, N.; de Faria, E. H.; Ricci, G. P.; Calefi, P. S.; Nassar, E. J.; Castro, K. A. D. F.; Nakagaki, S.; Ciuffi, K. J.; Trujillano, R.; Vicente, M. A.; Gil, A.; Korili, S. A. Porphyrin-kaolinite as Efficient Catalyst for Oxidation Reactions. *ACS Appl. Mater. Interfaces* 2009, *1*, 2667-2678.

Bollag, J.-M. Decontaminating soil with enzymes. *Environ. Sci. Technol*. 1992, *26*, 1876-1881.

Buschmann, H. J.; Fink, H.; Schollmeyer, E. Preparation of cucurbituril. *Chem. Abstr.* 1997, *127*, 205599.

Cantor, C. R.; Schimmel, P. R. *Biophysical Chemistry. Part II: Techniques for the Study of Biological Structure and Function*; Freeman and Co.: New York, 1980.

Conte, P.; Piccolo, A. Conformational arrangement of dissolved humic substances. Influence of solution composition on the association of humic molecules. *Environ. Sci. Technol.* 1999, *33*, 1682-1690.

Cozzolino, A.; Conte, P.; Piccolo, A. Conformational changes of humic substances induced by some hydroxy-, keto-, and sulfonic acids. *Soil Biol. Biochem.* 2001, *33*, 563-571.

Cozzolino, A.; Piccolo, A. Polymerization of dissolved humic substances catalyzed by peroxidase, Effects of pH and humic composition. *Org. Geochem.* 2002, *33*, 281-294.

Crestini, C.; Saladino, R.; Tagliatesta, P.; Boschi, T. Biomimetic degradation of lignin and lignin model compounds by synthetic anionic and cationic water soluble manganese and iron porphyrins. *Bioorgan. Med. Chem.* 1999, *7*, 1897-1905.

Crestini, C.; Pastorini, A.; Tagliatesta, P. Metalloporphyrins immobilized on montmorillonite as biomimetic catalysts in the oxidation of lignin model compounds. *J. Mol. Catal. A - Chem.* 2004, *208*, 195-202.

Cui, F.; Wijesekera, T.; Dolphin, D.; Farrel, R.; Skerker, P. Biomimetic degradation of lignin. *J. Biotechnol.* 1993, *30*, 15-26.

Day, A. I.; Arnold, A. P.; Blanch, R. J.; Snushall, B. J. Controlling factors in the synthesis of cucurbituril and its homologues. *Org. Chem.* 2001, *66*, 8094-8100.

Day, A. I.; Blanch, R. J.; Arnold, A. P.; Lorenzo, S.; Lewis, G. R.; Dance, I. A cucurbituril-based gyroscane: A new supramolecular form. *Angew. Chem. Int. Ed.* 2002, *41*, 275-277.

Dec, J.; Bollag, J.-M. Phenoloxidase-mediated interactions of phenols and anilines with humic materials. *J. Environ. Qual.* 2000, *29*, 665-676.

Dec, J.; Haider, K.; Bollag, J.-M. Decarboxylation and demethoxylation of naturally occurring phenols during coupling reactions and polymerization. *Soil Sci.* 2001, *166*, 660-671.

Dec, J.; Haider, K.; Bollag, J.-M. Release of substituents from phenolic compounds during oxidative coupling reactions. *Chemosphere* 2003, *52*, 549-556.

Fontaine, B.; Piccolo, A. Co-polymerization of penta-halogenated phenols in humic substances by catalytic oxidation using biomimetic catalysis. *Environ. Sci. Pollut. Res.* 2011, DOI 10.1007/s11356-011-0626-x.

Freeman, W. A.; Mock, W. L.; Shih, N.-Y. Cucurbituril. *J. Am. Chem. Soc.* 1981, *103*, 7367-7368.

Fukushima M.; Sawada A.; Kawasaki M.; Ichikawa H.; Morimoto K.; Tatsumi K. Influence of humic substances on the removal of pentachlorophenol by a biomimetic catalytic system with a water-soluble Iron(III)-Porphyrin complex. *Environ. Sci. Technol.* 2003, *37*, 1031-1036.

Gianfreda, L.; Bollag, J. - M. Effect of soil on the behavior of immobilized enzymes. *Soil. Sci. Soc. Am. J.* 1994, *58*, 1672–1681.

Gianfreda, L.; Bollag, J. - M. Influence of natural and anthropogenic factors on enzyme activity in soil. In G. Stotzky and J.- M. Bollag (ed.) *Soil biochemistry* 1996, *9*, 123-193, Marcel Dekker, New York.

Gonsalves, A. M. d'A. R.; Pereira, M. M. State of the art in the development of biomimetic oxidation catalysts. *J. Mol. Catal. A - Chem.* 1996, *113*, 209-211.

Groves, J. T.; Haushalter, R. C.; Nakamura, M.; Nemo, T. E.; Evans, B. J. High-valent iron-porphyrin complexes related to peroxidase and cytochrome P-450. *J. Am. Chem. Soc.* 1981, *103*, 2884-2886.

Hahn, D.; Cozzolino, A.; Piccolo, A.; Armenante, P. M. Reduction of 2,4-dichlorophenol toxicity to *Pseudomonas putida* after oxidative incubation with humic substances and a biomimetic catalyst. *Ecotoxicol. Environ. Safety* 2007, *66*, 335-342.

Haouaj, M. E.; Ko, Y. H.; Luhmer, M.; Kim, K.; Bartik, K. NMR investigation of the complexation of neutral guests by cucurbituril. *J. Chem. Soc. Perkin Trans. 2* 2001, 2104-2107.

Hendrickson, D. N.; Kinnard, M. G.; Suslick, K. S. Photochemistry of (5,10,15,20-tetraphenylprphyrinato)iron(III) halid complexes, Fe(TPP)(X). *J Am. Chem. Soc*. 1987, *109*, 1243-1244.

Idso, S. B.; Kimball, B. A. Tree growth in carbon-dioxide enriched air and its implications for global carbon cycling and maximum levels of atmospheric CO_2. *Global Biogeochemistry Cycles* 1993, *7*, 537-555.

Jastrow, J. D.; Miller, R. M. Soil aggregate stabilization and carbon sequestration: Feedbacks through organo-mineral associations. In *Soil Processes and the Carbon Cycle*; Lal, R.; Kimble, J. M.; Follett, R. F.; Stewart, B. A.; Eds.; CRC Press: New York, 1998.

Jeon, Y.-M.; Kim, J.; Whang, D.; Kim, K. Molecular Container Assembly Capable of Controlling Binding and Release of Its Guest Molecules: Reversible Encapsulation of Organic Molecules in Sodium Ion Complexed Cucurbituril. *J. Am. Chem. Soc*. 1996, *118*, 9790-9791.

Jiao, D.; Zhao, N.; Scherman, O.A. A "green" method for isolation of cucurbit[7]uril *via* a solid state metathesis reaction. *Chem. Commun.* 2010, *46*, 2007-2009.

Jiao, D.; Zhao, N.; Scherman, O.A. PCT/GB2010/002330.

Kahraman, M. V.; Kuğu, M.; Menceloğlu, Y.; Kayaman-Apohan, N.; Güngör, A. The novel use of organo alkoxy silane for the synthesis of organic-inorganic hybrid coatings. *J. Non-Crist. Solids* 2006, *352*, 2143-2151.

Kim, J.; Jung, I.-S.; Kim, S.-Y., Lee, E.; Kang, J.-K.; Sakamoto, S.; Yamaguchi, K.; Kim, K. New Cucurbituril Homologues: Syntheses, Isolation, Characterization, and X-ray Crystal Structures of Cucurbit[*n*]uril (*n*) 5, 7, and 8). *J. Am. Chem. Soc.* 2000, *122*, 540-541.

Kitamura, Y.; Mifune, M.; Hino, D.; Yokotani, S.; Saito, M.; Tsukamoto, I.; Iwado, A.; Saito, Y. Peroxidase-like catalytic activity of Mn- and Fe-tetrakis(4-carboxyphenyl)porphines bound to aminopropyl-glass bead in oxidative reaction of heterocyclic amines. *Talanta* 2006, *69*, 43-47.

Kobayashi, S.; Uyama, H.; Kimura, S. Enzymatic polymerization. *Chem. Rev*. 2001, *101*, 3793.

Kurioka, H.; Komatsu, I.; Uyama, H.; Kobayashi, S. Enzymatic oxidative polymerization of alkylphenols. *Macromol. Rapid Commun.* 1994, *15*, 507-510.

Lagona, J.; Mukhopadhyay, P.; Chakrabarti, S.; Isaacs, L. The cucurbit[n]uril family. *Angew. Chem. Int. Ed.* 2005, *44*, 4844-4870.

Lee, J. W.; Samal, S.; Selvapalam, N.; Kim, H.-J.; Kim, K. Cucurbituril Homologues and Derivatives: New Opportunities in Supramolecular Chemistry. *Acc. Chem. Res.* 2003, *36*, 621-630.

Lee, T.-M.; Ma, C-C M.; Hsu, C.-W.; Wu, H.-L. Effect of molecular structures and mobility on the thermal and dynamical mechanical properties of thermally cured epoxy-bridged polyorganosiloxanes. *Polymer* 2005, *46*, 8286-8296.

Liu, Y.; Han, B.-H.; Chen, Y.-T. Molecular Recognition and Complexation Thermodynamics of Dye Guest Molecules by Modified Cyclodextrins and Calixarenesulfonates *J. Phys. Chem. B* 2002, *106*, 4678-4687.

Liu, S.; Zavalij, P. Y.; Isaacs, L. Cucurbit[10]uril. *J. Am. Chem. Soc.* 2005, *127*, 16798-16799.

Liu, L.; Zhao, N.; Scherman, O. A. Ionic liquids as novel guests for cucurbit[6]uril in neutral water. *Chem. Commun.* 2008, 1070-1072.

Liu, L.; Nouvel, N.; Scherman, O. A. Controlled catch and release of small molecules with cucurbit[6]uril *via* a kinetic trap. *Chem. Commun.* 2009, 3243-3245.

Machado, A. M.; Wypych, F.; Drechsel, S. M.; Nakagaki, S. Study of the Catalytic Behavior of Montmorillonite/Iron(III) and Mn(III) Cationic Porphyrins *J. Colloid Interface Sci.* 2002, *254*, 158-164.

Maldotti, A.; Molinari, A.; Amadelli, R. Photocatalysis with organized systems for the oxofunctionalization of hydrocarbons by O_2. *Chem. Rev.* 2002, *102*, 3811-3836.

Mansuy, D. Activation of alkanes : the biomimetic approach. *Coord. Chem. Rev.* 1993, *125*, 129-141.

Mansuy, D. Biocatalysis and substrate chemodiversity: Adaptation of aerobic living organisms to their chemical environment. *Catal. Today* 2008, *138*, 2-8.

Marquez, C.; Hudgins, R. R.; Nau, W. M. Mechanism of Host-Guest Complexation by Cucurbituril. *J. Am. Chem. Soc.* 2004, *126*, 5806-5816.

Martin, J. P.; Haider, K. Microbial activity in relation to soil humus formation. *Soil Sci.* 1971, *3*, 54-63.

Martinez-Lorente, M.A.; Battioni, P.; Kleemiss, W.; Batoli, J.F.; Mansuy, D. Manganese porphyrins covalently bound to silica and montmorillonite K10 as efficient catalysts for alkene and alkane oxidation by hydrogen peroxide. *J. Mol. Catal. A - Chem.* 1996, *113*, 343-353.

Meunier, B. In: *Metalloporphyrins Catalyzed Oxidations;* Montanari, F.; Casella L.; Eds.; Kluwer Academics Publishers: Dordrecth, 1994; pp. 11-19.

Meunier, B.; Sorokin, A. Oxidation of pollutants catalyzed by metallophtalocyanines. *Acc. Chem. Res.* 1997, *30*, 470-476.

Mifune, M.; Hino, D.; Sugita, H.; Iwado, A.; Kitamura, Y.; Motohashi, N.; Tsukamoto, I.; Saito, Y. Peroxidase-Like Catalytic Activity of Anion-Exchange Resins Modified with Metal-Porphyrins in Oxidative Reaction of Hetrocyclic Amines with Hydrogen Peroxide. *Chem. Pharm. Bull.* 2005, *53*, 1006-1010.

Milos, M. A comparative study of biomimetic oxidation of oregano essential oil by H_2O_2 or $KHSO_5$ catalyzed by Fe (III) meso-tetraphenylporphyrin or Fe (III) phthalocyianine. *Appl. Catal. A - Gen.* 2001, *216*, 157-161.

Mock, W. L. *Cucurbituril*; Elsevier: New York, 1996; Vol. 2.

Mohajer, D.; Solati, Z. Rapid and highly selective epoxidation of alkenes by tetrabutylammonium monopersulfate in the presence of manganese meso-tetrakis(pentafluorophenyl)porphyrin and tetrabutylammonium salts or imidazole co-catalysts. *Tetrahedron Lett.* 2006, *47*, 7007-7010.

Moro-oka, Y. Reactivities of active oxygen species and their roles in the catalytic oxidation of inactive hydrocarbon. *Catal. Today* 1998, *45*, 3-12.

Nakagaki, S.; Ramos, A.R.; Benedito, F.L.; Peralta-Zamore, P.G.; Zarbin, A.J.G. Immobilization of iron porphyrins into porous vycor glass: characterization and study of catalytic activity. *J. Mol. Catal. A - Chem.* 2002, *185*, 203-210.

Nam, W.; Lee, H. J.; Oh, S.-Y.; Kim, C.; Jang, H. G. First success of catalytic epoxidation of olefins by an electron-rich iron(III) porphyrin complex and H_2O_2: imidazole effect on the activation of H_2O_2 by iron porphyrin complex in aprotic solvents. *J. Inorg. Biochem.* 2000, *80*, 219-225.

Nam, W.; Park, S.E.; Lim, I.K.; Lim, M.H.; Hong, J.; Kim, J. First Direct Evidence for Stereospecific Olefin Epoxidation and Alkane Hydroxylation by an Oxoiron(IV) Porphyrin Complex. *J. Am. Chem. Soc.* 2003, *125*, 14674-14675.

Nardi, S.; Pizzeghello, D.; Muscolo, A.; Vianello, A. Physiological effects of humic substances on higher plants. *Soil Biol. Biochem.* 2002, *34*, 1527-1536.

Nuzzo, A.; Piccolo, A. Enhanced catechol oxidation by heterogeneous biomimetic catalysts immobilized on clay minerals. 2011. Manuscript to be submitted for *J. Mol. Catal. A – Chem, also reported in this thesis.*

Nieder, R.; Benbi, D. K.; Isermann, K. Soil organic matter dynamics. In *Handbook of Processes and Modeling in the Soil-Plant System*; Benbi, D. K.; Nieder, R.; Eds.; Food products press, The Haworth Reference Press: New York, 2003.

Oguchi, T.; Tawaki, H.; Uyama, S.-i.; Kobayashi, S. Soluble polyphenol. *Macromol. Rapid Commun.* 1999, *20*, 401-403.

Park, J.-W.; Dec, J.; Kim, J.-E.; Bollag, J.-M. Effect of humic constituents on the transformation of chlorinated phenols and anilines in the presence of oxidoreductive enzymes or birnessite. *Environ. Sci. Technol.* 1999, *33*, 2028-2034.

Paustian, K.; Andrén, O.; Janzen, H. H.; Lal, R.; Smith, P.; Tiang, G.; Tiessen, H.; van Noordwijk, M.; Woomer, P. L. Agricultural soils as a sink to mitigate CO_2 emissions. *Soil Use and Management* 1997, *13*, 230-244.

Peuravuori, J. NMR spectroscopy study of freshwater humic material in light of supramolecular assembly. *Environ. Sci. Technol.* 2005, *39*, 5541-5549.

Piccolo, A. Humus and Soil Conservation. In *Humic Substances in Terrestrial Ecosystems*; Piccolo, A., Ed.; Elsevier: Amsterdam, The Netherlands, 1996; pp 225-264.

Piccolo, A. The supramolecular structure of humic substances. *Soil Sci.* 2001, *166*, 810-832.

Piccolo, A. The supramolecular structure of humic substances: A novel understanding of humus chemistry and implications in soil science. *Adv. Agron.* 2002, *75*, 57-134.

Piccolo, A.; Nardi, S.; Concheri G. Macromolecular changes of soil humic substances induced by interactions with organic acids. *Eur. J. Soil Sci.* 1996, *47*,319-328.

Piccolo, A.; Conte, P.; Cozzolino, A. Conformational association of dissolved humic substances as affected by interactions with mineral and monocarboxylic acids. *European Journal of Soil Science* 1999, *50*, 687-694.

Piccolo, A.; Cozzolino, A.; Conte, P.; Spaccini, R. Polymerization of humic substances by an enzyme-catalyzed oxidative coupling. *Naturwissenschaften* 2000, *87*, 391-394.

Piccolo, A.; Conte, P.; Cozzolino, A.; Spaccini, R. In *Humic Substances And Chemical Contaminants*; Clapp, C. E., Hayes, M. H. B., Senesi, N., Bloom, P., Jardine, P. M., Eds.; Soil Science Society of America: Madison, WI, 2001; pp 89-118.

Piccolo, A.; Cozzolino A.; Conte, P. Chromatographic and spectrophotometric properties of dissolved humic substances as compared to macromolecularpolymers. *Soil Sci.* 2001, *166*, 174-185.

Piccolo, A.; Conte, P.; Trivellone, E.; Van Lagen, B.; Buurman, P. Reduced heterogeneity of a lignite humic acid by preparative HPSEC following interaction with an organic acid. Characterization of size-separates by PYR-GC-MS and ^{1}H-NMR spectroscopy. *Environ. Sci. Technol.* 2002, *36*, 76-84.

Piccolo, A.; Spiteller, M. Electrospray ionization mass spectrometry of terrestrial humic substances and their size fractions. *Anal. Bioanal. Chem.* 2003, *377*, 1047-1059.

Piccolo, A.; Conte, P.; Cozzolino, A.; Spaccini, R. The conformational structure of humic substances. In *Handbook of Processes and Modeling in the Soil-Plant System*; Benbi, D. K.; Nieder, R.; Eds.; Food products press, The Haworth Reference Press: New York, 2003.

Piccolo, A.; Conte, P.; Tagliatesta, P. Increased Conformational Rigidity of Humic Substances by Oxidative Biomimetic Catalysis. *Biomacromolecules* 2005, *6*, 351-358.

Piccolo A., Spiteller M., Nebbioso A. Effects of sample properties and mass spectroscopic parameters on electrospray ionization mass spectra of size-fractions from a soil humic acid. *Anal. Bioanal. Chem.* 2010, *397*, 3071-3078.

Piccolo, A.; Spaccini, R.; Nebbioso A.; Mazzei P**.** Carbon sequestration in soil by *in situ* catalyzed photo-oxidative polymerization of soil organic matter. *Environ. Sci. Technol*. 2011, *45*, 6697–6702.

Powell, M.F.; Pai, E.F.; Bruice, T.C. Study of (Tetraphenylporphinato)manganese(111)-Catalyzed Epoxidation and Demethylation Using p-Cyano-N,N-dimethylanilinNe -Oxide as Oxygen Donor in a Homogeneous System. Kinetics, Radiochemical Ligation Studies, and Reaction Mechanism for a Model of Cytochrome P-450. *J. Am. Chem. Soc*. 1984, *106*, 3277-3285.

Que, L. Jr.; Tolman, W. B. Biologically inspired oxidation catalysis. *Nature* 2008, *455*, 333-340.

Rocha-Gonsalves, A.M.A.; Pereira, M.M. State of the art in the development of biomimetic oxidation catalysts. *J. Mol. Catal. A - Chem.* 1996, *113*, 209-221.

Rebelo, S.L.H.; Gonçalves, A.R.; Pereira, M.M.; Simoes, M.M.Q.; Neves, M.G.P.M.S.; Cavaleiro, J.A.S. Epoxidation reactions with hydrogen peroxide activated by a novel heterogeneous metalloporphyrin catalyst. *J. Mol. Catal. A - Chem.* 2006, *256*, 321-323.

Saiz-Jimenez, C. The chemical structure of humic substances. In *Humic Substances in Terrestrial Ecosystems*; Piccolo A.; Ed.; Elsevier: Amsterdam, 1996.

Sánchez-Cortés, S.; Francioso, O.; García-Ramos, J.V.; Ciavatta, C.; Gessa, C. Catechol polymerization in the presence of silver surface. *Colloids Surf., A* 2001, *176*, 177-184.

Schlesinger, W. H. *Biogeochemistry. An analysis of Global Change*; 2nd ed.; Academic Press: San Diego (CA) 1997.

Shaik, S.; Hirao, H.; Kumar, D. Reactivity of high-valent iron_oxo species in enzymes and synthetic reagents: a tale of many states. *Acc. Chem. Res.* 2007, *40*, 532-542.

Sheldon, R. A. Oxidation catalysis by metalloporphyrins. In *Metalloporphyrins in Catalytic Oxidations*; Sheldon, R. A.; Ed. Dekker: New York, 1994.

Simpson, A. J. Determining the molecular weight, aggregation, structures and interactions of natural organic matter using diffusion ordered spectroscopy. *Magn. Reson. Chem.* 2002, *40*, S72-S82.

Six, J.; Conant, R. T.; Paul, E. A.; Paustian, K. Stabilization mechanisms of soil organic matter: implications for C-saturated soils. *Plant Soil* 2002, *241*, 155-176.

Šmejkalová, D.; Piccolo, A. Enhanced Molecular Dimension of a Humic Acid Induced by Photooxidation Catalyzed by Biomimetic Metalporphyrins. *Biomacromolecules* 2005, *6*, 2120-2125.

Šmejkalová, D.; Piccolo, A. Rates of Oxidative Coupling of Humic Phenolic Monomers Catalyzed by a Biomimetic Iron-Porphyrin. *Environ. Sci. Technol*. 2006, *40*, 1644-1649.

Šmejkalová, D.; Piccolo, A.; Spiteller, M. Oligomerization of Humic Phenolic Monomers by Oxidative Coupling under Biomimetic Catalysis *Environ. Sci. Technol*. 2006, *40*, 6955-6962.

Šmejkalová, D.; Conte, P.; Piccolo, A. Structural Characterization of Isomeric Dimers from the Oxidative Oligomerization of Catechol with a Biomimetic Catalyst. *Biomacromolecules* 2007, *8*, 737-743.

Šmejkalova, D.; Piccolo, A. Aggregation and disaggregation of humic supramolecular assemblies by NMR Diffusion Ordered Spectroscopy (DOSY-NMR). *Environ. Sci. Technol.* 2008, *42*, 699–706.

Smith, T. M.; Shugart, H. H. The transient response of terrestrial carbon storage to a perturbed climate. *Nature* 1993, *361*, 523-526.

Song, J.; Huang, W.; Peng, P.; Ma, B. X. Y. Humic Acid Molecular Weight Estimation by High-Performance Size-Exclusion Chromatography with Ultraviolet Absorbance Detection and Refractive Index Detection. *Soil Sci Soc. Am. J.* 2010, *74*, 2013-3020.

Stenson, A. C.; Landing, W. M.; Marshall, A. G.; Cooper, W. T. Ionization and fragmentation of humic substances in electrospray ionization fourier transform-ion cyclotron resonance mass spectrometry. *Anal. Chem.* 2002, *74*, 4397–4409.

Stenson, A. C.; Marshall, A. G.; Cooper, W. T. Exact masses and chemical formulas of individual Suwannee river fulvic acids from ultrahigh resolution electrospray ionization Fourier Transform Ion Cyclotron Resonance mass spectra. *Anal. Chem.* 2003, *75*, 1275–1284.

Stephenson., N.A.; Bell, A.T. The influence of substrate composition on the kinetics of olefin epoxidation by hydrogen peroxide catalyzed by iron(III) [tetrakis(pentafluorophenyl)] porphyrin. *J. Mol. Catal. A - Chem.* 2006, *258*, 231-235.

Stevenson, F. J. *Humus Chemistry: Genesis, Composition, and Reactions*; 2nd ed.; John Wiley and Sons: New York, 1994.

Swift, R. S. Macromolecular properties of soil humic substances: fact, fiction, and opinion. *Soil Sci.* 1999, *164*, 790-802.

Tan, K. H. *Environmental Soil Science*, Marcel Dekker: New York, 1994.

Tan, K. H. *Principles of Soil Chemistry*; 3rd ed.; Marcel Dekker: New York, 1998.

Tisdall, J. M.; Oades, J. M. Organic matter and water-stable aggregates in soils. *J. Soil Sci.* 1982, *33*, 141–163.

Traylor, T.G.; Hill, K.W.; Fann, W.P.; Tsuchiya, S.; Dunlap, B.E. Aliphatic Hydroxylation Catalyzed by Iron(111) Porphyrins. *J. Am. Chem. Soc.* 1992, *114*, 1308-1312.

Traylor, T.G.; Tsuchiya, S.; Byun, Y.S.; Kim, C. High-Yield Epoxidations with Hydrogen Peroxide and tert-Butyl Hydroperoxide Catalyzed by Iron(111) Porphyrins: Heterolytic Cleavage of Hydroperoxides. *J. Am. Chem. Soc.* 1993, *115*, 2775-2781.

Wang, Y.; Hsieh, Y-P. Uncertainties and novel prospects in the study of the soil carbon dynamics. *Chemosphere* 2002, *49*, 791-804.

Weber, L.; Hommel, R.; Behling, J.; Haufe, G.; Hennig, H. Photocatalytic Oxygenation of Hydrocarbons with (Tetraarylporphyrinato)iron(III) Complexes and Molecular Oxygen. Comparison with Microsomal Cytochrome P-450 Mediated Oxygenation Reactions. *J. Am. Chem. Soc.* 1994, *116*, 2400-2408.

Wershaw, R. L. Evaluation of conceptual models of natural organic matter (Humus) from a consideration of the chemical and biochemical processes of humification. U.S. Geological Survey; *Scientific Investigation Report 2004-5121*: Reston, VA, 2004.

Whang, D.; Heo, J.; Park, J.; Kim, K. A Molecular Bowl with Metal Ion as Bottom: Reversible Inclusion of Organic Molecules in Cesium Ion Complexed Cucurbituril. *Angew. Chem. Int. Ed.* 1998, *37*, 78-80.

Yau, W. W.; Kirkland, J. J.; Bly, D. D. *Modern Size Exclusion Chromatography*; Wiley Interscience: New York, 1979; p 318-326.

Zucca, P.; Mocci, G.; Rescigno, A.; Sanjust, E. 5,10,15,20-Tetrakis(4-sulfonato-phenyl)porphine-Mn(III) immobilized on imidazole-activated silica as a novel lignin-peroxidase-like biomimetic catalyst. *J. Mol. Catal. A - Chem.* 2007, *278*, 220-227.